5-2004

# Structural Analysis of CO2 Leakage Through the Salt Wash and Little Grand Wash Faults from Natural Reservoirs in the Colorado Plateau, Southeastern Utah

Anthony P. Williams
*Utah State University*

# STRUCTURAL ANALYSIS OF $CO_2$ LEAKAGE THOUGH THE SALT WASH AND LITTLE GRAND WASH FAULTS FROM NATURAL RESERVOIRS IN THE COLORADO PLATEAU, SOUTHEASTERN UTAH

by

Anthony P. Williams

A thesis submitted in partial fulfillment
of the requirements for the degree

of

MASTER OF SCIENCE

in

Geology

Approved:

UTAH STATE UNIVERSITY
Logan, Utah

2005

# ABSTRACT

Structural Analysis of $CO_2$ Leakage Through the Salt Wash and Little Grand Wash Faults from Natural Reservoirs in the Colorado Plateau, Southeastern Utah

by

Anthony P. Williams, Master of Science

Utah State University, 2004

Major Professor: James P. Evans
Department: Geology

The Little Grand Wash fault and the Salt Wash Graben in the Colorado Plateau of southeastern Utah emit $CO_2$ gas from abandoned drillholes, springs, and a hydrocarbon seep. Similar $CO_2$-charged water has also been emitted in the past, as shown by large localized travertine deposits and veins along and near the fault traces. The faults cut natural $CO_2$ reservoirs and provide an excellent analog for geologic $CO_2$ sequestration. The faults cut a north-plunging anticline of rocks consisting of siltstones, shales, and sandstones from the Permian Cutler Formation through the Cretaceous Mancos Shale. The Little Grand Wash fault has 260 m of throw and the stratigraphic separation across the Salt Wash Graben is 50 m. The fault rocks in the damage zone show hundreds of fractures, which decrease in density farther away from the faults. In specific areas, fractures with the presence of calcite mineralization indicate fluid migration and bleach zones from a few millimeters to 30 cm. This is evidence of past fluid migration directly

associated with the fault zone. Calcite mineralization fills these fractures and is also deposited in a variety of other bed forms. Foliated fault gouge, 5 to 20 cm thick, forms clay smear structures with a scaly shear fabric in a zone 10 to 15 cm thick is seen in the fault core. The leakage is constrained to the footwalls of the northernmost faults throughout the area. Clay-rich gouge structures should be effective barriers to cross-fault flow. Well log, surface geologic, and geochemical data indicate that the $CO_2$ reservoirs have been cut by the faults at depth, providing a conduit for the vertical migration of $CO_2$ to the surface, but not for horizontal flow across the fault plane. Even though lateral cross-fault migration may be impeded, this study clearly indicates that there are possible migration pathways for the escape of $CO_2$ from faulted subsurface aquifers, including aquifers faulted by "low-permeability" faults with clay gouge. Three-dimensional flow models show how the fault's maximum permeability in the damage zone is parallel to the faults, and the leakage though the damage zone is localized near the fold axis of the regional anticline. Direct dating of the clay in the fault gouge was done by ExxonMobil with $^{40}Ar/^{39}Ar$ methods, indicating that fault movement occurred between the middle Eocene and the end of the Miocene. During this time, the Colorado Plateau is interpreted to have been experiencing rapid uplift. The middle Jurassic, upper Jurassic, and Cretaceous rocks at the surface have been uplifted approximately 1.8 km since the end of the Eocene. This uplift may have influenced fault movement in the Colorado Plateau and along the Little Grand Wash fault, and Salt Wash and Ten Mile Graben. In evaluating these deep aquifers for $CO_2$ sequestration, careful design and monitoring of the geological structure and stress regimes must be considered to avoid leakage.

(94 Pages)

Dedicated to

Pete McKilop

# ACKNOWLEDGMENTS

The number of people that helped, encouraged, and inspired me to undertake the challenges of completing this thesis is certainty too long to mention here. There are many people in this field of study and many more on a personal level that gave me the support I needed to finish this thesis.

At the top of the list let me first thank my advisor, James P. Evans. Jim's content guidance has always encouraged me to supersede goals that I did not even think were achievable. Jim has also provided me with financial support, allowing me to focus completely on achieving the goals of this thesis. Without his support on many levels, I never could have made it this far, nor have the confidence to tackle whatever is next on the horizon.

My committee members, Zoe Shipton and Thomas E. Lachmar, have also been instrumental in the completion of the research. Zoe has spent time with me in the field listening to my ideas and countless hours helping me convey these ideas in writing. She has been extremely patient with me and in understanding my weaknesses.

Tom has been the light at the end of the tunnel, always encouraging me to make the next step closer to completion. His door is always open to help me when I need it most.

You will read the names of other people throughout this thesis that must be thanked. Rick Allis, Paul Lillis, Ben Dockrill, Dawn Matindale, Eleanor Dixon, and Scott Gerwe have all at some point added data and support helping me complete this work.

I would also like to thank the Geology Department of Utah State University, including all the professors and staff. I cannot think of a better learning atmosphere and thank you for creating a pleasant working environment.

The friendship and support from many of the people in the department helped me stay on the course to completion. I would like to thank all my office mates and other graduate students who have stepped in when needed and helped out whenever they could. Graduate student Jason Heath and I worked closely together and I would like to thank him for the amount of time we spent tossing around ideas.

There are many friends and family members that have supported my efforts here at Utah State University. Without there support and patience I would not be where I am today. At times my sanity was questionable and these friends and family members have been there to bring me back down to earth.

Again, I thank you and all the others who deserve my thanks. I could not have done it with the help from all of you.

Anthony Williams

# CONTENTS

Page

# LIST OF TABLES

# LIST OF FIGURES

# INTRODUCTION

Field-based structural analyses of clay-rich fault zones can be used to help constrain the geometry and properties of leaky subsurface aquifers and oil reservoirs. Faults bound a variety of subsurface reservoirs and may act as conduits, barriers, or combined conduit-barrier systems that enhance or impede fluid flow (Smith, 1980; Randolph and Johnson, 1989; Scholz, 1990; Caine et al., 1996). The questions that this field-based study examines include, but are not limited to, the following:

1. Why and where might leakages occur and have they occurred in the past?
2. What is leaking: water, oil, and/or gas?
3. Where are the fluids coming from?
4. What is the effect of faults on the storage integrity of potential sequestration reservoirs?
5. What is the geochronology of the system?

## Motivation

Field-based studies of reservoir-scale, clay-rich faults are few (Aydin and Yehuda, 2002). The above questions are addressed in this study by examining three fault systems located in the northwestern region of the Paradox Basin in southern Utah, in the Colorado Plateau (Fig. 1). The Little Grand Wash fault, the Salt Wash fault system, and the Ten Mile fault system cut rocks that contain water, oil, and carbon dioxide. These systems may provide insight to the geometry and properties of leaky subsurface aquifers

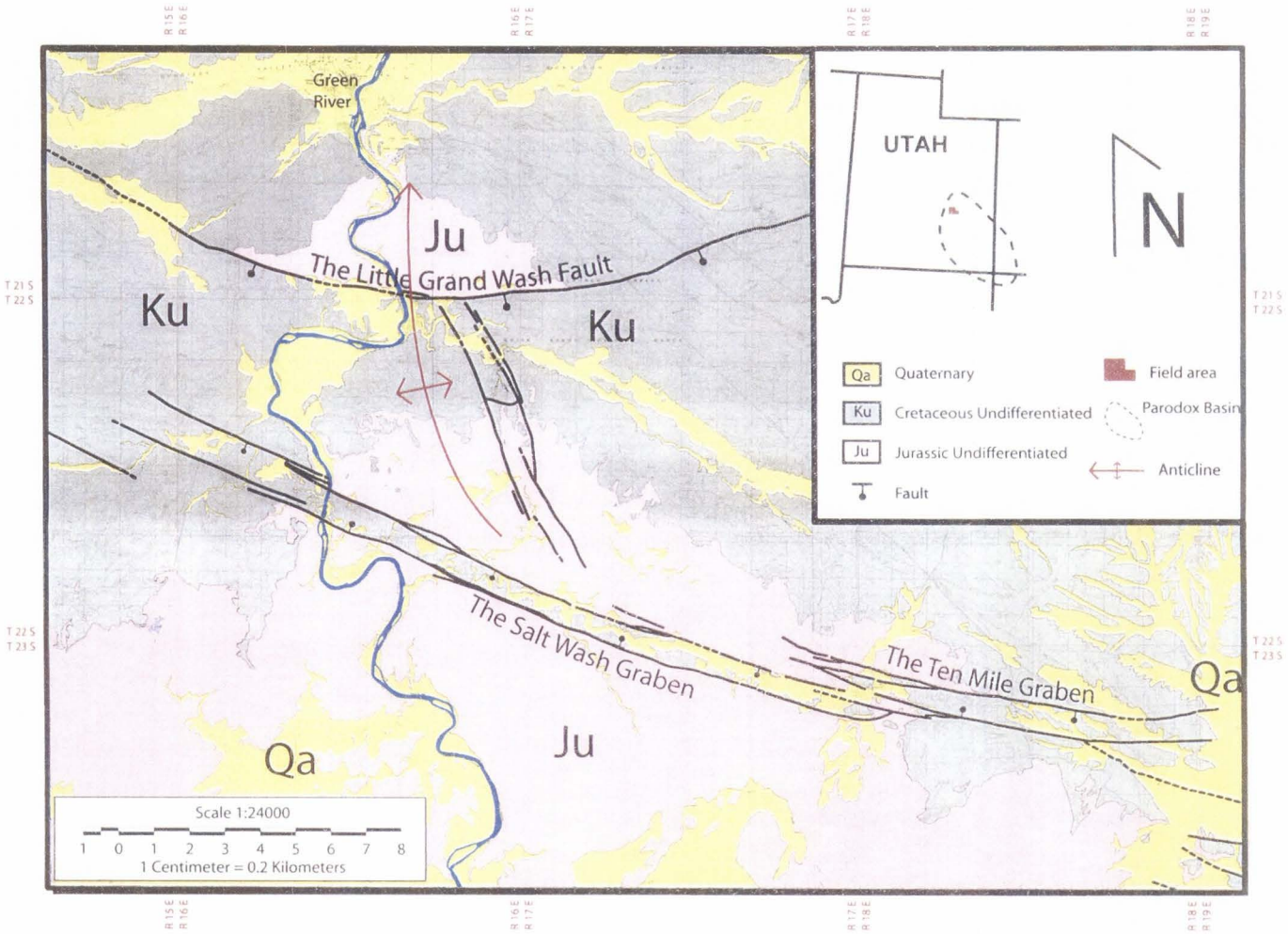


Figure 1 Location map and generalized regional geology of the study region in the Colorado Plateau, central Utah. Major faults are labeled (modified from Doelling, 2000).

and oil reservoirs. Two of the three systems, the Little Grand Wash fault and the Salt Wash fault system, appear to fail to constrain these fluids (Baer and Rigby,1978; Doelling, 1994). Past fluid flow is evidenced by numerous tufa/travertine and carbonate vein mineralizations localized along the fault traces (Baer and Rigby, 1978; Heath, 2004). Today, an oil seep, gas seeps, geysers, and springs near the faults leak carbon dioxide into the atmosphere. Geysers, oil, and gas seeps have been reported in the area as early as 1912 (Anonymous, 1912) and the travertine terraces near Crystal Geyser were documented as far back as 1867 (Powell, 1875). These faults are systems that presently cannot contain fluids and clearly have failed to do so in the past. This site provides an excellent opportunity to study clay-rich leaky faults.

The second motivation of this research is to examine a natural laboratory that can be used to study $CO_2$ sequestration. Due to the amount of $CO_2$ escaping, this area also provides a unique opportunity to study the impact of faults in $CO_2$ reservoirs. Hundreds of scientists across the world have participated in the study of the effects on the climate of increasing $CO_2$ in our atmosphere (Pearce et al., 1996; IPCC, 2001). Their studies have shown that the global average surface temperature has increased since 1861. In the past 140 years the increase has been $0.6 \pm 0.2^{o}C$ (Fig. 2). It is suggested that the temperature increase in the $20^{th}$ century is likely (66-90% probability) to have been the largest of any century during the past 1,000 years (Fig. 2 b). Increasing concentrations of $CO_2$ and other greenhouse gases tend to warm the Earth's lower atmosphere (Pearce et al., 1996; IPCC, 2001). Carbon dioxide, methane, and nitrous oxide concentrations have all increased in the past 100 years (Fig. 3). This change in climate can result from anthropogenic internal variability within the climate system, and from external factors.

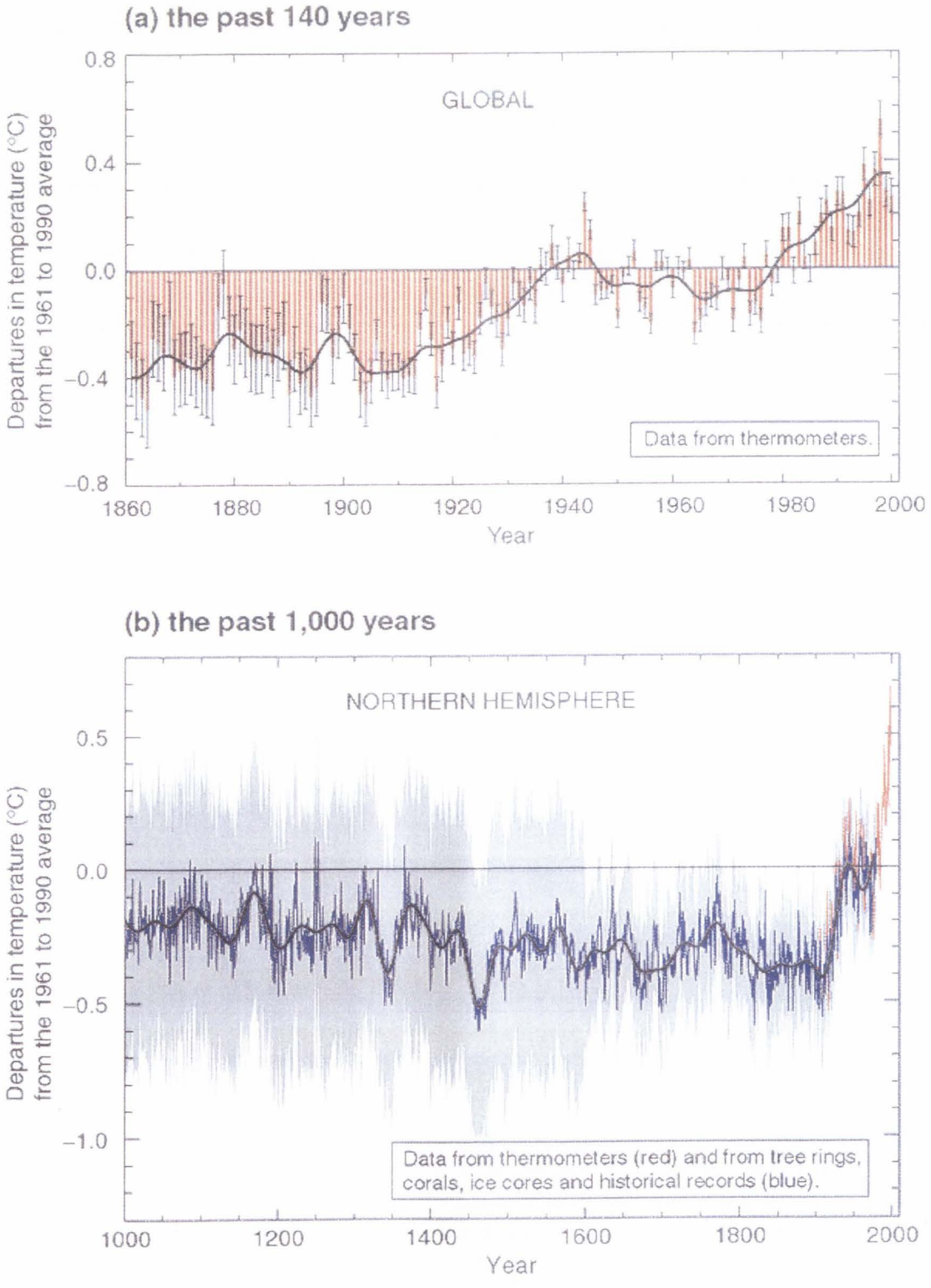


Figure 2 Temperature changes at the Earth's surface: a) the past 140 years and b) the past 1,000 years (taken from IPCC, 2001).

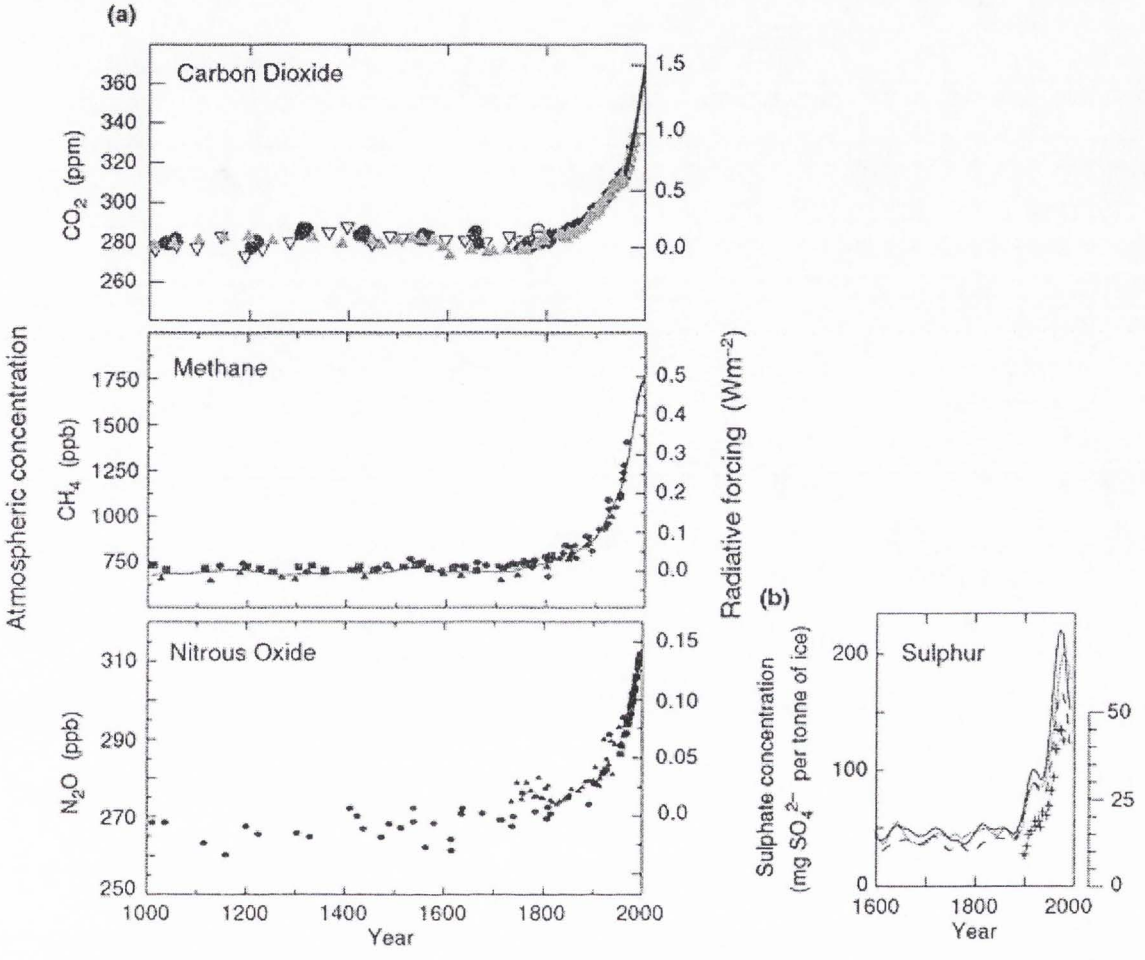


Figure 3 Graphs showing greenhouse gas concentrations during the past 1000 years: a) these three charts show the atmospheric concentrations of carbon dioxide, methane, and nitrous oxide and b) shows the sulphur concentrations (taken from IPCC, 2001).

It is widely accepted that during the 21st century, the dominant influence on the trends in atmospheric $CO_2$ concentration will be from the burning of fossil fuels.

One possibility for reducing carbon dioxide emissions is to dispose of excess $CO_2$ underground in geologic reservoirs (Pearce et al., 1996). $CO_2$ can be pumped into a variety of geological reservoirs and when the CO2 remains in the formation, it is referred

to as $CO_2$ sequestration. Pilot studies of injecting $CO_2$ into a deep aquifer include the Sleipner $CO_2$ project in the North Sea and the Weyburn study of a depleted oil reservoir (Gale, 2002).

## Rationale

### $CO_2$ sequestration implications

Currently, there are extensive governmental research programs on geologic storage of carbon dioxide in the U.S., Canada, Japan, and Europe. In addition to governmental support, there are major industry projects underway in Australia and the U.S., and there is also support from the multi-company Carbon Capture Project led by BP, Inc. (Gale, 2002). These research programs aim to build a scientific understanding of $CO_2$ capture while they increase the understanding of the effects of geologic storage. It is important that this research address all the issues and concerns relating to geologic storage of $CO_2$ so it can achieve general recognition as a global mitigation option (Gale, 2002). The study of natural occurrences of $CO_2$ assists in this goal. Natural $CO_2$ fields are potential analogs of $CO_2$ disposal and storage that can provide useful information of the behavior of $CO_2$ in subsurface reservoirs (Pearce et al., 1996). There are numerous natural $CO_2$-dominated gas reservoirs that have been discovered as a result of petroleum exploration in the greater Colorado Plateau and the Rocky Mountain region (Fig. 4).

### Fault sealing integrity

Some of these $CO_2$ reservoirs have been cut by faults that appear to create flow paths for $CO_2$ and other fluids to escape. The Little Grand Wash and Salt Wash faults cut

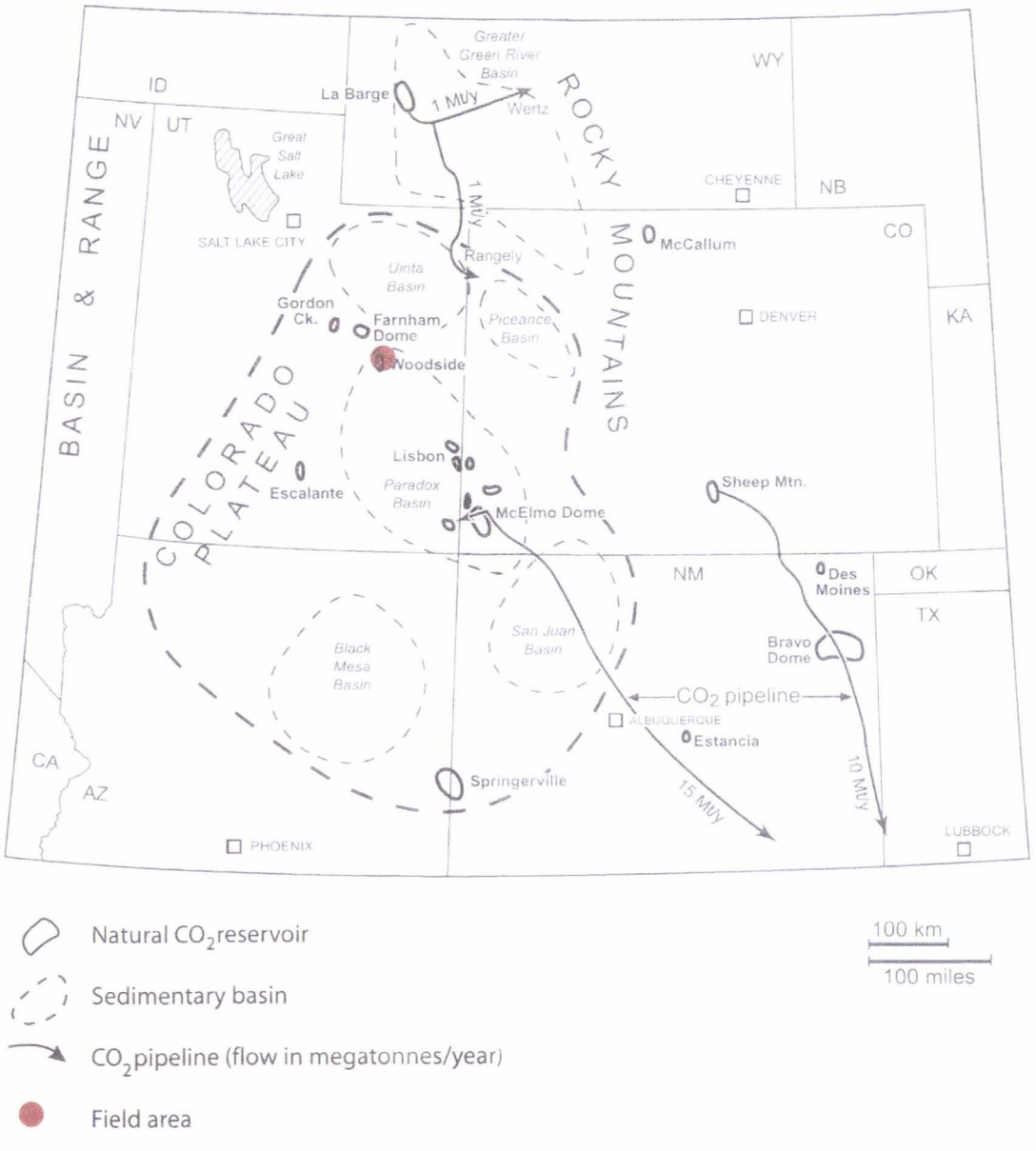


Figure 4 Synthesis map of the data pertaining to $CO_2$ fluxes and concentrations around the Colorado Plateau (modified from Allis et al., 2000).

$CO_2$-charged reservoirs, and it is these structures that are the focus of this research.

To begin to understand these structures, one must first consider the primary components of fault zone deformation. Caine et al. (1996) recognize these components as fault core, damage zone, and protolith. They define the fault core as the structural, lithologic, and morphologic portion of a fault zone where most of the displacement is accommodated. They further define a damage zone as the network of subsidiary structures that bound the fault core and may enhance fault zone permeability related to the core and the undeformed protolith. They describe the protolith as the surrounding county rock where fault-related permeability structures are absent.

These primary components and other factors influence whether faults act as barriers or conduits to the flow of fluids (Caine et al., 1996), or they may act as a mixed barrier-conduit system. Some of the other factors discussed by Caine et al. (1996) that influence the behavior of a fault and can play a major role in fault zone integrity, include, but are not limited to: unconsolidated clay-rich gouge in the fault core, the amount of fractures in the fault zone, the connectivity of the fractures, the presence and amount of mineralization in the fractures, and the permeability and thickness changes, both down dip and along strike, of the rocks that are cut by the fault (Caine and Forster, 1999). This field-based study explores the above elements associated with faults, and also reviews regional structures that may influence fault zone permeability.

There are fault-induced fractures near the Little Grand Wash fault, the Salt Wash fault system, and the Ten Mile fault system. They likely contribute to the gas leakage of the area, but do not completely explain the location of this leakage. These localized fractures are associated with all three fault systems; however, leakage is only seen in

areas of the Little Grand Wash fault and the Salt Wash fault zones. Rocks in the damage zones of these faults clearly show leakage. Many fractures are filled with mineral deposits and/or rocks are also bleached near the fractures.

Fault zone permeability in outcrop is also important to consider in terms of sealed or leaky faults. The reduction of pore space through granulation and the presence of clay or shale in the fault zones are two major mechanisms that are proposed to explain the relatively low permeability of faults (Aydin and Yehuda, 2002). In faulted sandstone reservoirs, fault rocks tend to exhibit reduced permeability in comparison to the host rocks. This is a result of denser grain packing, clay-enriched fault gouge, clay/shale smear and occasionally cataclasis and/or cementation (Antonellini and Aydin, 1994; Shipton et al., 2002; Helgesen and Vold, 2003). Faulting in granular media can cause cataclasis and changes in porosity (Antonellini and Aydin, 1994). These processes may affect the quality of porous media and, in multiphase flow, can cause compartmentalization and fault sealing (Nelson, 1985; Hardman and Booth, 1991). Compartmentalization of juxtaposed porous reservoirs caused by fault sealing has been recognized in the Gulf Coast (Smith, 1980), in the Niger Delta (Weber and Daukoru, 1975; Seeburger et al., 1991), in California, and in Central Sumatra (Harding and Tuminas, 1988). Clay smearing is the mechanism thought to explain this process (Smith, 1966, 1980; Downey, 1984; Watts, 1987; Bouvier et al., 1989).

The occurrence of shale in subsurface fault zones is common (Aydin and Yehuda, 2002). This information is largely obtained from gamma-ray and dipmeter logs. Core recovery of clay-rich faults studied by Aydin and Yehuda (2002) is very poor, and the resolution of seismic data is not high enough to reveal fault zone architecture and its

content. However, Aydin and Yehuda (2002) did find that well tests largely from gamma-ray and dipmeter logs, together with seismic data and well logs, show that clay-rich faults have relatively low permeability, thereby providing lateral seals for fluids. Furthermore, there is evidence that flow parallel to the shale-bearing fault zones does occur (Weber et al., 1978) and that some faults may leak laterally (Perkins, 1961; Smith, 1966). These problems have necessitated field studies of the geometry and distribution of shale bodies along fault zones in structural analogs, and the mechanisms of their emplacement (Weber et al., 1978; Gibson, 1994; Weber, 1997; Aydin and Yehuda, 2002).

Previous work done in the area studied in this thesis does not address the relationship between sealing capabilities and the integrity of these faults. It is important to understand the sealing characteristics and structure of shale-rich faults for a variety of oil and gas reservoir production models. It is essential to understand fluid flow through and around faults to predict subsurface flow from possible reservoirs. These faults provide a unique opportunity to study a natural carbon dioxide-charged reservoir that has failed. This also is very important for examining the problems associated with $CO_2$ sequestration due to the unique leaky nature of the faults.

## Objectives

The purpose of this study is to determine the lithology, fault characteristics, and fault geometry that influence the flow of fluids along and around the Little Grand Wash fault, the Salt Wash fault system, and Ten Mile fault system/. The specific objectives of this study are to: 1) map the field area (approximately 240 $km^2$) at a scale of 1:24,000,

and at 1:6,000 where evidence of fault failure is most abundant; 2) collect and collate drillhole data; 3) create a lithologic column for the area; 4) draw a cross section for each of the faults; 5) attempt to date the age of the faulting and carbonate deposits along them; 6) develop timing relationships between faults, mineral deposits and the regional anticline; and 7) develop a 3-D conceptual model of the reservoir-flow system.

These objectives were met by performing a field-based study of the Little Grand Wash fault, the Salt Wash fault system, and Ten Mile fault system. This study addresses these objectives, which can help the understanding of effects that $CO_2$ sequestration may have in faulted subsurface aquifers.

# GEOLOGICAL SETTING

Previous work in the area shows that the Colorado Plateau and Four Corners region of the western United States contains at least nine producing or abandoned $CO_2$ fields with over 28 trillion cubic feet (TCF) of $CO_2$ gas in place (Allis et al., 2000). Some of this $CO_2$ gas has actively been produced from hydrocarbon and $CO_2$ fields (e.g., the Lisbon and McElmo Dome fields) (Fig. 4) within the Paradox Basin (Allis et al., 2000). These $CO_2$ gas fields lie beneath rocks that have a gentle regional dip to the north and are superimposed by local structural features (McKnight, 1940). The Little Grand Wash fault, the Salt Wash fault system, and the Ten Mile fault system are part of a WNW trending set of 70- to 90°-dipping normal faults in the region (Fig. 5). Some of these structures fail to seal fluid flow as shown by gas and oil seeps, springs and mineral deposits (McKnight, 1940; Baer and Rigby, 1978; Doelling, 1994). This study addresses these regional structures. The area has been subject to numerous tectonic loads, including Cretaceous (early Tertiary) repeated salt movement, Tertiary intrusive igneous activity, burial, uplift, and is currently under NNE extension (Davatzes et al., 2003; Reinecker et al., 2004).

## Springs

A series of carbonate deposits found by active and inactive springs, and an active $CO_2$-charged geyser are localized along a 2-km section of the Little Grand Wash fault zone (Baer and Rigby, 1978; Campbell and Baer, 1978; Doelling, 1994). The Salt Wash

fault system also has many carbonate mineralizations, springs, and a $CO_2$-charged geyser studied in this thesis, and will be discussed in the results section.

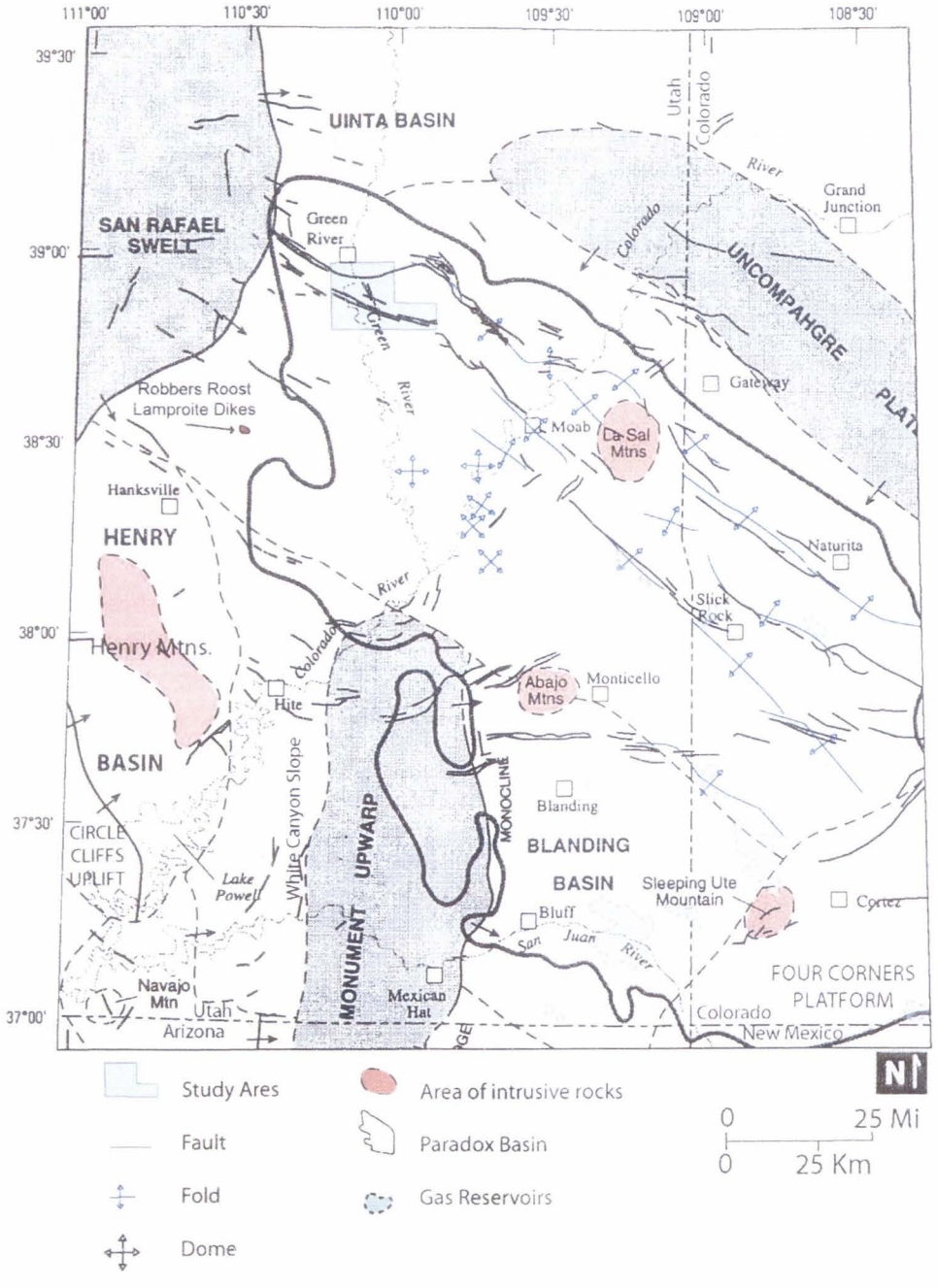


Figure 5 Regional map showing the study area, NW fault and fold trends, intrusive rocks and gas reservoirs (taken from Heath, 2004).

## Carbonate Deposits

Calcite deposits with a variety of textures are located in and near the damage zones of both faults (Heath, 2004; Shipton et al., 2004). Brilliant layered, fibrous, and impure white veins are present in all calcite-rich areas (Fig. 6). These veins have thicknesses varying from a few millimeters to a few meters, and in one location alone the Salt Wash fault veins extend for lateral distances of up to 90 m from the fault. Globular calcite and tufa deposits are commonly integrated with the veins. Textures that appear to be sub-aerial rimstone are found at active depositional areas. Rimstone texture is also seen in ancient inactive deposits. The mineralization is layered. The color is variable throughout these deposits, and is generally white or white with light shades of yellow, orange, red, brown, green and gray. A detailed textural and isotopic analysis of these deposits is presented in Dockrill et al. (in review).

## Stratigraphy

### Subsurface rocks

Formations cut by the faults in the subsurface range from the Permian Cutler Formation to the Jurassic Carmel Formation. These rocks do not outcrop anywhere in the field area, and therefore their surface expressions are not described.

### Surface rocks

The depositional environment of the surface rocks includes broad floodplains with occasional lakes and ponds, lacustrine mudstone, sporadic channel-point bar deposits,

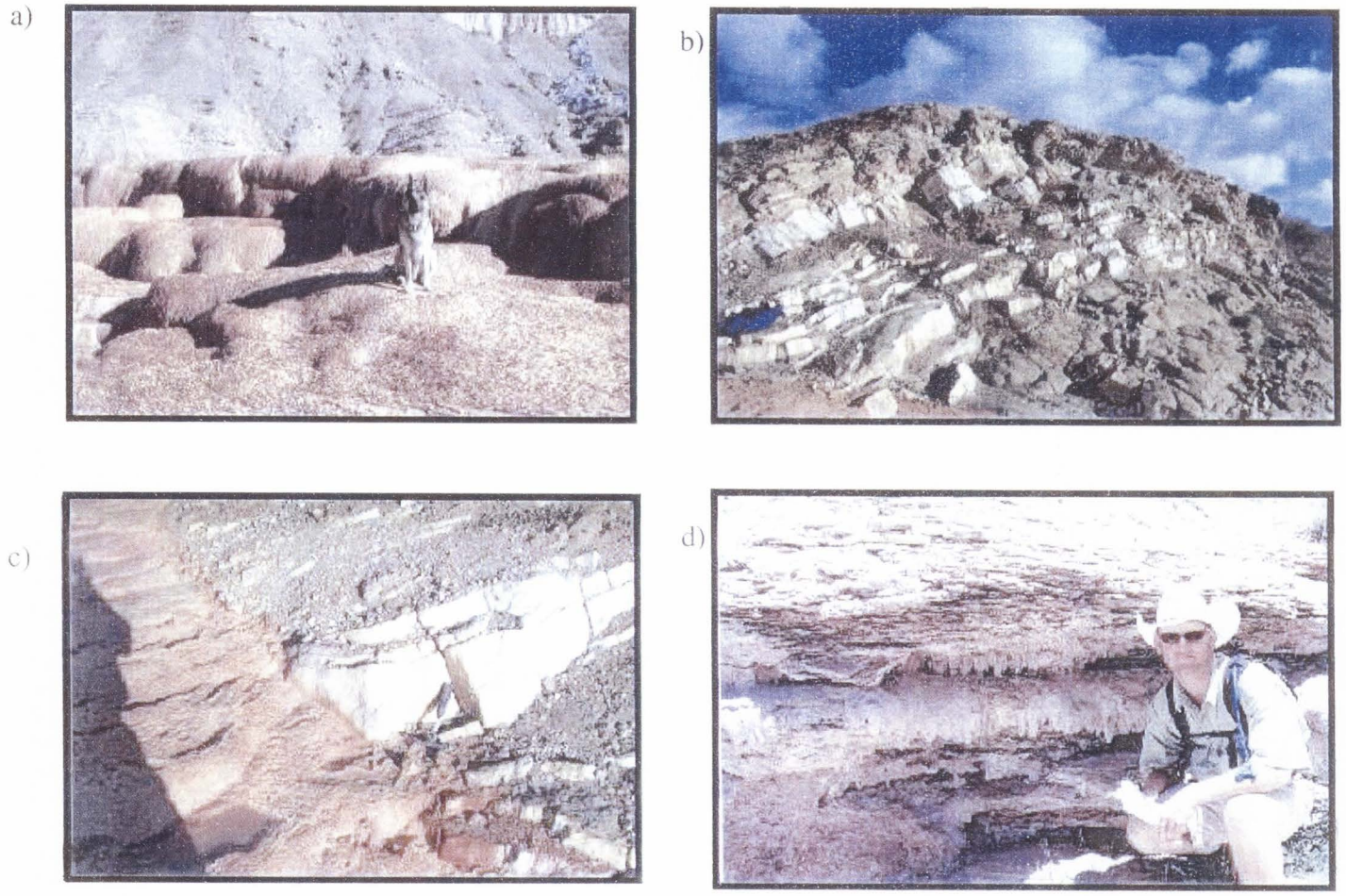


Figure 6 Calcite deposits found at different locations in the field area. a) Travertine terraces actively being deposited by waters from the Crystal Geyser. b) Sub-horizontal veins that appear to have been deposited from past fluid flow (Crystal Geyser area). c) The modern-day deposit (left) is cross-cutting past deposits (right) (Crystal Geyser area). d) Stalactite structures deposited in the voids within the calcite mounds (Salt Wash north fault). e) Chaotic calcite veins that completely obliterate the preexisting host rock and fault structures (Little Grand Wash fault). f) Weathered calcite veins that show a box-work pattern (Little Grand Wash fault). g) Globular structures that may also form in sub-aerial caverns (Little Grand Wash fault).

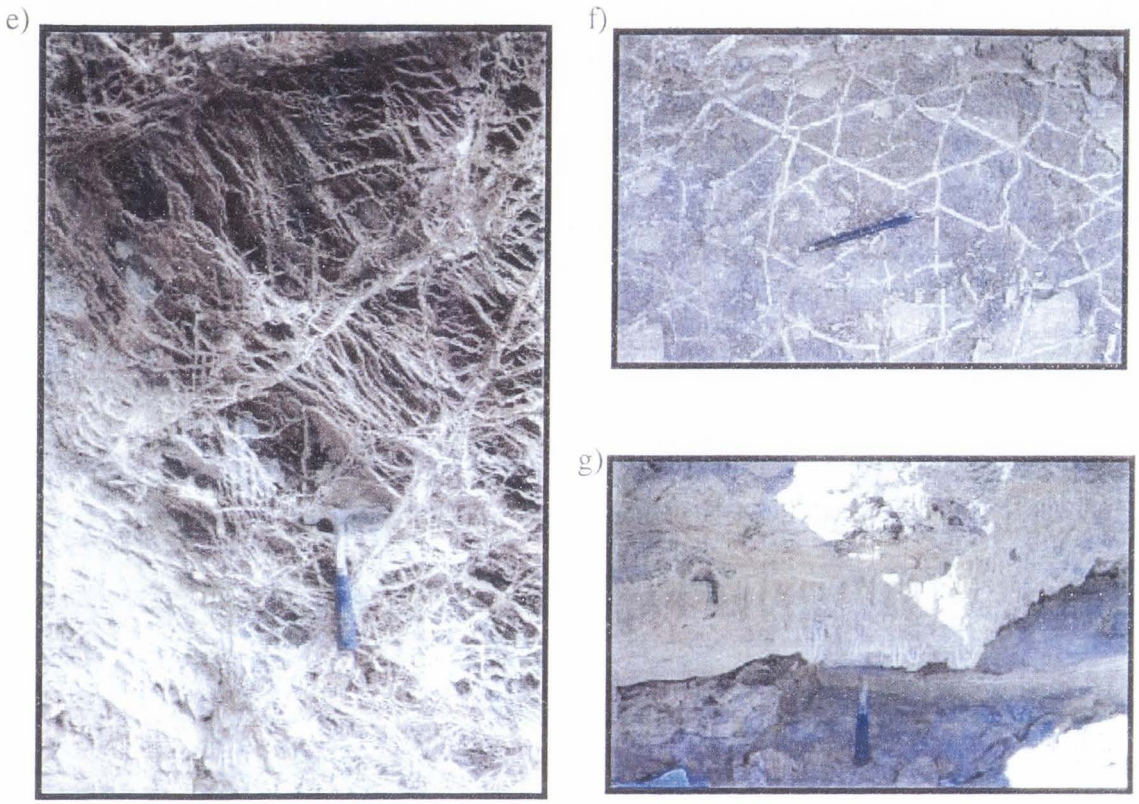


Figure 6 Continued.

channel-fill sandstone, braided streams, migrating fluvial channel sandstone and conglomerates. This fluctuation introduces dramatic changes in thickness that can occur within short distances. Some evidence of the variability of thickness in these formations can be seen in uranium excavations near the field area. Previous field work was done (Trimble and Doelling, 1978) throughout 1975 and the spring of 1976 about 22 km west of the field area, near the San Rafael Swell. The study was completed to investigate the production of uranium and vanadium. According to these records, formations change thickness as much as 91 m within several kilometers (Trimble and Doelling, 1978). Work of this nature has been conducted in this study near the Little Grand Wash fault and the Salt Wash faults with the aid of some previously drilled wells that have provided some

simple well logs. A summary of these logs can be seen in Table 1. The wells show the tops of some of the formations in the subsurface of the field area. Geologic investigations of these boreholes, combined with detailed surface mapping, have provided clues to the relationship between these formations and the faults that cut them.

The rocks cut by the faults along their surface traces range from the Jurassic Entrada Sandstone through the Cretaceous Mancos Shale. This section includes brief descriptions of these formations observed in the field, both in this study and by many others (Doelling, 1975; Trimble and Doelling, 1978; Petersen and Roylance, 1982; Johnson, 1988; Peterson, 1988; Peterson and Turner-Peterson, 1989; O'Sullivan, 1992; Vrolijk et al., 2005).

Middle Jurassic Curtis and Entrada Formations

The Jurassic Entrada Sandstone is primarily composed of red, fine-grained, silty sandstone, which has distinct massive bedding. It weathers into rounded mounds and slick slopes with medium-grained and coarse-grained cross-beds. The Entrada has a varying thickness of 59 to 164 m (Fig. 7) and a total average thickness of 112 m (Table 2) are seen in the wells across the area.

The Jurassic Curtis Formation lies conformably above the Entrada and is comprised of sandstones, siltstones, and shales. The base of the unit is mostly resistant, fine- to medium-grained sandstone. In many places an interval of interbedded sandstone and siltstone lies beneath the resistant sandstone, but locally may be absent. The upper section of the Curtis Formation is less resistant than the lower, slope-forming base and

becomes progressively more silty and shaly towards the top. The total thickness of the Curtis ranges from 11 to 104 m (Fig. 7), with an average thickness of 57 m (Table 2).

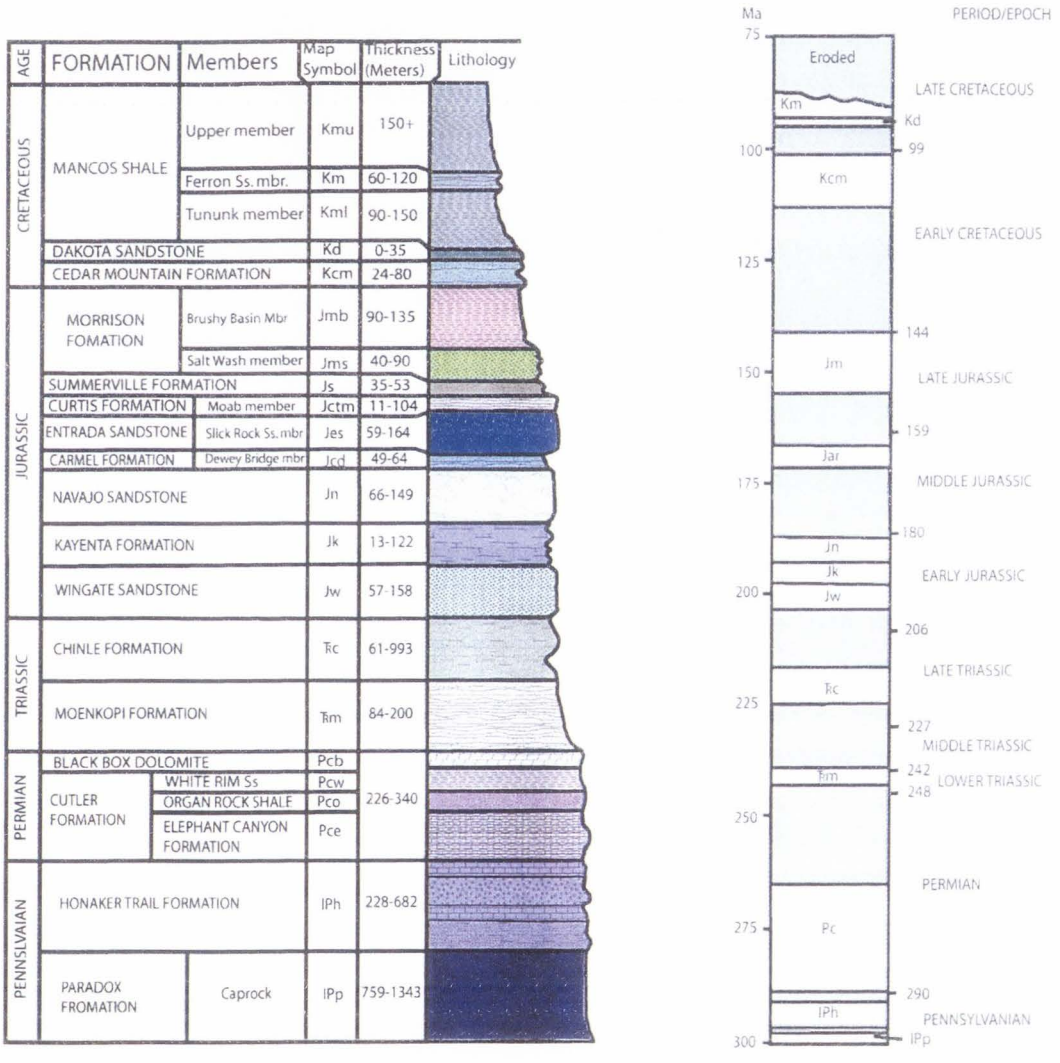


Figure 7 Formations and ages of the rocks cut by the Little Grand Wash fault, the Salt Wash faults and the Ten Mile Graben. Stratigraphic column (left) shows the formation (capitalized) and members (lower case) with their relationship to thickness and outcrop signature. The correlation diagram (right) shows formations and members with respect to time and age of deposition. Shaded areas indicate when rocks were not deposited and/or deposited and subsequently eroded. In the correlation diagram, Jm represents all the members of the Morrison Formation. Js represents the Summerville, Curtis, Entrada, and Carmel Formations. Ma (millions of years ago) shows the times the formations were deposited (after Doelling, 2001).

Table 1 Data compiled from well logs available in the field area (depths are in feet).

| Well Number | Well Name | Date completed | Total Depth (ft.) | Formation at T.D. | Summary of Oil and Gas shows (ft.) |
|---|---|---|---|---|---|
| | **Emery County** | | | | |
| # 1 | Superior Oil Co. no. 14-24 Grand Fault Unit | May-61 | 10,608 | Lynch Dolomite (Cambrian) | Gas show in Pardox Fm. 6947-7014 and 9412-8454 |
| #2 | Skyline Oil Co. no. 1 Green River Unit | May-65 | 9,621 | Leadville Ls. (Mississippian) | Gauged 15 mcfpd rate from Paradox Fm. 7017-7080 |
| #3 | California-Utah Oil Co. no.1 | Dec-1899 | 1,600 | Probably Morrison Fm. (Jurassic) | 30ft. Probably Morrison Fm. Gas flared at 1100ft. |
| #4 | Amax Petroleum no. 9-7 Green River Desert Unit | Jan-64 | 8,991 | Leadville Ls. (Mississippian) | None |
| #5 | Texas Eastern Transmission no. 1 Fed | Nov-57 | 8,490 | Leadville Ls. (Mississippian) | Local oil saturation and bleeding gas from cores of post salt Hermosa Group, 5322-5327, 5821-5874 and 6117-6177 |
| #6 | Equity Oil Co. no. 1 gov't | Feb-52 | 6,201 | Leadville Ls. (Mississippian) | None |
| #7 | American Metals Climax/Sinclair O.&G. no. 29-4 Nine Mile-Gov't | Dec-61 | 6,201 | Paradox Fm (Pennsylvanian) | None |
| #8 | Whienant no. 1 | Sep-43 | 435 | Morrison Fm. (Jurassic) | None |
| | **Grand County** | | | | |
| #9 | Bamberger and Mills no. 1 | Mar-05 | 1,000 | Morrison Fm. (Jurassic) | None. |
| #10 | Glen Ruby et al. no. 1-x | Jun-36 | 2,627 | Kiabab Ls. (Permian) | Minor shows. Well erupts carbon dioxide and water (see text) |
| #11 | Marland Oil Co. Culbertson no. 1 | Sep-26 | 3,820 | Elephant Canyon Fm. (Permian) | Oil show 400 (Morrison): gas show 1500-1530 (Navajo/Kayenta); oil show 2396, oil show 3060-3070 (White Rim); gas show 3170-3180 (White Rim) 83% CO2 |
| #12 | Crescent Drilling Co. no. 1 | Oct-13 | 2,100 | Entrada Fm. (Jurassic) | Gas show at 850 (top of Dakota Ss.) 976 (Morrison Fm.) and 1980 |
| #13 | Shell Oil Co. no. 1-26 Federal | Jul-69 | 11,895 | Pinkerton Trail Fm. (Pennsylvanian) | Minor gas shows in Honker Trail and Paradox Formations |
| #14 | Crescent Drilling Co. no. 2 | Mar-05 | 1,600 | Morrison Fm. (Jurassic) | Gas show at 350 ft., died |
| #15 | Amerada Petroleum Corp. Green River no. 1 | Jan-49 | 5,645 | Paradox Fm. (Pennsylvanian) | Temporary flow of gas; condensate and salt water at T. D. (see text) |
| #16 | Amerada Petroleum Corp. Green River no. 2 | Jul-49 | 5,896 | Paradox Fm. (Pennsylvanian) | None |
| #17 | Ferguson Oil Co. no. 1-14 U-tex | Nov-71 | 6,730 | Leadville Ls. (Mississippian) | Gauged 1.27 MMcf rate from Paradox Fm. 5860-6108; died |
| #18 | Mountain Fuel Supply Co. Skyline OU Co. no 1-25 | Mar-73 | 9,508 | Morrison Fm. (Jurassic) | Gauged 3 mcfgpd rate in Honaker Trail Fm.; other minor gas shows in same |
| #19 | British-American Petroleum Co. no. 3 | Mar-05 | 425 | Paradox Fm. (Pennsylvanian) | None. Well drilled to intersect surface showing downdip |
| #20 | Pacific-Western Oil Co. no1 Sharp State | Sep-49 | 5,046 | Jurassic | None |
| #21 | Delany Petroleum Corp. no. 1 | Oct-49 | 980 | Leadville Ls. (Mississippian) | None |
| #22 | Superior Oil Co. no. 22-34 Salt Wash Unit | Nov-49 | 10,293 | Leadville Ls. (Mississippian) | Minor gas show in Honaker Trail Fm. |
| #23 | British-American Petroleum Co. Levi no. 2 | Dec-49 | 1,500 | | None |
| Bonus #1 | Megadon ENT Inc | Mar-82 | 9,110 | Leadville Ls. (Mississippian) | None |
| Pan America #1 | Pan America | Apr-61 | 9,523 | Lynch Dolomite (Cambrian) | Gas cap encroaching water |

Table 2 Recorded formation thicknesses found in the wells in the field area. The average thickness is seen on the bottom of the table. These thicknesses are in meters. Formation names are abbreviated and the full names can be seen on Figure 7. Well numbers shown on Table 1.

| Well number | Kcm | Jmb | Js | Jctm | Jes | Jcd | Jn | Jk | Jw | Trc | Trm | Pc | IPh | IPp |
|---|---|---|---|---|---|---|---|---|---|---|---|---|---|---|
| 1 | | | | | | 52 | 76 | 122 | 99 | 76 | | 245 | | |
| 2 | | | | | | | | | | | | 261 | 381 | |
| 3 | | | | | | | | | | | | | | |
| 4 | | 90 | | | 102 | 58 | 132 | 51 | 123 | 74 | | | 302 | |
| 5 | | | | | | 68 | 149 | | | 75 | | | 303 | |
| 6 | | | | | | | | | | 61 | | | 536 | |
| 7 | | | 52 | 68 | 133 | 67 | 140 | 59 | 111 | 80 | | | | |
| 8 | | | | | | | | | | | | | | |
| 9 | | | | | | | | | | | | | | |
| 10 | | | | | | | | | | | | | | |
| 11 | | | | | | | | | | | | | | |
| 12 | | | | | | | | | | | | | | |
| 13 | | | | 104 | 96 | 39 | 121 | 29 | 138 | 84 | | | | |
| 14 | | | | | | | | | | | | | | |
| 15 | | | 35 | 11 | 164 | 51 | 119 | | | | | | 508 | |
| 16 | | | 39 | 27 | 158 | 45 | | | 135 | | | | | |
| 17 | | | | | | 36 | 119 | 30 | 130 | 69 | 188 | | | |
| 18 | | | | | 49 | 47 | 139 | 42 | 57 | 73 | 200 | 340 | 228 | 1201 |
| 19 | | | | | | | | | | | | | | |
| 20 | | | | | 103 | 38 | 66 | 62 | 146 | 74 | 94 | | 558 | |
| 21 | | | | | | | | | | | | | | |
| 22 | | | | | | | | | 137 | 93 | 84 | 277 | 692 | 1343 |
| Bonus Drill Hole 1 | 24 | | 53 | 75 | 93 | 58 | 141 | 13 | 151 | 76 | 154 | 334 | 314 | 759 |
| Pan Am 1 | | | | | | | 130 | | 158 | 88 | 181 | 226 | 478 | 991 |
| **Average Thickness** | 24 | 90 | 45 | 57 | 112 | 51 | 121 | 51 | 125 | 77 | 150 | 281 | 430 | 1073 |

Middle to Upper Jurassic

In addition to the observations I have made in the section, Lee Fairchild (ExxonMobil, written comm., 2002) measured a detailed stratigraphic section of the Summerville Formation, the Morrison Formation and the lower Mancos Shale along the Little Grand Wash fault (Fig. 8).

The Summerville Formation represents fluvial deposition. Mudstone and siltstone, and sporadic channel-point bar deposits are preserved as sandstone interbeds. Coarsening upward channel deposits across floodplain and lacustrine mud are recorded by the thicker cross-stratified sandstone beds near the top of the Summerville (Peterson, 1988). At the surface, the Summerville weathers out in laminated red slopes with the contrasting sandstones of the Salt Wash cliffs above them. The average thickness of the Summerville is 45 m (Table 2) and the change in thickness is 35 to 53 m (Fig.7).

The Jurassic Morrison Formation covers much of the Colorado Plateau and is divided into up to seven members in eastern Colorado and locations in Utah (Peterson and Turner-Peterson, 1989). Two of those members crop out in the field area: the lower Salt Wash Member, and the upper Brushy Basin Member.

The Salt Wash Member is described as consisting of cliff-forming lenticular, cross-bedded, channel-fill sandstone and conglomeratic sandstone interbedded with reddish-brown to grayish and purple laminated mudstone (Doelling, 1975; Petersen and Roylance, 1982; Peterson, 1988; O'Sullivan, 1992). In the field area, the Salt Wash Member consists of 0.5- to 4-m-thick, white, cross-stratified sandstone beds divided by

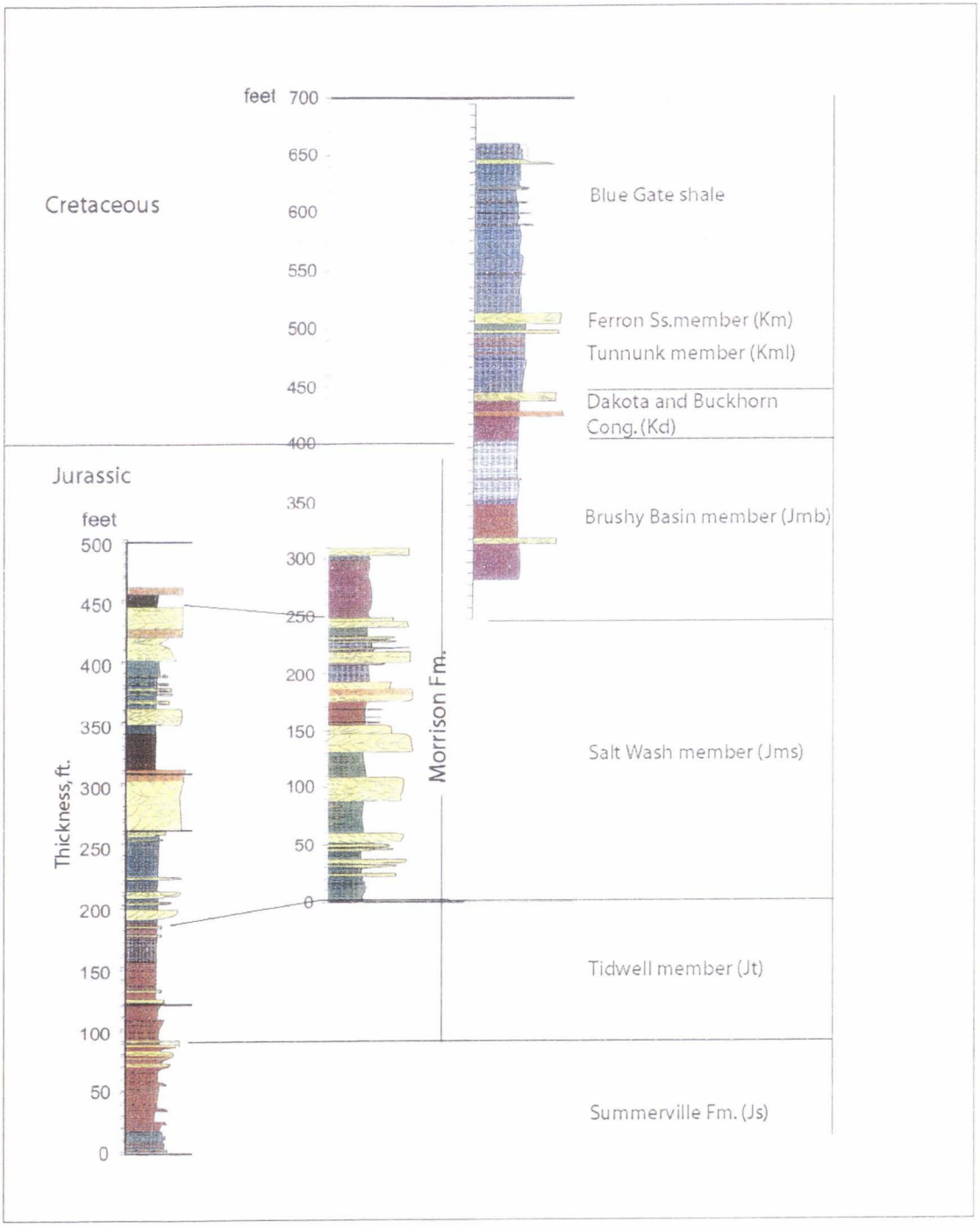


Figure 8 The formations and ages of the rocks cut by the Little Grand Wash fault. These three stratigraphic columns are interpreted from three of the shallow wells ExxonMobil drilled near the Little Grand Wash fault. ExxonMobil used well logs and conventional core samples to add to the interpretations. Formation names have been added from this study (modified from ExxonMobil, written comm., 2002).

red and white mudstone and green siltstone layers less than 0.5 m thick. The mudstone layers pinch out within 3 to 5 m. This member thins and thickens irregularly (40 to 90 m, Fig. 7) and is sometimes difficult to separate from the other members exposed in the field.

The Brushy Basin member represents changing environments, as the braided streams of the Salt Wash were gradually replaced by migrating fluvial channel sandstone and conglomerate and increasing floodplain and lacustrine mudstone (Johnson, 1988; Peterson, 1988). Johnson believes the fluvial systems changed from bed-load to mixed- and suspended-load channels when large amounts of volcanic ash covered the river's headwaters in the western and southern highlands. The volcanic ash was reworked and redeposited as floodplain mudstone more than 90 m thick.

Cretaceous

The younger Cretaceous Cedar Mountain Formation is divided into two members in the field area—a basal unit named the Buckhorn Conglomerate and the upper shale. The Buckhorn Conglomerate is discontinuously exposed and rests disconformably on the Brushy Basin. It is comprised of gray, black, and tan chert, and quartzite pebbles and cobbles (Trimble and Doelling, 1978). It has abundant petrified logs and branches that are completely silicified. The shale member is similar to the Brushy Basin Member of the Morrison Formation, but its colors are more faded (Trimble and Doelling, 1978).

The Cretaceous Mancos Shale has five members, but has previously been separated in this area into three members; the Tununk and Ferron Members, and above

them a thick indivisible unit mapped as upper Mancos Shale (Trimble and Doelling, 1978).

The Tununk is blue-gray marine shale with occasional thin sandy limestone beds. Near the middle of the member, a conspicuous zone of sandy, fossiliferous, limestone outcrops. The Ferron Sandstone Member is a thin unit of tan, fine-grained, thin-bedded, fossiliferous sandstone interbedded with gray shale. The contact between the Ferron and upper Mancos is placed where the thin sandstones give way to the blue-gray marine shales in the overlying unit (Trimble and Doelling, 1978). In this study, these three units were noted in the field and were mapped as undivided Cretaceous Mancos Shale.

## Little Grand Wash Fault

The Little Grand Wash fault zone is on the Colorado Plateau of southern Utah, approximately 5 km south of Green River (Fig. 1). The fault is located on the north-plunging part of the broad Cane Creek-Big Flat salt anticline (Campbell and Baer, 1978). The Little Grand Wash fault is an arcuate, high-angle normal fault downthrown to the south (Campbell and Baer, 1978). Campbell and Bear (1978) report a total displacement of 290 m near the Green River that is accommodated by two primary slip surfaces. Previous studies disagree on the surface trace length of these slip surfaces and the surface trace length of the entire fault. This work has better constrained these lengths.

Active and inactive carbonate spring deposits are localized along a 2.4-km-long section at the center of the fault (Baer and Rigby, 1978; Campbell and Baer, 1978; Doelling, 1994). An active $CO_2$ charged geyser erupted from an abandoned exploration

well (Glen Ruby et al. no 1-X well drilled in 1935) approximately every 4 to 6 hours in the 1940's to 1960's (Baer and Rigby, 1978), but the eruptions are every 11 to 14 hours today (Fig. 9). An oil seep has been previously mapped east of the geyser (McKnight, 1940), and surface oil seepage, approximately in the same area, was also reported by Hager (1956). This seep is still observed today. The mineral deposits, oil seep, and geyser are near a zone where the fault consists of two major fault strands. The strands merge together to the east and to the west (McKnight, 1940), but surface separation and the length of the two strands are poorly understood. The mapping in this study helps to better understand the architecture of the faults.

## Salt Wash Fault

The Salt Wash fault system is 15 km south of the Little Grand Wash fault in the Colorado Plateau of southern Utah (Fig. 1). The Salt Wash faults also cut the north-plunging part of the broad Cane Creek-Big Flat salt anticline (Campbell and Baer, 1978). The system forms a graben and has a straight N 70° W trace with an average width of 731 m (McKnight, 1940). Two primary, parallel normal faults define the northern and southern boundaries of the Salt Wash Graben. The maximum displacements have been estimated to be approximately 320 m on the north fault and 244 m on the south fault (McKnight, 1940). From the Green River in the west to the Ten Mile Graben in the east, the surface trace length was reported by McKnight (1940) to be approximately 16 km, but this study shows an approximate length of 23 km.

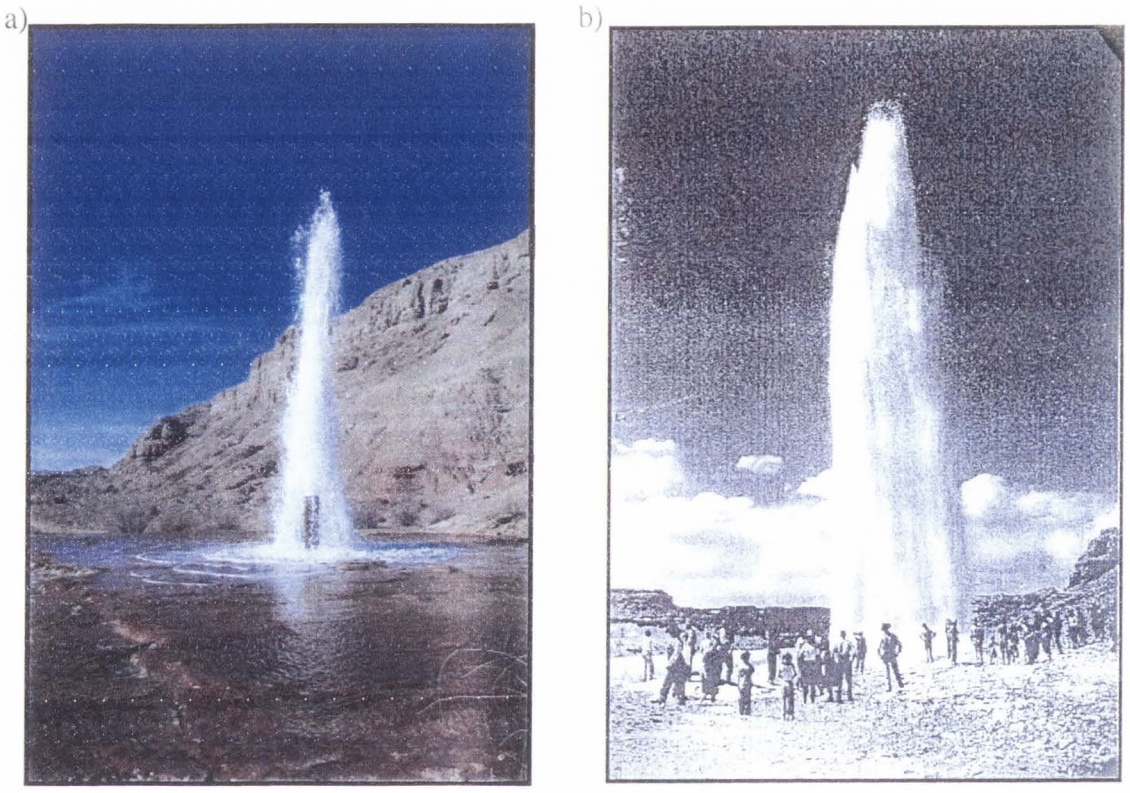


Figure 9 The Crystal Geyser (Glen Ruby et al. no 1-X well drilled in 1935). a) An eruption from the Crystal Geyser in 2000 (casing shown is 1.5 m). b) Past eruption from the Crystal Geyser. Date of photo uncertain; (possibly taken 1950's-1960's). Photo obtained by D. Martindale. The UTM coordinates are northing 575001, easting 4310087.

As with the Little Grand Wash fault, large active springs and inactive calcite deposits are found here, near the center of the north strand of the graben. Uncapped, abandoned boreholes allow water to flow freely to the surface, releasing $CO_2$ gas and depositing calcite. The Ten Mile $CO_2$-charged geyser erupts from an abandoned exploration well (Fig. 10).

## Ten Mile Graben

The Ten Mile Graben is east of the Salt Wash Graben and is defined by two parallel normal faults (Fig. 1). The maximum displacement was previously believed to be 244 m on the north fault and 214 m on the south fault (McKnight, 1940). Early studies by McKnight (1940) reported the width of the graben to be 244 m in the west and1.1 km in the east. The Ten Mile Graben has a surface trace length of approximately 11 km. (McKnight, 1940). The strand associated with the south strand of the graben may be the northern extension of the Moab fault (McKnight, 1940) (Fig. 1).


Figure 10 The Ten Mile Geyser located in the central section of the Salt Wash fault system approximately 100 m west of the north fault trace. The UTM coordinates are northing 578105, easting 4302058.

# METHOD OF STUDY

Previous mapping of this field area was conducted by McKnight (1940) at 1:62,500 and Doelling (2001) 1:100,000. Although the scale of this mapping was useful and greatly appreciated, it is not adequate for the objectives of this study. With the aid of this mapping and the use of formation descriptions previously described (Trimble and Doelling, 1978), detailed mapping in various locations was conducted in this study. Geological mapping at scales of 1:6,000 and 1:24,000 was done on Mylar topographic maps. In addition, a fly-over, at an altitude of approximately 200 m above the surface, was used to constrain areas of leakage and to take oblique air photos. Air photos, oblique air photos and orthoquads with were used as base maps. These photos were used to determine specific locations in the field area that would yield the best results for the objectives of this study. This fly-over revealed well-exposed fault regions, the locations of tufa/travertine and veins, spring locations, and zones of bleaching.

The geology of these locations was mapped in the field along with detailed outcrop- scale descriptions. Descriptions of the fault zone characteristics included the following: orientations, dips, and slickenlines of the major fault strands; fracture density at and near the fault zones; the presence of clay gouge, mineralization, bleached zones, rocks cut by the fault, and altered bedding orientation. Carbonate deposits in the area were studied and are briefly described in this thesis. Further description of these deposits can be found in Dockrill et al. (in review). Springs associated with the deposits were located and the geologic setting described. Heath (2004) sampled and studied these spring waters to determine their origin.

Unit descriptions and the location of the formation boundaries were guided by

the use of previous formation descriptions (Trimble and Doelling, 1978). Formation thicknesses were determined by compiling available well log data for wells drilled in the field area (Table 1). Formations found in the area and the thicknesses of these formations were used for a lithologic column of the area.

Using the maps, formation types, and lithology column, cross sections for the Little Grand Wash fault and the Salt Wash fault were compiled. A conceptual block diagram of a complex step-over zone from the Salt Wash Graben to the Ten Mile Graben was also constructed. Utilizing the lithology and the cross-sectional data, and mapping, a 3-D flow model was generated to determine the general geometry of the water, gas, and/or oil reservoirs that underlie the area.

A handheld GPS unit was used to record geologic data digitally. As the faults were mapped, orientation data on the faults and their associated calcite deposits were recorded. Digital mapping of this type confirmed fault orientations for the Little Grand Wash fault, the Salt Wash fault and the step-over zone in the Ten Mile Graben. The GPS data also confirmed sample locations, springs, wells, and access roads, strike and dip data in the study area, and vein orientations and locations.

Digital Elevation Models (DEM's) for this study were downloaded from the Utah Automated Geographic Reference Center database (Utah AGRC, 2002). These were reclassified into UNIX-compatible files. After conversion, they were copied into a directory and imported to ArcView as grid data sources. Orthoquads were downloaded from the AGRC and added to ArcView as image data sources. GPS fault and geology data collected in the field were downloaded in Pathfinder and then differentially corrected. Any discrepancies in the data sets were then addressed and corrected. These

data were converted into shape files with attribute tables. Shape files with similar attribute tables were combined and then exported as DBF files. These files can be opened in Excel and imported into StereoWin. These shape files, with associated attribute tables, provide an excellent digital database to store information that aids in the interpretation and analysis of the Little Grand Wash fault, the Salt Wash fault and the Ten Mile Graben.

## Seismic Data

ExxonMobil (P. Vrolijk, written comm., 2001, 2002) conducted a detailed two- and three-dimensional seismic survey across the Little Grand Wash fault in order to test seismic reflection methods that might yield detailed information regarding the thickness and nature of the fault zone, including tests for identifying fluid pathways. Data provided for this study included figures that summarized their 2D and 3D surveys and processed data; no data were processed for this study. The study consisted of a vertical seismic profile (VSP) conducted in one borehole, a high-resolution 2D reflection line to test their acquisition parameters, and a 3D survey that was designed from the VSP model and ray tracing. The examined area is in the eastern part of the region mapped, and consisted of an area ~200 m long as measured in a line bearing 020°, and ~240 m measured at ~290°. Fifteen lines of data were acquired along the north-south trend, and the northern edge of the data lies ~5 m south of the surface trace of the fault. A sledge hammer was used for the seismic source.

## Geochronology

Geochronology of faults was examined with two methods. The first method was again provided for this study by ExxonMobil. Direct dating of the clay in the fault gouge was done with $^{40}Ar/^{39}Ar$ methods outlined in van der Pluijm et al. (2001), Pevear et al. (1998) and Dong et al. (1995). This technique reduces the problems of Argon recoil and contamination by analyzing different clay-size grains separated in encapsulated sample holders (van der Pluijm et al., 2001). Quantitative x-ray diffraction of the clay-grain size populations is performed, and a ratio of authigenic and detrital clays is determined for each size fraction. Each grain size fraction is then analyzed, and combined with the percentage of detrital clay in each fraction. The end-member ages (all authigenic and all detrital) are thus constrained. The data presented here were provided by Exxon Mobil.

The second method used to date the faults is uranium series dating. This method is based on the fact that in U-bearing water, no thorium is transported, and thus during deposition, carbonates will contain $^{238}U$ and $^{234}U$, but no $^{230}Th$. With time, $^{238}U$ decays to $^{234}U$, which also decays to $^{230}Th$, and the $^{234}U$ and $^{230}Th$ are in equilibrium with $^{238}U$. The build up of $^{230}Th$ is used determine $^{230}Th$ /$^{234}U$ values, which can then be used to estimate ages if the carbonates are less than 250,000-300,000 years old. As of this writing, samples are still being analyzed by E. Dixon (Los Alamos National Lab). These methods help constrain the history of faulting during basin evolution ($^{40}Ar/^{39}Ar$) and the timing of travertine and tufa deposition ($^{230}Th$ /$^{234}U$).

Using the previous mapping (McKnight, 1940; Doelling, 2001) and the detailed mapping of this study, the areas of fault zone leakage can be studied to help answer the questions why and where leakage might occur at the surface, and where it has occurred in

the past. In addition, it can help determine what is leaking. Seismic and well log subsurface data can assist in answering these questions and help constrain where the fluids are coming from. This type of data analysis can also tease out the subsurface fault architecture and geometry of the aquifers cut by the faults. These data, coupled with geochronological data, can determine the rate at which the leakage is occurring.

# RESULTS

## Lithology

Permian, Triassic, Jurassic, and some Cretaceous formations are cut by the faults. They are comprised of mudstone and siltstone, lenticular cross-bedded channel-fill sandstone, and conglomeratic sandstone interbedded with reddish-brown to grayish and purple laminated mudstone (Fig. 7) (Doelling, 1975; Petersen and Roylance, 1982; Peterson, 1988; O'Sullivan, 1992). The thickness of the units in the field area, (seen in Fig. 7) was determined in this study by compiling all the available well logs that were drilled throughout the region (Table 1); their locations can be seen on Figure 11 and in Table 1. There are inconsistencies in thickness of up to 110 m compared to the results of Trimble and Doellings (1978) west of the field area (Table 2). These can be seen in the stratigraphic column of the area (Fig. 7).

## Regional Structures

Mapping at 1:24,000 is compiled in Figure 12. Mapping at 1:6,000 was completed in specific areas of the study area and will be discussed later in this thesis. This study confirms the following: 1) the 1:24,000 map-scale structures show that the Little Grand Wash fault is an arcuate normal fault; 2) the Salt Wash fault system forms a graben; its east end steps to the north and continues in the same orientation, becoming the fault system of the Ten Mile graben, which fault may be linked to the Moab fault farther southeast of the field area (Fig. 12); 3) the Cane Creek Anticline is cut by the Little Grand Wash fault and the Salt Wash fault system.

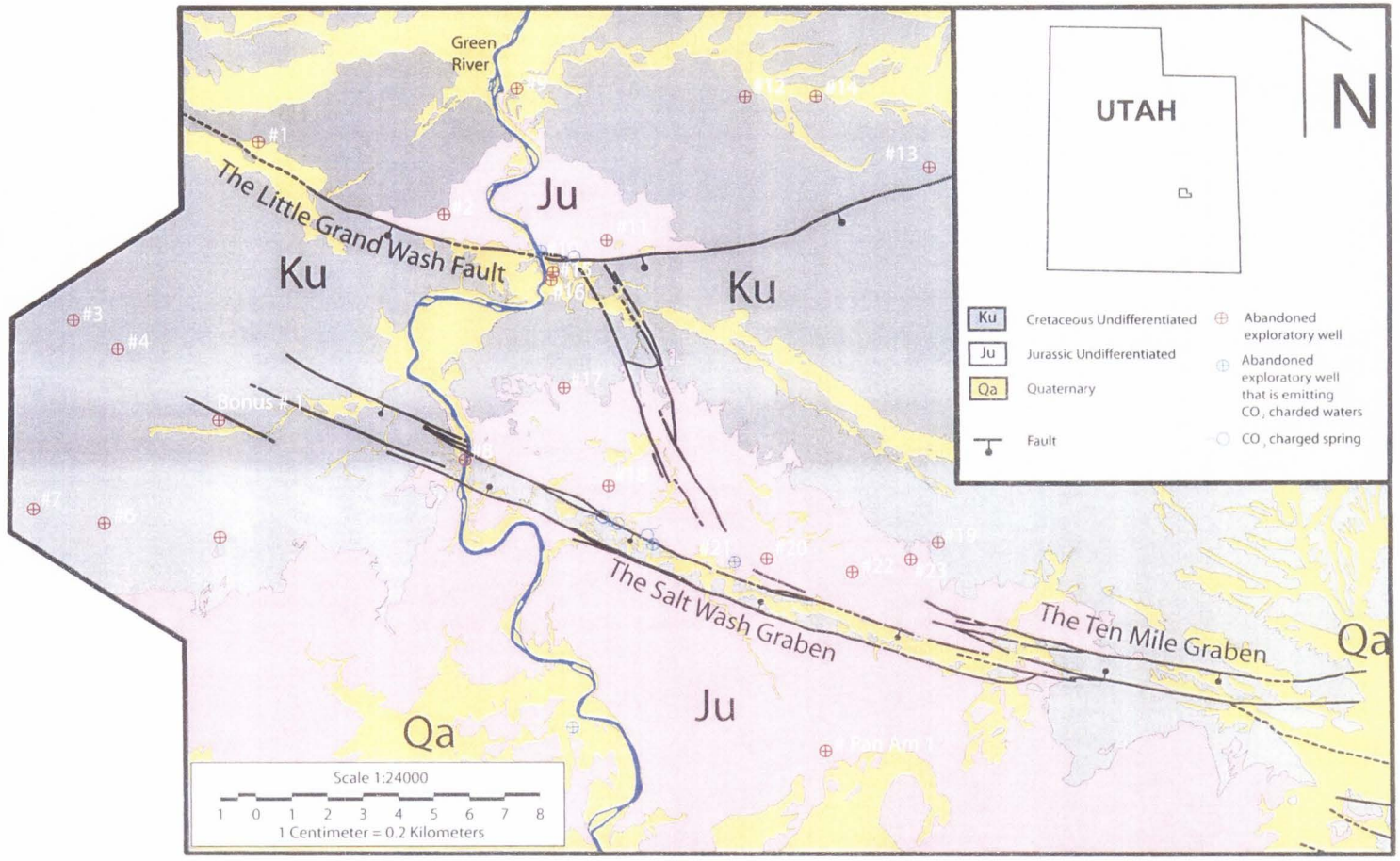


Figure 11. Regional geologic map showing the abandoned exploratory wells, abandoned exploratory wells emitting $CO_2$-charged waters, and $CO_2$-charged springs. Well numbers correspond with the numbers on Tables 1, 2, and 3.

a)

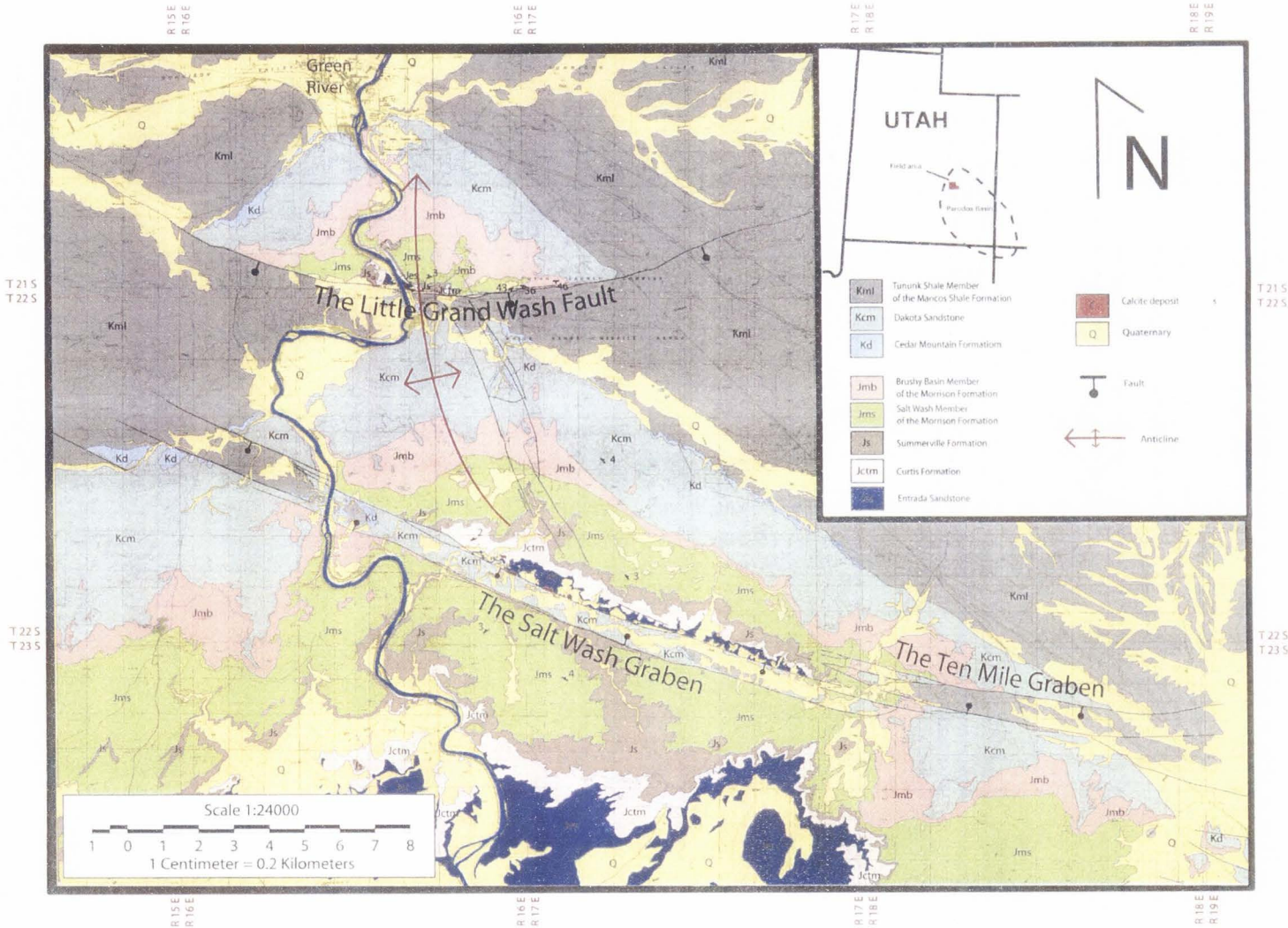


Figure 12. Compiled 1:24,000-scale geologic map of the field area.

b)

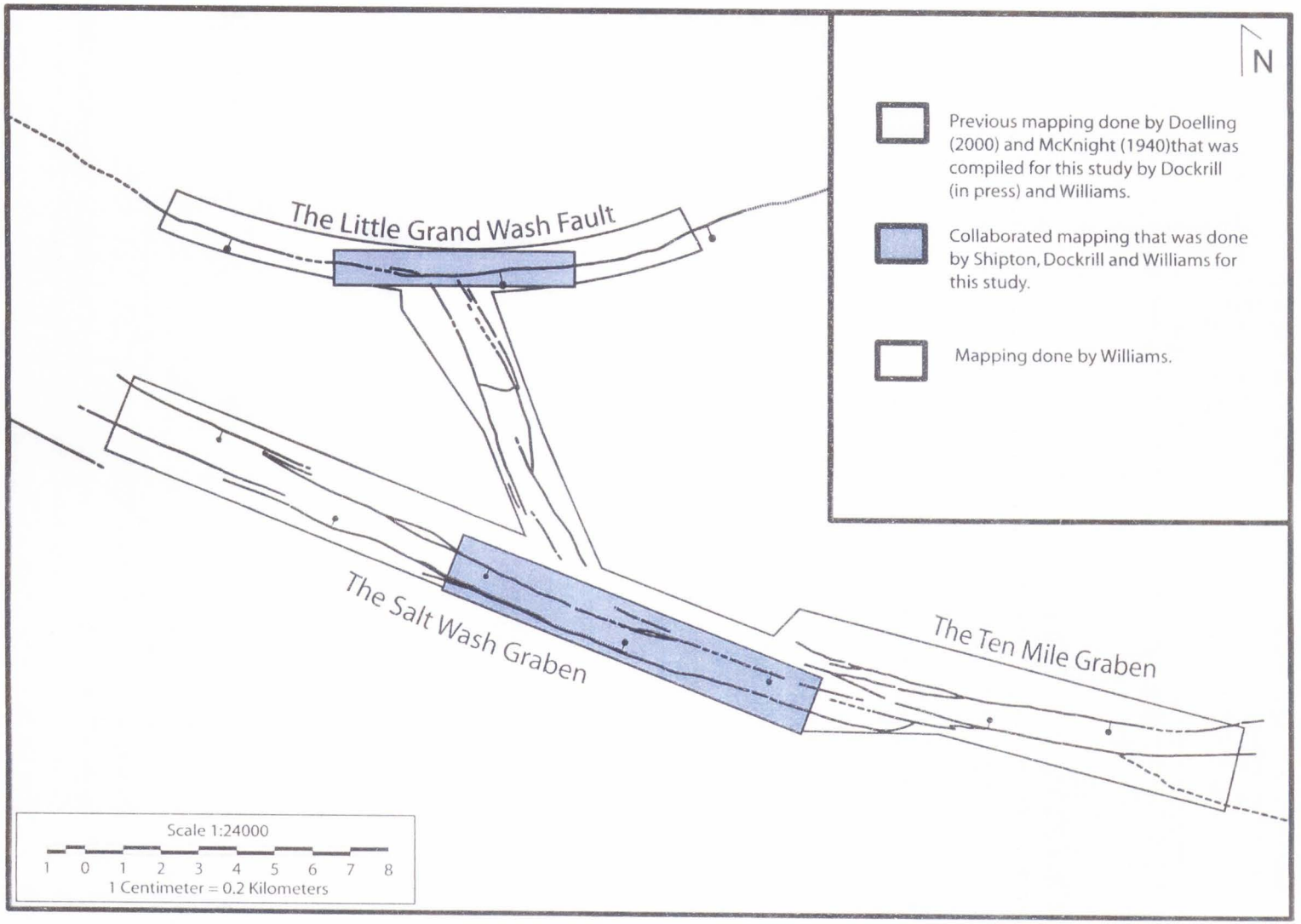


Figure 12 Continued.

# Little Grand Wash Fault

## Structures related to the Little Grand Wash fault

The Little Grand Wash fault has a clear surface expression of 24 km in the field area (Fig. 12). The fault strikes 108° in the west section, 075° in the east section, and 091° near the center. The dip along the major fault strand varies from 78° to 88° S (Fig. 13). This indicates that the Little Grand Wash fault is an arcuate, south-dipping normal fault. Well logs show this steeply-dipping normal fault displaces Pennsylvanian rocks that are at least 1 km deep and has a maximum vertical separation of 260 m. Air photos, oblique air photos, and field investigations showed that the central region of the fault, near the Crystal Geyser (Glen Ruby et al. no 1-X well drilled in 1935), is an excellent area to do detailed mapping at 1:6,000 (Fig. 14) and outcrop-scale analysis. It is in this central region that this study concentrates its efforts along the Little Grand Wash fault.

The slip is accommodated along several slip surfaces in many locations along the fault. Most of these surfaces account for small amounts of slip. The majority of the slip is accommodated along one fault that bifurcates into two major slip surfaces in at least three locations. Two of these areas offset the Jurassic Morrison members along the north fault, and the Jurassic Morrison Brushy Basin Member against the Cretaceous Mancos Shale along the south fault, and will be discussed in more detail in this section. The third area offsets the Jurassic Morrison and the Cretaceous Dakota Sandstone along the north fault, and offsets the Cretaceous Dakota Sandstone against the Cretaceous Mancos Shale along the south fault (Fig. 14).

In this central region of the Little Grand Wash fault, a variety of locations with fault-related structures are present, including rotated bedding, localized small-scale

folding, small-displacement synthetic faults, fractures, and calcite deposits (Fig. 15). Two of the best-exposed locations will be described in this section. It is also important to note rotated bedding is seen almost everywhere the faults are exposed. This rotation can be substantial near both major fault strands and some subsidiary faults (Fig. 15 a). The dip of the beds decreases farther away from the fault trace. This rotation is illustrated in the Figure 15 and will be discussed later.

Little Grand Wash outcrop location one

In the eastern section of the central region of the Little Grand Wash fault, there are at least five slip surfaces expressed in the Salt Wash Member of the Jurassic Morrison Formation seen on Figure 14. These surfaces have small offsets (2 cm to1.3 m), dip steeply to the south, and appear to be subsidiary faults associated with the two major fault strands in this section. At this location, the majority of the stratigraphic separation on the Little Grand Wash fault is accomodated by these two major sub-parallel strands (Fig 16). The north fault strand juxtaposes the Jurassic Morrison Salt Wash Member in the footwall against the Morrison Brushy Basin Member in the hanging wall. The Salt Wash cliff-forming sandstone resists weathering, and the interbedded mudstone underlying it is cut by the north fault (Fig. 17 a and c). Along the south fault, the Brushy Basin Member is juxtaposed against the Cretaceous Tununk Member of the Mancos Shale. The laminated mudstones of the Salt Wash Member and the shales of the Brushy Basin and Mancos cut by the faults are extremely weathered and poorly exposed. Trenching, done

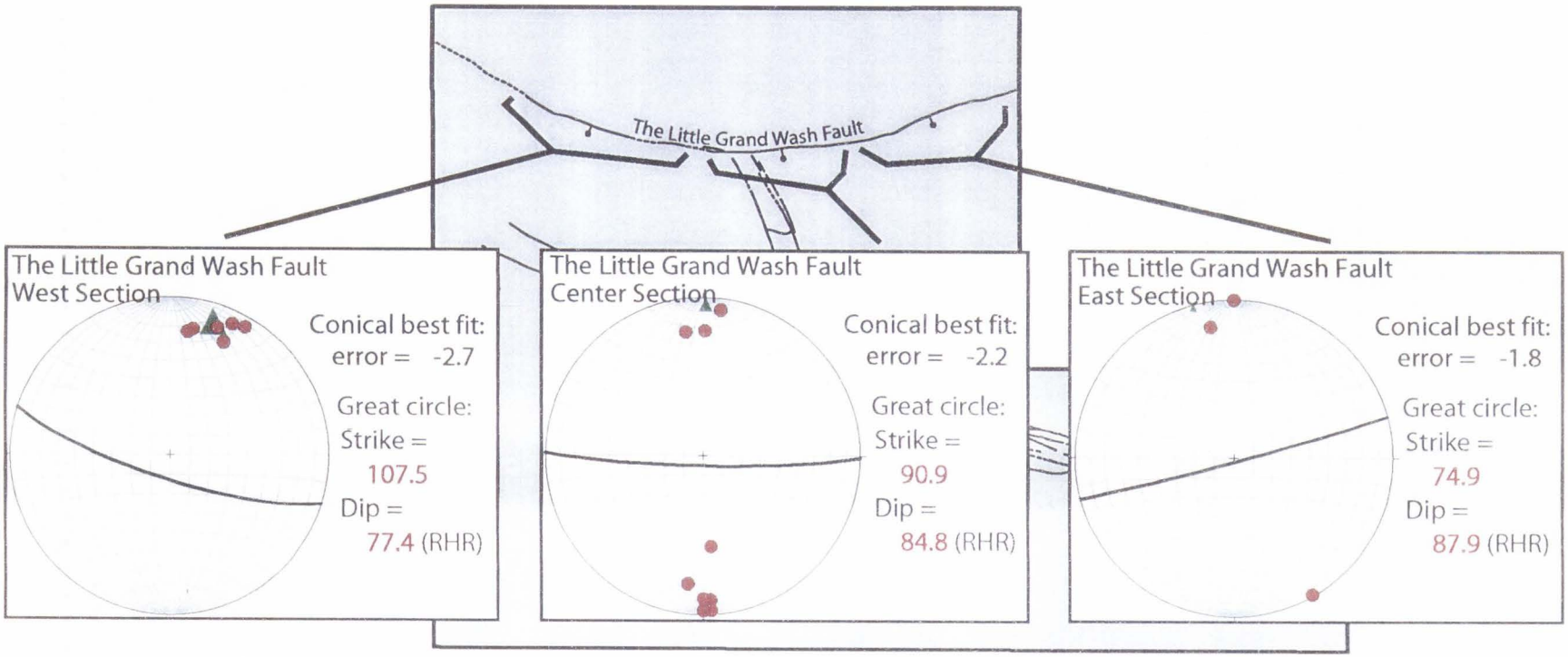


Figure 13 Stereograms compiled from fault data showing fault strike and dip in different sections along the Little Grand Wash fault.

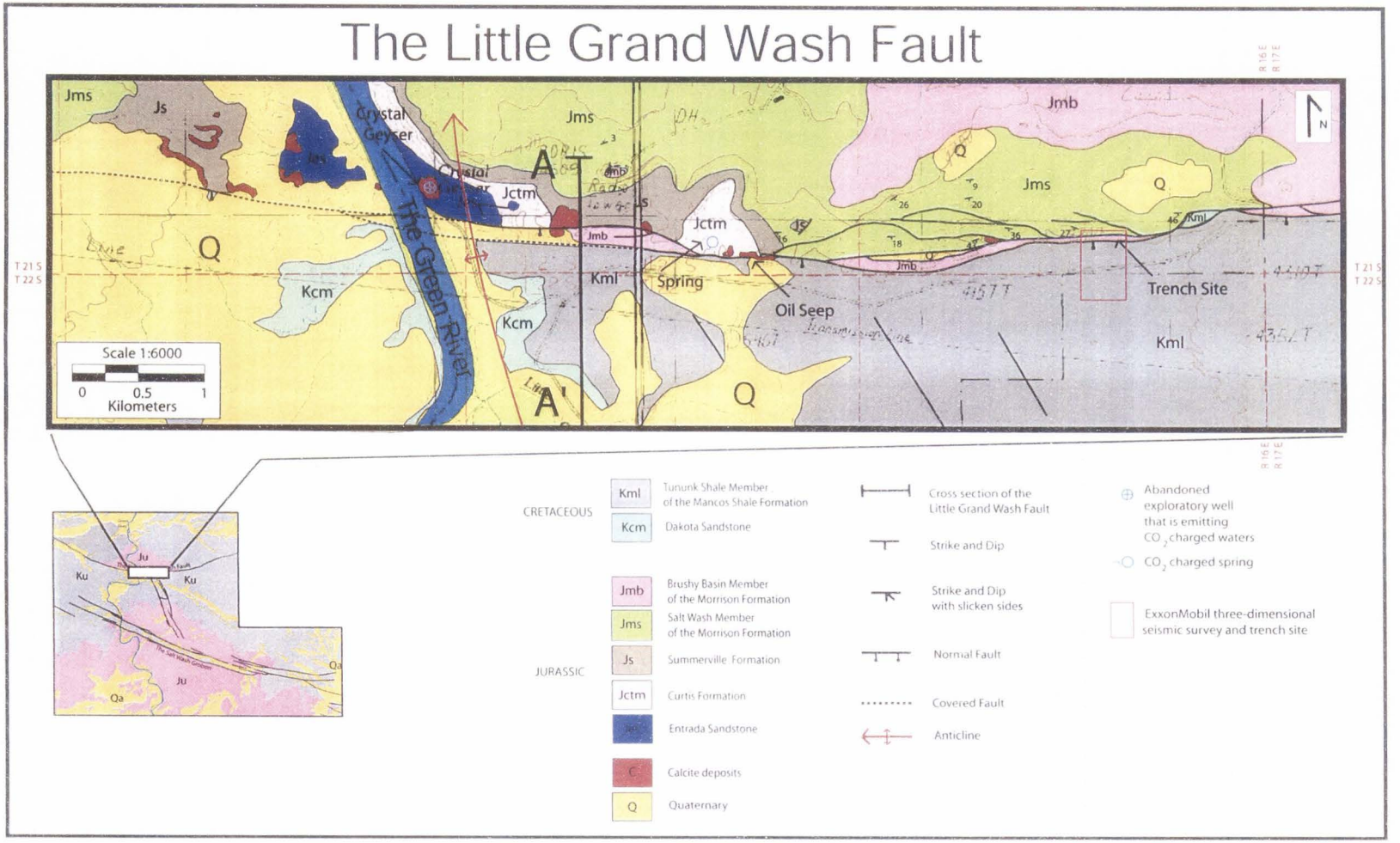


Figure 14 A detailed geologic map showing the central region of the Little Grand Wash fault.

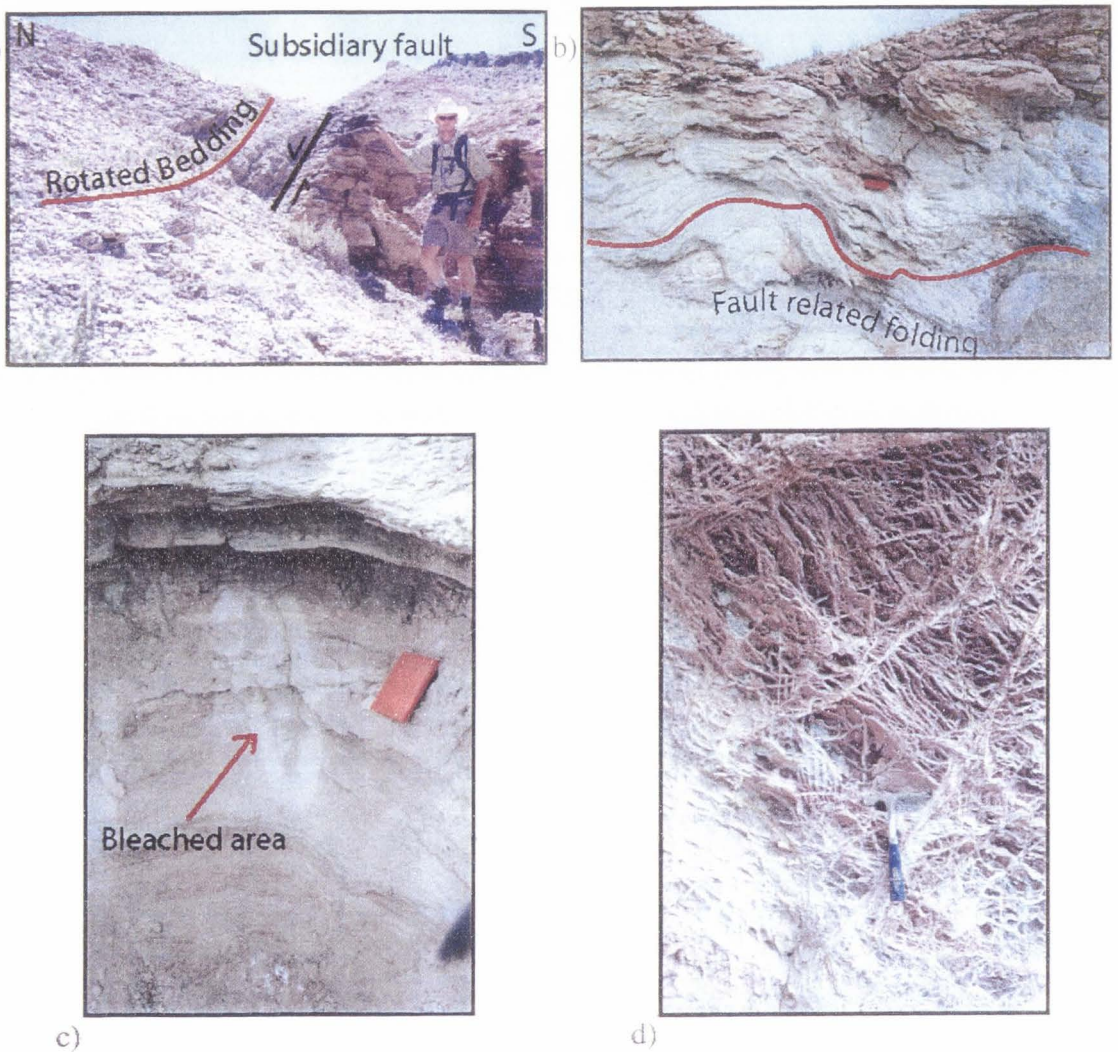


Figure 15 Structures seen in the Little Grand Wash fault zone. a) Looking to the east at rotated beds associated with an antithetic subsidiary fault located in the fault damage zone. b) Bleached host rock with small-scale folded beds in the damage zone, (field book for scale). c) Fault-related fracture with bleaching. d) Calcite veins that completely obliterate the host rock. e) Fracture or fault that was filled with calcite mineralization and then reactivated.

e)

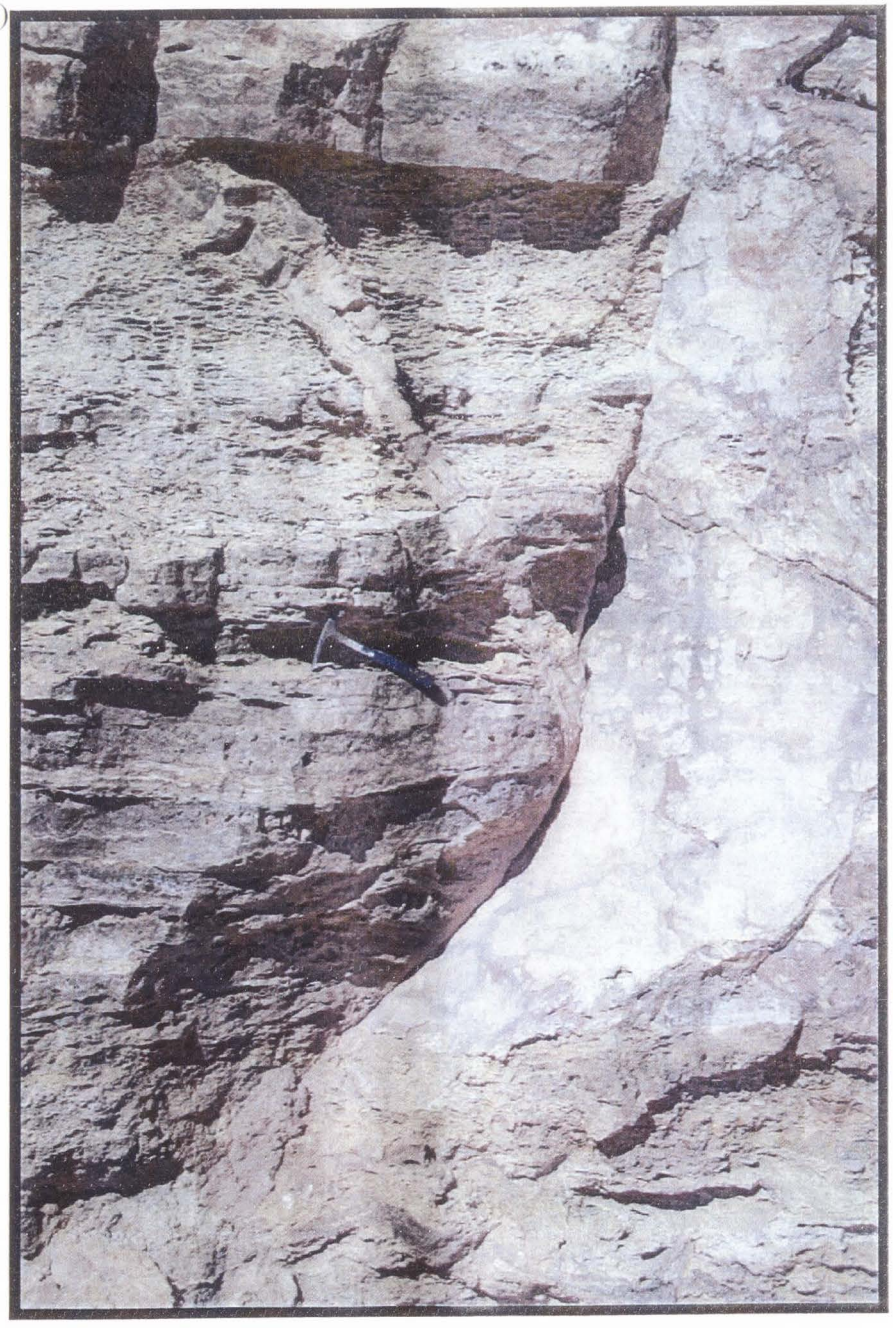

Figure 15 Continued.

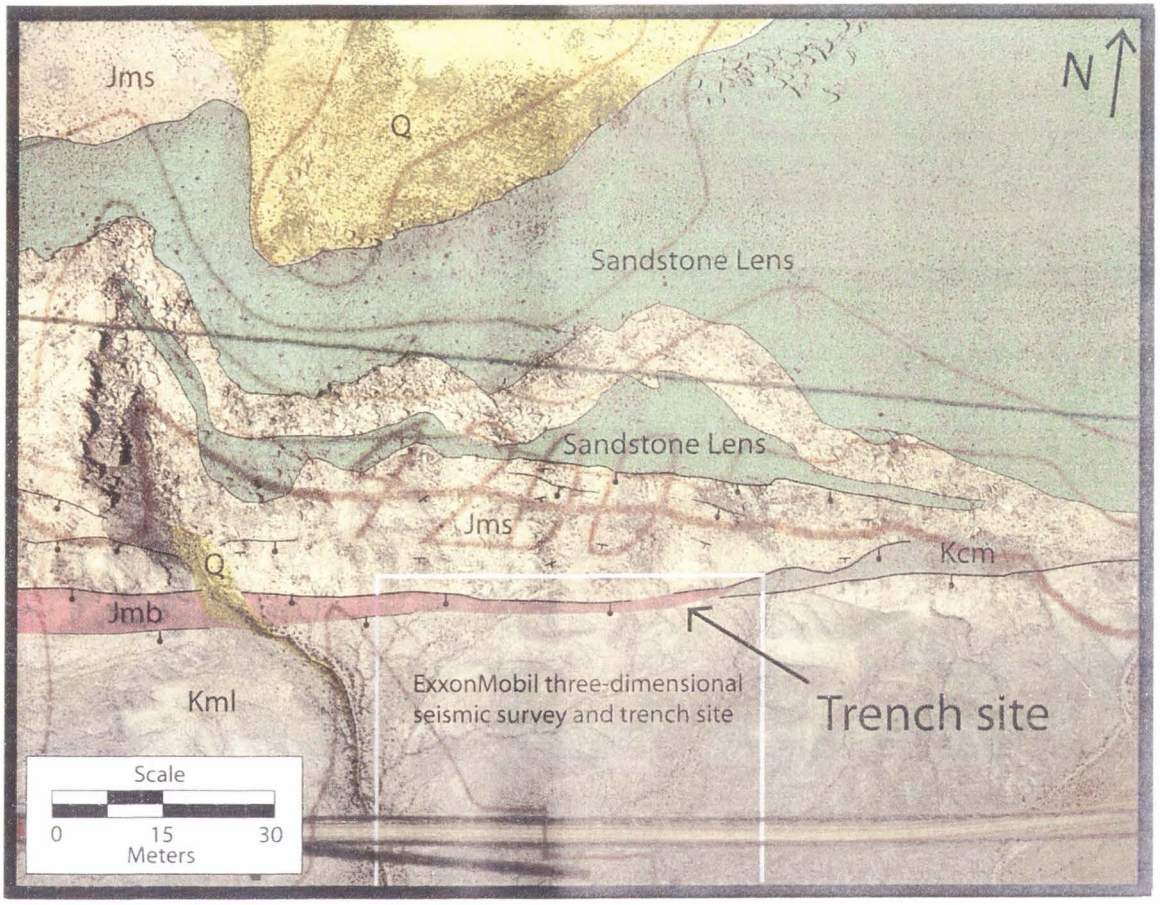


CRETACEOUS

Kml — Tununk Shale Member of the Mancos Shale Formation

Kcm — Dakota Sandstone

JURASSIC

Jmb — Brushy Basin Member of the Morrison Formation

Jms — Salt Wash Member of the Morrison Formation

Q — Quaternary

Strike and Dip

Strike and Dip with slicken sides

Normal Fault

Figure 16 Detailed map and air photo of the Little Grand Wash fault near the ExxonMobil trench site. Air photo is overlaid with rock types and topography lines that have 40-ft. intervals. The labeled sandstone lenses are within the Jms. Near the trench site, the north fault strand juxtaposes the Jurassic Morrison Salt Wash Member in the footwall against the Morrison Brushy Basin Member in the hanging wall. Along the south fault, the Brushy Basin Member is juxtaposed against the Cretaceous Tununk Member of the Mancos Shale and against the Salt Wash Member of the Morrison.

by ExxonMobil and cleared by this study, exposes a 2-m to 10-m-wide damage zone with a fault core that consists of fractured, extremely altered, poorly consolidated host rock. What appear to be slivers of members of the Morrison Formation have been dragged into the fault zone (Fig. 17 b and c). Interbedded sections of washed out, bleached sandstone (possibly the Salt Wash) are mixed with a clay-rich, purple-black, 5-cm to 20-cm-thick, foliated fault gouge that forms clay smear structures with a scaly shear fabric in a zone 10 to 15 cm thick (Fig. 17). Further detailed transects of the clay-rich fault core have been done by Dockrill et al. (in review.).

At this same location, ExxonMobil personnel (P. Vrojlijk, written comm., 2001, 2002) conducted a detailed two- and three-dimensional seismic survey across the Little Grand Wash fault in order to test seismic reflection methods that might yield detailed information regarding the thickness and nature of the fault zone, including tests for identifying fluid pathways. The location of the survey can be seen on Figures 14 and 16. A 2D trace of the data that has been processed and depth-migrated (Fig. 18) shows the near-surface structure of the hanging wall of the fault (P. Vrolijk, written comm., 2001, 2002). Formation tops picked in this study (Fig. 8) suggest prominent reflectors in the upper 70 m of the record are probably continuous beds within the Mancos Shale, and possibly the top of the Morrison Formation. Correlating the seismic data with the well data (Fig. 7; Fig. 8) suggests that reflectors at 200 to 210 m are in the base of the Morrison.

The fault at depth appears to be consistent with the surface expression mapped in this study and has two primary slip surfaces. This is shown in a 3D survey that was

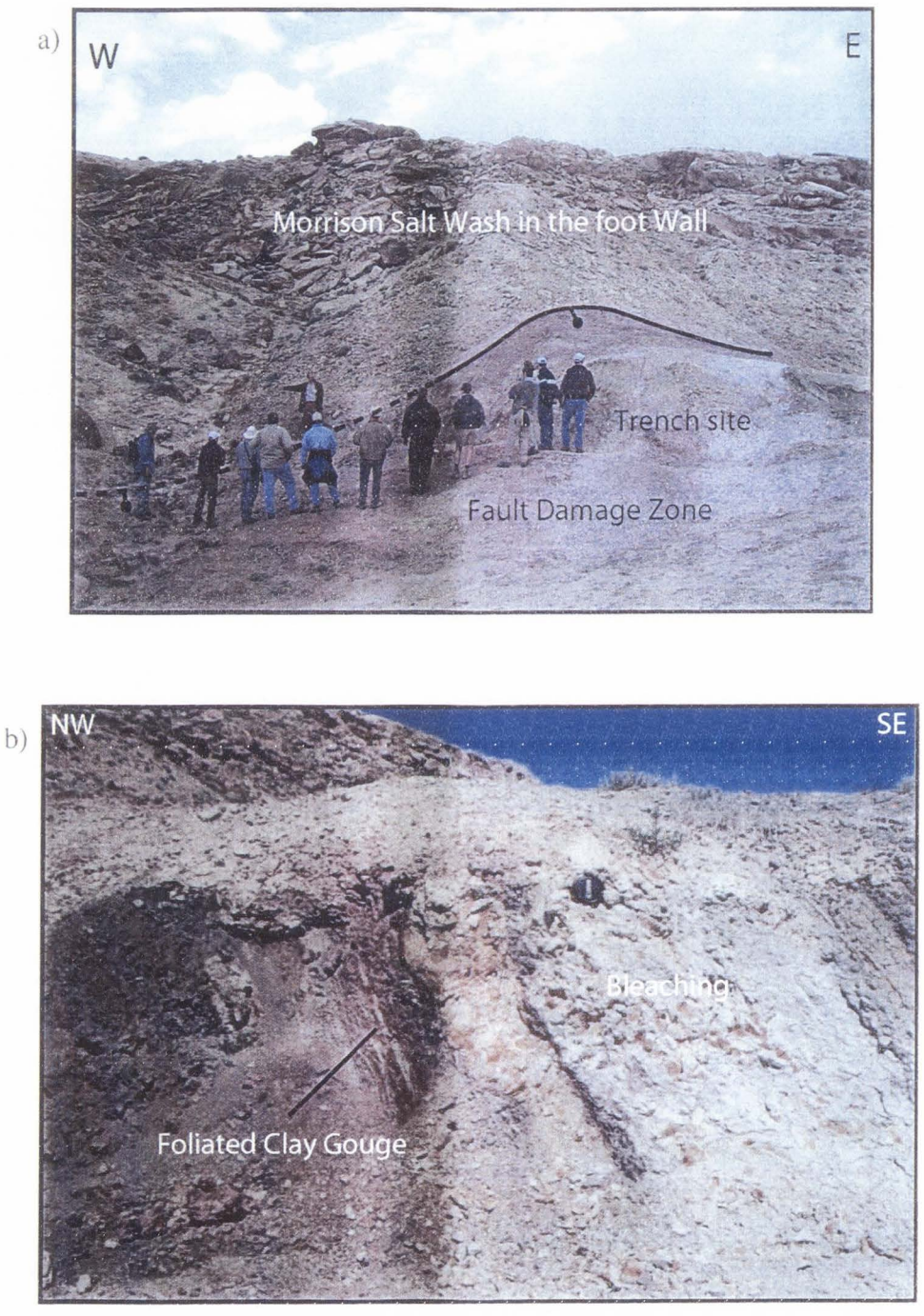


Figure 17 Trench site area (see Figure 16) of the Little Grand Wash fault. a) North viewing photograph showing the trench site across the Little Grand Wash fault damage zone. b) Sub-parallel fault gouge and bleached sandstone that has been dragged into the fault zone. c) Cartoon showing in cross section: 1) subsidiary faults associated with the two major fault strands, and 2) shallow beds of the Morrison steeply dipping near the major fault zone and in the fault damage zone between both faults.

c)

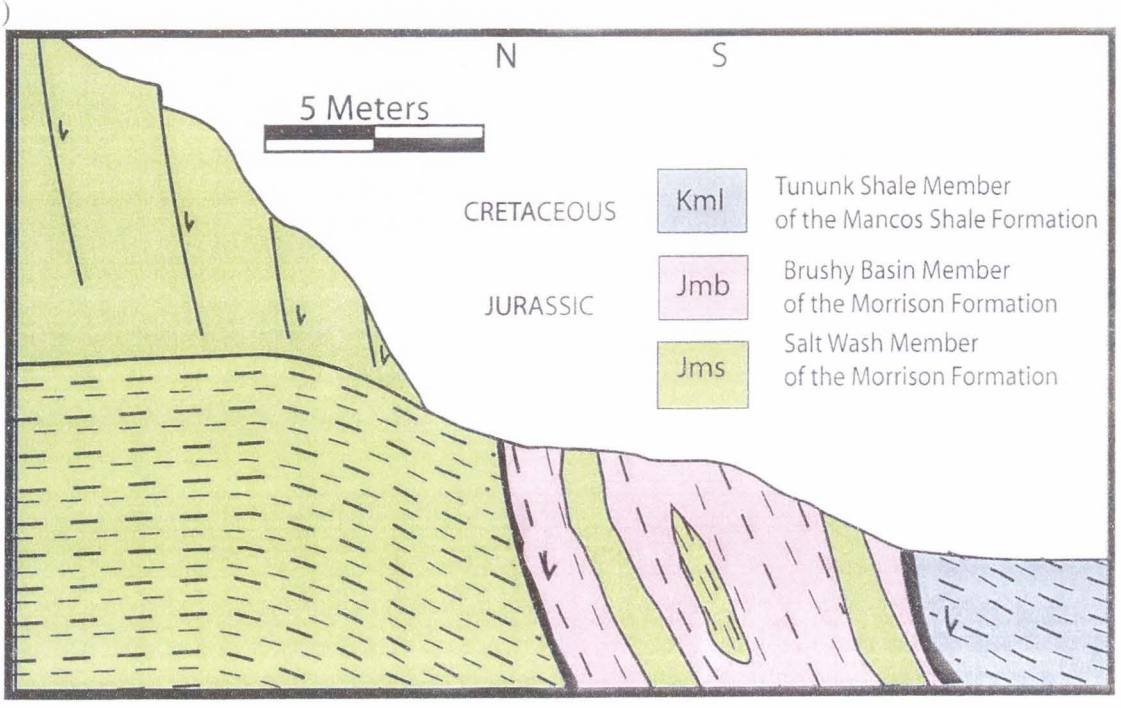


Figure 17 Continued.

designed from combining a vertical seismic profile (VSP) conducted in one borehole and a high-resolution 2D reflection to create a VSP model and ray tracing (Fig. 18).

Little Grand Wash outcrop location two

In the central region of the fault, near the Crystal Geyser (Glen Ruby et al. no 1-X well drilled in 1935), the slip of the fault is accommodated by two major sub-parallel strands. The surface separation of the two faults varies from 10 m, where the fault splays in the east, to 125 m in the west. This is illustrated in map view in Figure 14 near cross section line A to A' and in oblique air photos in Figure 19. The clay-rich members of the

a)

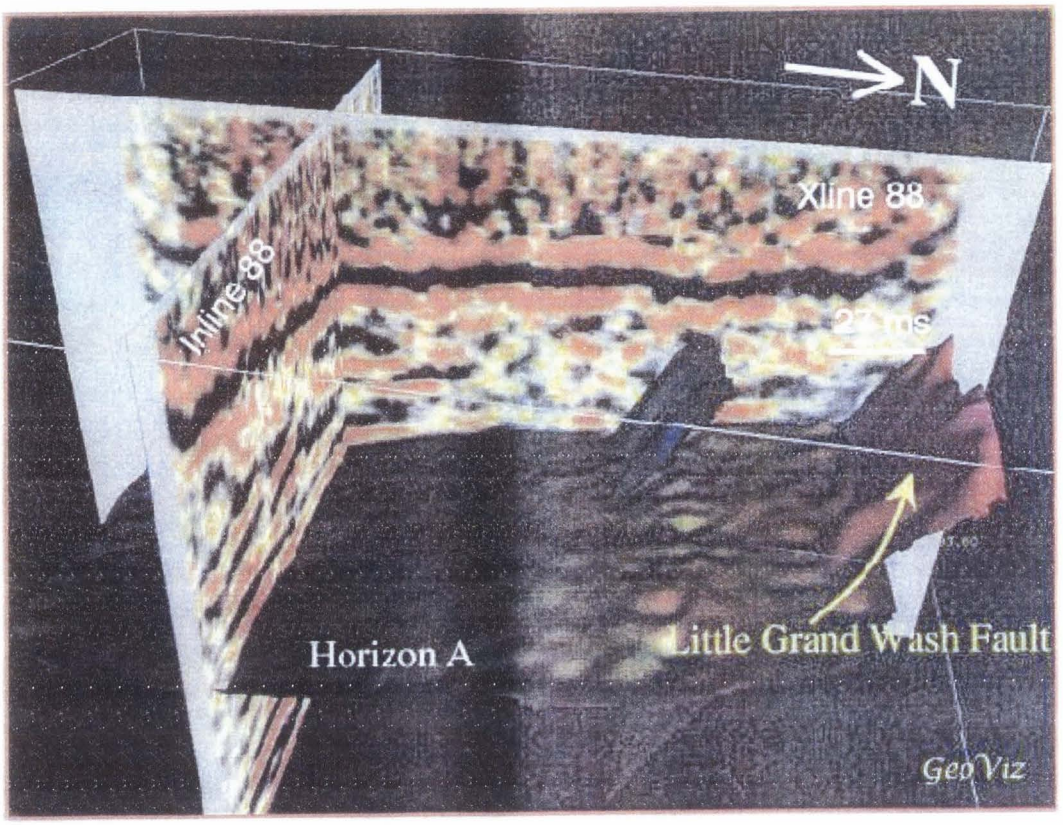


Figure 18 A detailed two- and three-dimensional seismic survey across the Little Grand Wash fault. The base of the Morrison is shown as horizon A. a) View of the Little Grand Wash fault looking west. b) View of the Little Grand Wash fault looking northwest. Gridding artifacts result in uncertain fault interpretation due to poor quality and lack of reflectors deeper in the section. c) View of the Little Grand Wash fault looking northeast.

Morrison Formation are very difficult to separate throughout the trace of the fault, in this section of the fault. The Jurassic Curtis Formation, Summerville Formation and Morrison Salt Wash and Brushy Basin Members are covered in many locations by a thin veneer of sandstone float from the Jurassic Morrison Salt Wash Member and the Cretaceous Dakota, and Cedar Mountain Formations (Fig. 19). Some of the larger

b)

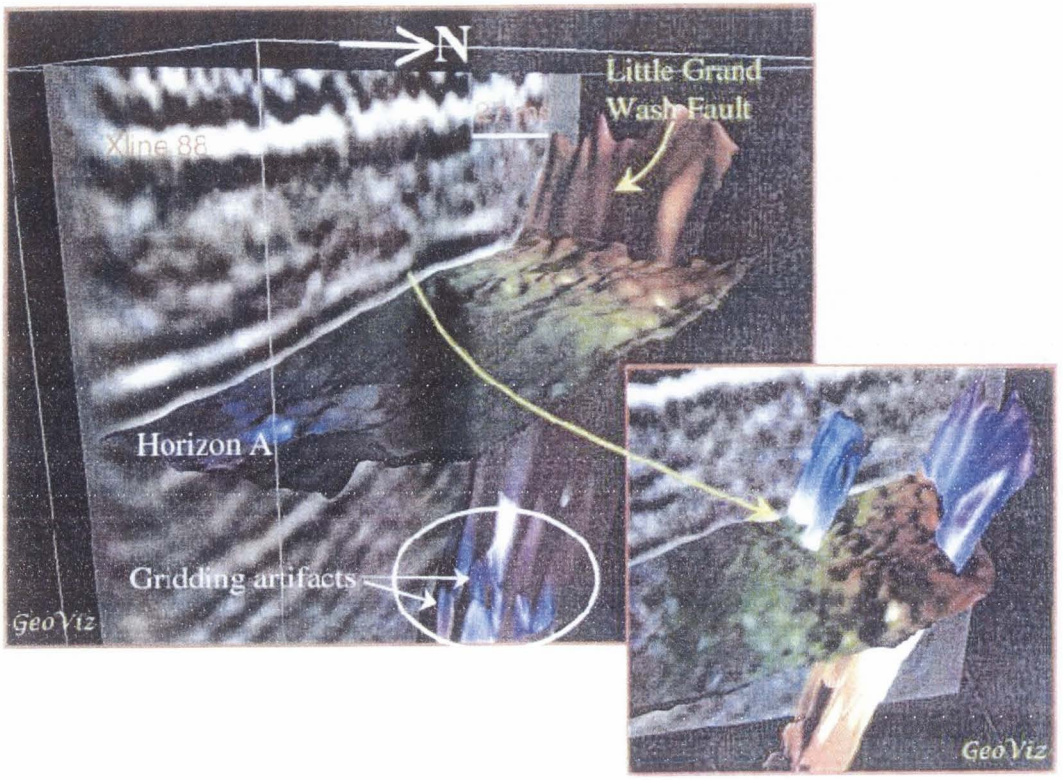


Figure 18 Continued.

sandstone outcrops, possibly discontinuous river channels in the Salt Wash, appear to be insitu, though highly altered by fractures and in many cases bleached from fluid migration. In some locations, these fractures can be seen in the clay-rich formations as well. The fractures increase in density the closer they are to a major fault strand. This pattern will be discussed later. The northern fault strand cuts gently north-dipping beds of the Jurassic Morrison Formation, and near its center, the Summerville Formation is in the footwall and juxtaposed against the Brushy Basin Member. The Brushy Basin clays are juxtaposed against the Cretaceous Tununk Member of the Mancos Shale along the same section of the south fault (Fig. 19).

c)

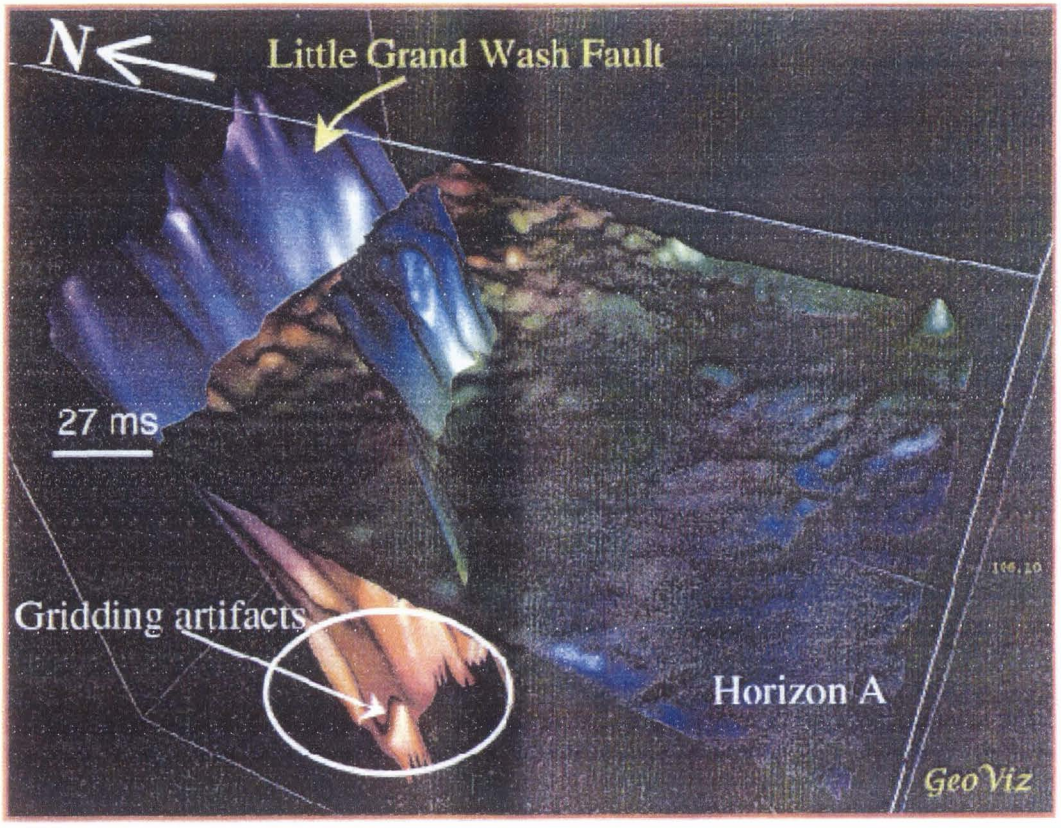


Figure 18 Continued.

Unfortunately, the south major fault strand cuts the Jurassic Brushy Basin Member and the Cretaceous Mancos Shale Formation and has poor outcrop expression. This remains the case towards the eastern section of the fault, and the fault is covered by Quaternary deposits in the immediate west. However, the north fault strand cuts rocks that are well exposed, and a large calcite deposit caps the faulted Summerville Formation (Fig. 20 a). This location is outlined with a box in Figure 19.

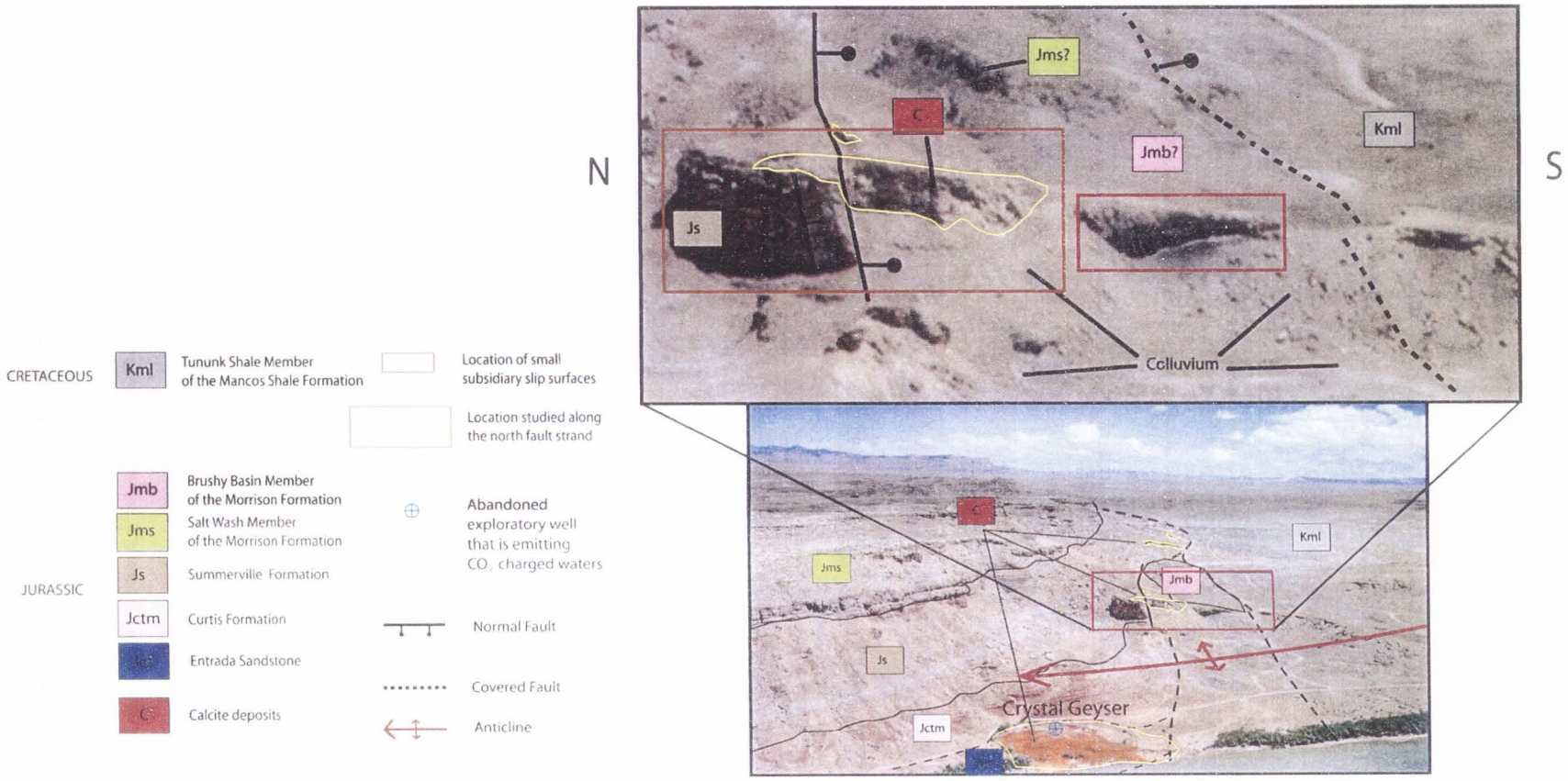


Figure 19 Air photo looking to the east along the strike of the Little Grand Wash fault. The two major sub-parallel strands are illustrated showing the juxtaposed Summerville Formation against the Jurassic Morrison members along the north fault, and the Cretaceous Tununk member juxtaposed against the Brushy Basin clays along the south fault. Outlined boxes in the upper photo are shown in more detail in Figures 20 and 21. Highlighted areas traced in yellow are areas where calcite deposits are found.

a)

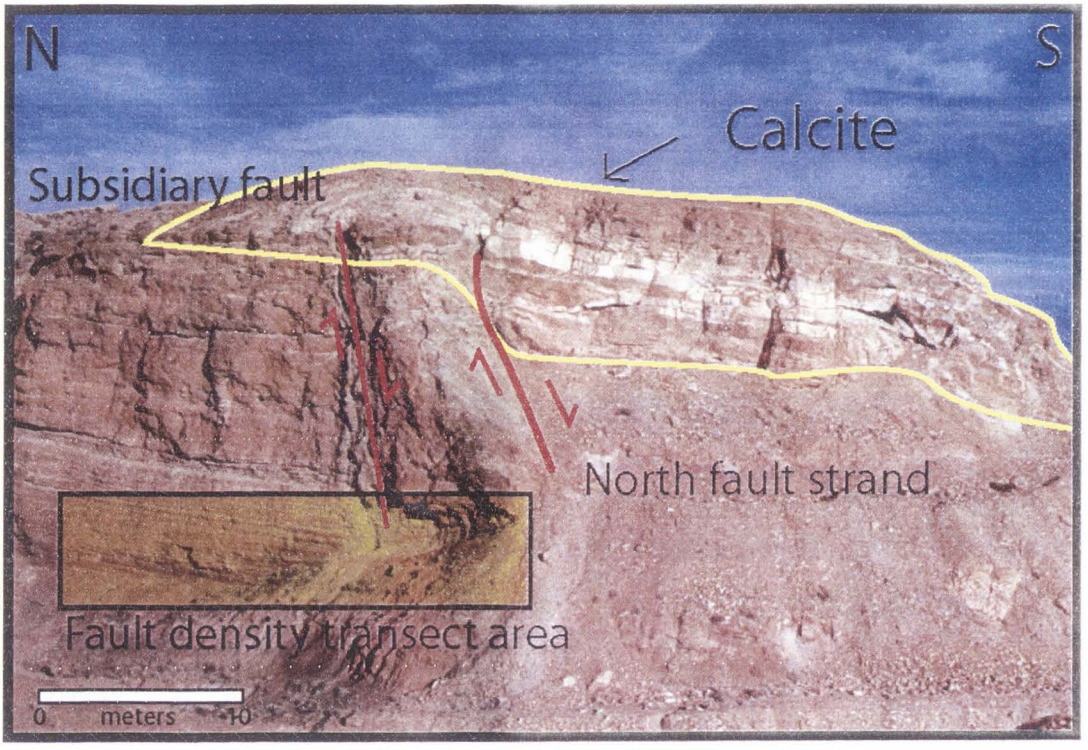


b)

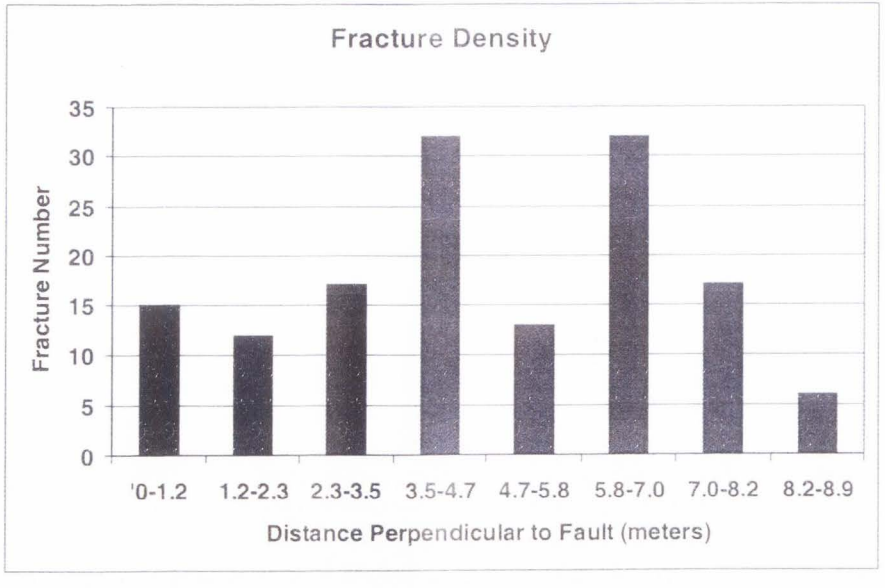


Figure 20 A calcite deposit caps the north fault strand of the Little Grand Wash fault. a) Northwest between the cross section A to A' line and the Crystal Geyser (Fig.14), the north fault strand cuts the Summerville Formation in the hanging wall of the fault. b) Fracture density of the Little Grand Wash fault. The number of fractures is on the y-axis and the distance perpendicular to the fault (in meters) is on the x-axis.

At this outcrop, the fault zone contains at least one subsidiary fault and more than 100 fractures (Fig. 20), which is similar to what is expressed at many locations along the fault. The fractures decrease in density farther away from the faults (Fig. 20 b). Some of these fractures in specific areas along the faults have experienced fluid migration—as evidenced by the presence of calcite mineralization and bleached zones from millimeters to 30 cm. This is evidence of past fluid migration directly associated with the fault zone. Calcite mineralization fills these fractures and is also deposited in a variety of other bed forms that will be briefly discussed later.

In between the north and south fault strands, near the line of cross section A to A' line illustrated in map view on Figure 14, there are more than 10 subsidiary slip surfaces too small to be mapped at this map scale. This section is outlined with a box in Figure 19. These small-displacement antithetic faults cut gently north-dipping Morrison clays and have a strike of 091° to 095° and a dip of 84° to 89° N (Fig. 21). Slicken lines measured on these faults indicate mostly oblique left-lateral dip-slip movement (48° rake). They crosscut fractures with a strike of 087° and dip 10° S, with offsets of approximately 10 to 20 cm. Similar to what is seen in the Salt Wash Member in the eastern section previously discussed, these smaller faults are likely related to the larger structures in this region.

With the use of this 1:6,000 mapping (Fig. 14), outcrop scale analysis, and well log compilation, a cross section of the Little Grand Wash fault was compiled (Fig. 22). The gently north-dipping Morrison Formation is cut by the north strand of the Little Grand Wash fault, as illustrated on the cross section. The poorly exposed south fault

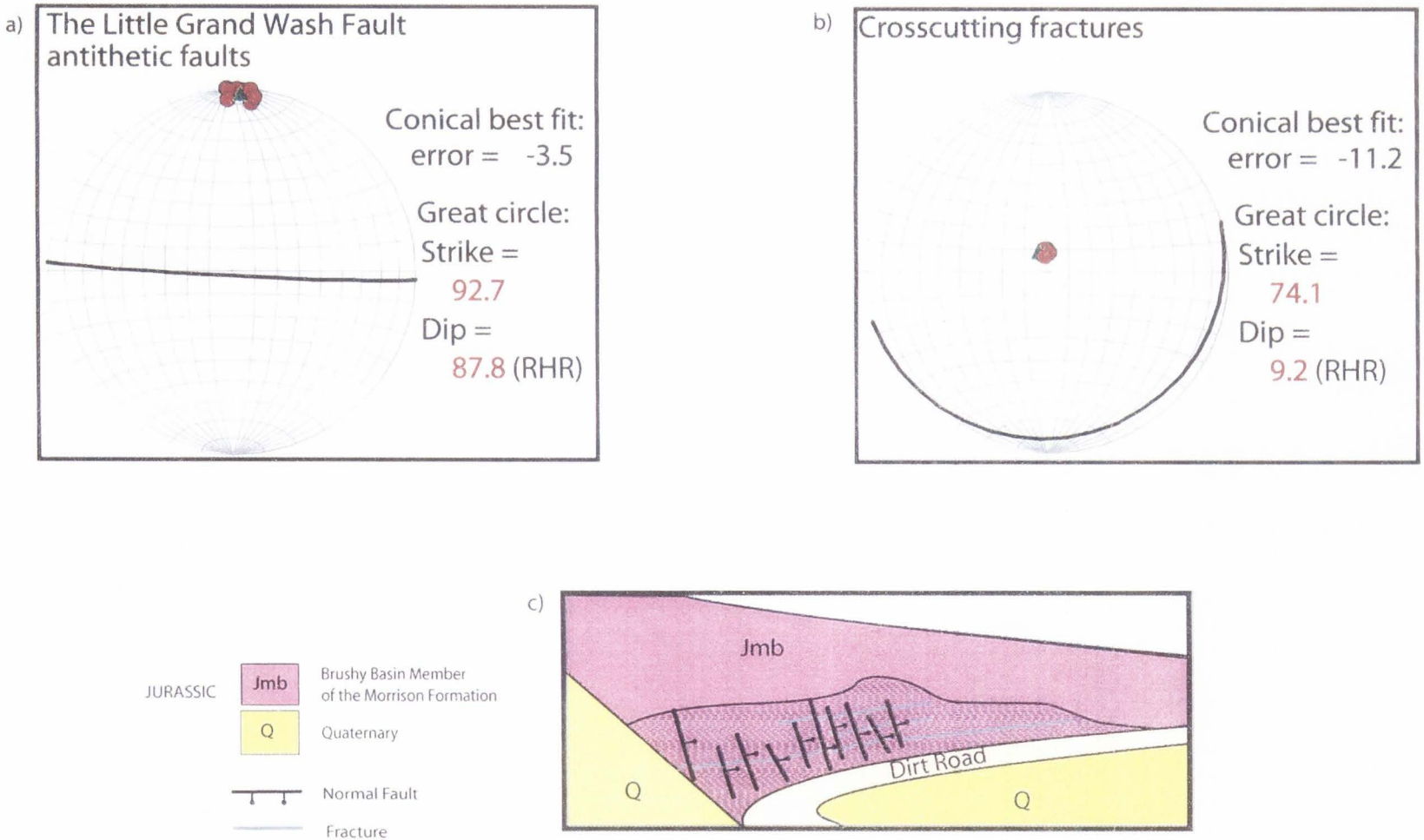


Figure 21 Small-displacement antithetic faults in the fault damage zone of the Little Grand Wash fault. a) Stereogram of the antithetic faults between the north and south major fault strands of the Little Grand Wash fault. b) Stereogram of the fractures cross-cut by the faults. c) Cartoon of this location (actual location can be seen in Figure 19).

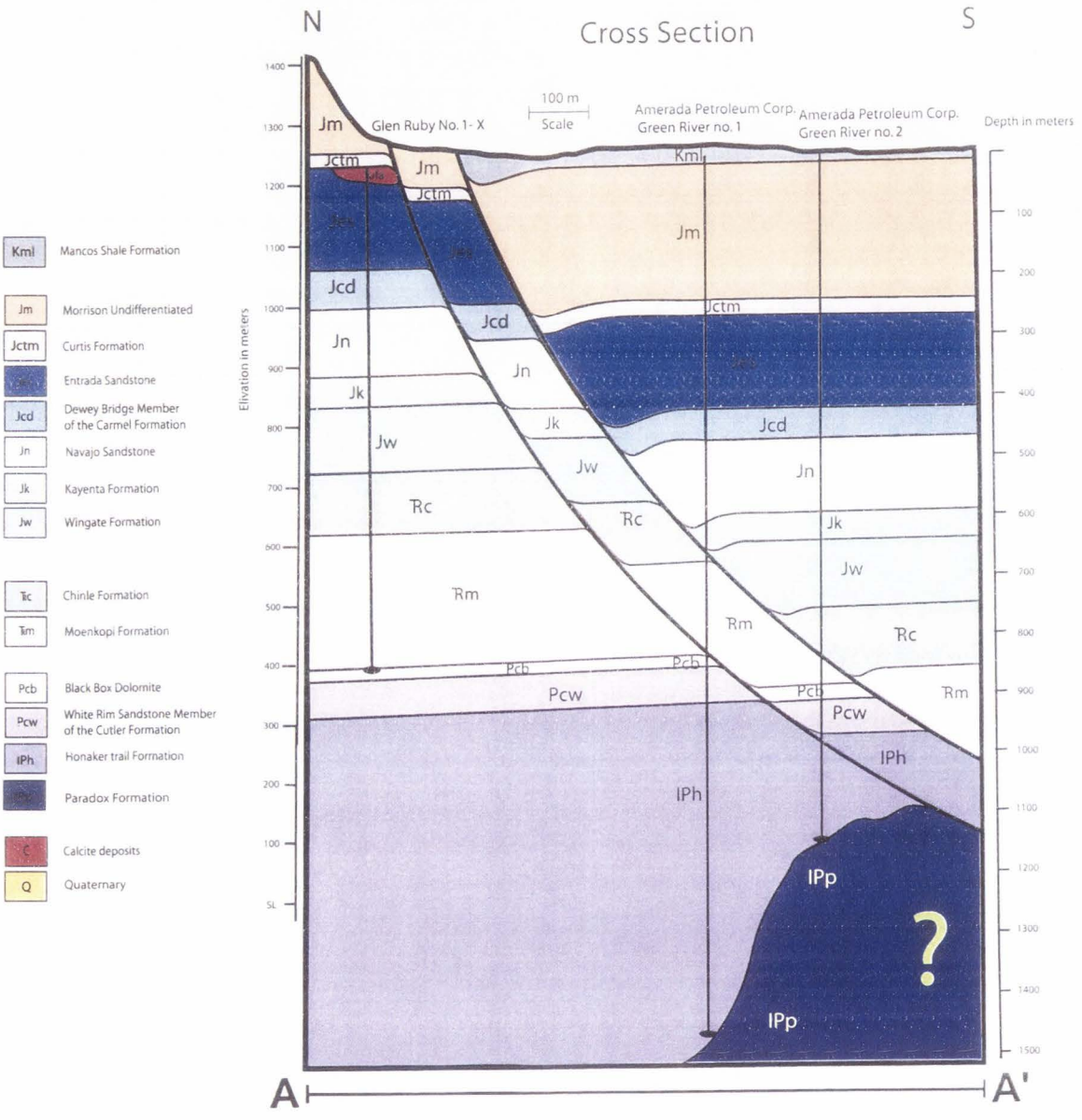


Figure 22 Cross section of the Little Grand Wash fault. Cross section shows rotated bedding near the fault, fault rollover in the hanging wall, and the listric nature of the faults interpreted from surface orientations and well log data.

strand cuts the Morrison Formation and has the Cretaceous Mancos Shale in the hanging wall.

The stratigraphic separation across the north strand is 60 m, whereas the south strand has a separation of 200 m (Fig. 22). Varying degrees of rotated bedding directly associated with faulting was noted at all outcrop locations studied. This altered bedding is illustrated on the two fault strands of the cross section. The faults dip steeply at the surface (91° S from Figure 13) and change dip at depth. Abandoned wells to the south of the fault (Amerada Hess, Green River no. 1, and Amerada Hess, Green River no. 2, drilled in 1949) (Table 1) indicate that the fault dip changes to 41° at a depth of 800 m and reaches a depth of at least 970 m. This change in dip is based on the assumption that the faults seen in the wells at depth are indeed the same faults seen at the surface. This suggests that the Little Grand Wash fault is a listric fault system and therefore, in order to reconstruct this cross section, the fault is likely to have antithetic or synthetic faults and/or fault-induced rollover in the hanging wall. It is possible that the faults seen in the Amerada Hess Green River no.1 and no. 2 wells are antithetic or synthetic faults (there are no dip data available in the well database). It is very difficult to discern if the mechanisms of fault rollover and/or antithetic or synthetic faults are not present or not seen in the highly weathered Mancos Shale. Therefore, for the purposes of this cross section, fault rollover was selected and is illustrated (Fig. 22). This style of fault geometry is commonly associated with listric faults (Ramsay and Huber, 1987). This interpretation also fits geometric models of listric normal faults and rollover folds (Dula, 1991). It also should be noted that the Paradox Formation is encountered at different

depths in wells no.1 and no. 2. If these well depths are correct, this suggests salt movement at depth. This is consistent with other areas throughout the Paradox Basin.

Evidence for fault leakage

The Little Grand Wash fault clearly affects present-day gas, water, and oil flow. Carbonate springs, an oil seep and oil stained rocks, an active $CO_2$-charged geyser, and actively forming travertine deposits are localized along the Little Grand Wash fault zone (Fig. 23). Field mapping and oblique air photos show that present-day leakage areas are constrained to the same section of the fault previously discussed (Fig. 14). In this region of the fault, near the Crystal Geyser (Glen Ruby et al. no 1-X well drilled in 1935), there are many indications of leakage. The Crystal Geyser has been unnaturally leaking water and $CO_2$ gas since it was drilled in 1935; and in this same area, reports as early as 1912 have noted the leakage of oil, gas, and water.

Previous work (Baer and Rigby, 1978; Campbell and Baer, 1978; Doelling, 1994), well logs, and field work support that the Glen Ruby well was drilled through preexisting, 21.5-m-thick calcite deposits (Fig. 14). Since it was drilled in 1935, bright orange-stained calcite has been deposited from periodic (11- to 15-hour) 20-m to 30-m-high eruptions (Fig. 9 and 23 c). This geyser has maintained its eruptions regardless of damage done to the well. The borehole has been dynamited, attempts at cementing it have been conducted, and railroad ties have been dumped into its 24-in. casing (D. Matindale, oral comm., 2003). A 1.5-m-high steel pipe was added to the top of the well casing in 2001. A small bubbling carbonate spring exists 10-m northeast of the geyser (Fig. 23 a). This spring increases and decreases discharge in correspondence with the

geyser. This spring has been observed during this study to be influenced by the same hydrologic system as the geyser.

Two km east of Crystal Geyser, there are $CO_2$ gas seeps, an oil seep, and a small spring (Fig. 14; Fig. 23 b and d). Gas seeps audibly from the ground in a wash approximately 30 m north of the Little Grand Wash fault. A small amount of water flows

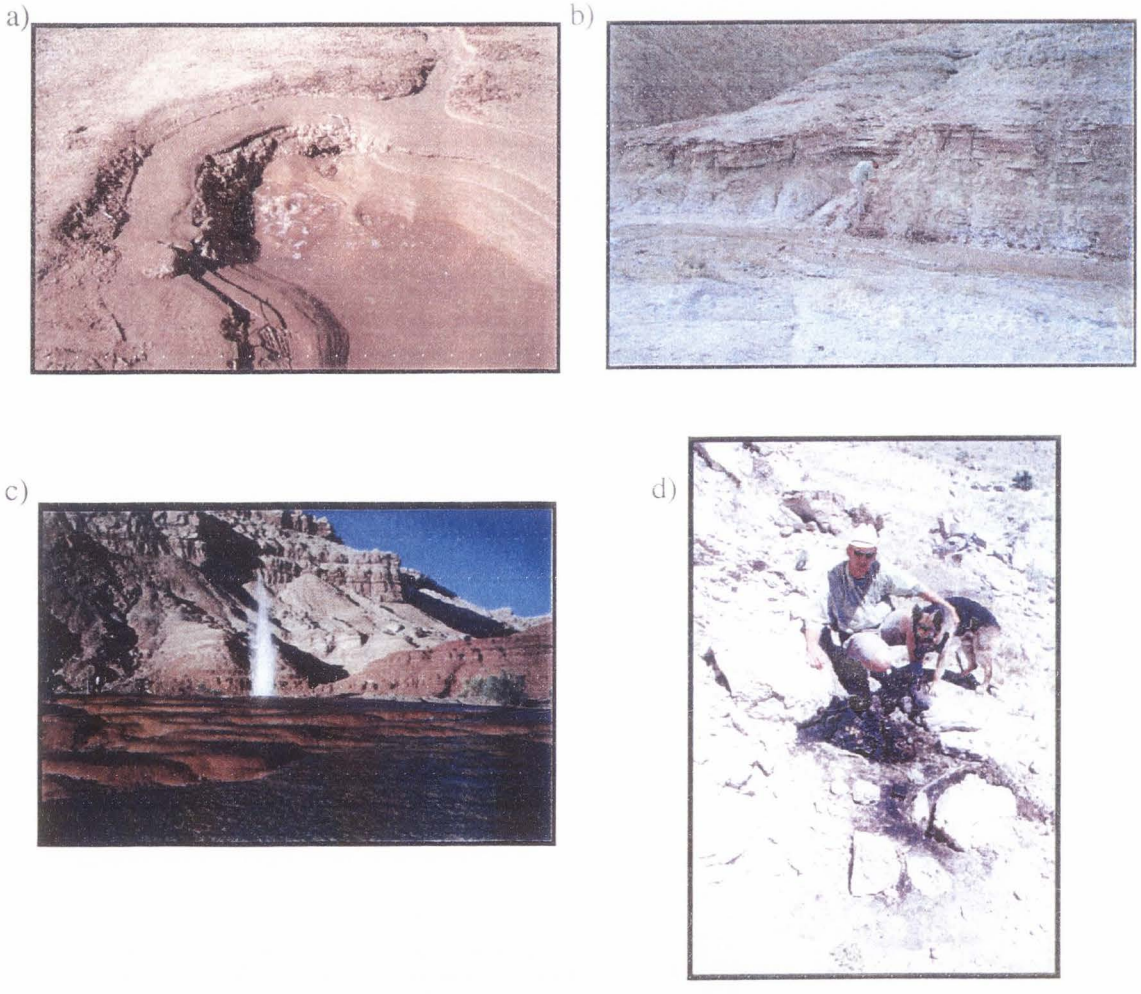


Figure 23 Photos of present-day leakage of the Little Grand Wash fault. a) Spring located 10 m northeast of the Crystal Geyser. b) Spring located along the fault's trace about 2 km east of the Crystal Geyser. c) The Crystal Geyser and active tufa deposits. d) An oil seep and oil stained rocks located 2.2 km east of the Crystal Geyser.

sporadically from upstream of this location, leaving salty deposits and wet sand in the base of the wash. Farther to the east, an oil seep lies on the fault strand. A shallow pit contains fresh oil, indicating that there is active flow of hydrocarbons to the surface. The host rock close to this seep contains patches of oil staining. The geochemical fingerprint of this oil suggests that it was sourced in the lower Permian (Lillis et al., 2003).

Throughout the central region of the Little Grand Wash fault, there are a number of calcite deposits (Fig. 14) that indicate leakage has occurred in the past. These terraces will be briefly discussed in the calcite description section of this paper.

## Salt Wash Fault

### Fault characteristics

The Salt Wash fault offset is primarily accommodated by a set of normal faults cutting the shallow north-plunging Caine Creek Anticline. Two sub-parallel normal faults with opposing steep dips form a graben over 23 km long (Fig 12). These major faults maintain an average orientation of 289.5° (Fig. 24), and at the surface, they displace Jurassic and Cretaceous sandstones, siltstones, and clays (Fig 25). The total maximum stratigraphic separation across this fault system, from east to west, is only about 50 m, but the down-dropped graben has stratigraphic separation across the north fault of about 300 m and across the south fault of about 250 m.

### Structures related to the Salt Wash fault

Surface data show the dip of the north fault is 78° S and the dip of the south fault is 87° N (Fig. 24). Similar to the Little Grand Wash fault, the central region of the Salt

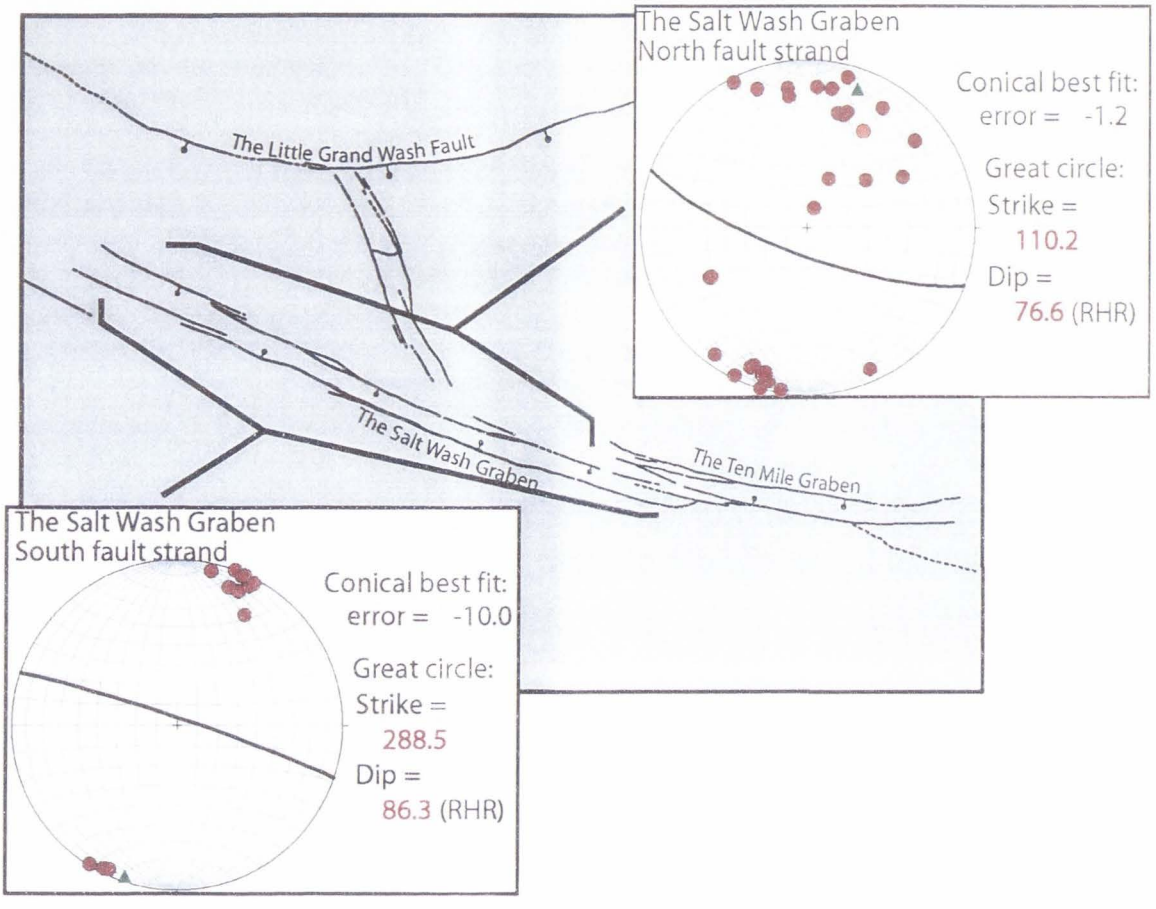


Figure 24 Stereograms compiled from fault data showing fault strike and dip along the Salt Wash Graben.

Wash fault shows the maximum separation, and is an excellent area to do outcrop-scale analysis and detailed mapping at 1:6,000 (Fig. 25). The Cedar Mountain Formation in the hanging wall is folded, and forms a shallow syncline with an axis sub-parallel to the trend of the Salt Wash Graben. The outer limbs of the syncline are cut by the north and south faults. In this central region, the southern stratigraphic separation of the Cedar Mountain Formation occurs on two faults stands (Fig. 25). These faults juxtapose the Cedar Mountain Formation against the Morrison Formation.

Similar to the Little Grand Wash fault, in this region of the Salt Wash fault, fault-related structures, including rotated bedding, localized small-scale folding, small-displacement synthetic faults, fractures, and calcite deposits, are present at a variety of locations. The best-exposed locations will be described in this section. It is noted that rotated bedding continues to be seen almost everywhere the faults are exposed (Fig. 26 c).

In the southeastern section, east of Torrey Spring (shown on Fig. 25), a subsidiary fault cuts the Jurassic Curtis Formation and has a very well exposed, 6.5-m-wide fault core (Fig. 26 a). Adjacent to the fault zone in the footwall, a variety of structures are present, including localized small-scale folding, small-displacement faults, fractures, rotated bedding, carbonate deposits, and bleaching.

In the footwall, shallow 3°-NE to 6°-NE-dipping beds of the Curtis Formation have been highly deformed by rotation, folding and small-displacement faults (Fig. 26 a). Near the fault core, in the hanging wall, the flat-lying Curtis beds have been rotated nearly vertical, sub-parallel to the fault plane. Clay-rich fault gouge can be seen in many places along the fault, and forms complex clay smear structures with a scaly shear fabric 1 to 6 cm thick. Farther up section in the hanging wall, poorly consolidated carbonate deposits are truncated by another clay-rich fault gouge slip surface. At least five 1-cm to 18- cm-thick calcite veins are separated by thinner 1-cm to 8-cm clay-rich layers. These layers are cut by at least nineteen 1-cm-thick perpendicular calcite veins. The red-stained Curtis Formation is bleached to a light tan to pale white along fractures 1 m farther south of the fault zone (Fig. 26 a).

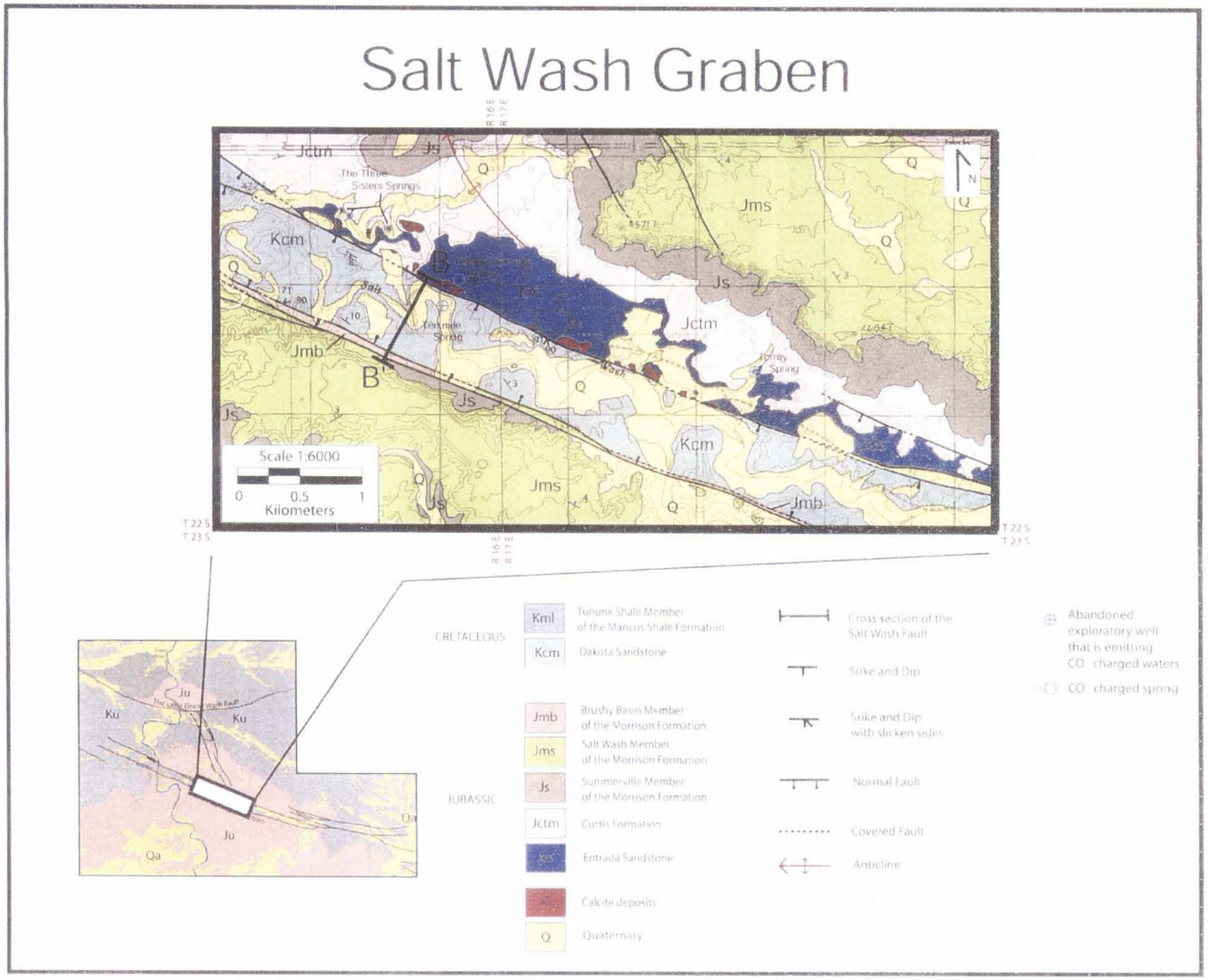


Figure 25 A detailed geologic map showing the central region of the Salt Wash fault.

About 200 m northwest of this location, along the fault trace, an outcrop shows substantial mineral rotation (Fig. 26 b). The rimstone texture of this deposit is seen in many locations in the field area. It consists of stacked sub-horizontal layers. These initially sub-horizontal layers appear to have been rotated by the fault at this location (Fig. 26 b).

There are numerous fault-related fractures seen in outcrops near the Salt Wash fault zones. Some of these fractures extend for long distances from the fault zone, are steeply dipping, and are at high angles to the faults. They are well exposed in the upper portion of the Entrada Sandstone in the footwall of the north strand of the Salt Wash Graben. It is noted that these fractures are located near the axis of the Caine Creek Anticline and have a similar trend (Fig. 25). In a number of places along the fault zone, the red-stained Entrada Formation is bleached to a light tan to pale white along fractures emanating from the fault zone. Chan et al. (2001) suggest that such bleaching is the result of the movement of a reducing fluid, such as might be associated with hydrocarbons, through the system.

A cross section of the Salt Wash Graben was complied with the use of 1:6,000 mapping, outcrop-scale analysis, and the well log data in Table 2 (Fig. 27). There are few wells near the Salt Wash Graben, and unfortunately even fewer of these wells have documented drilling records. This makes the depth that these faults extend to uncertain, but they may sole into the Paradox salt sequence, and could be related to the salt tectonics in the region. In order to constrain a cross section, well logs of the entire field area were compiled and the average thickness of subsurface formations was used (Table 2).

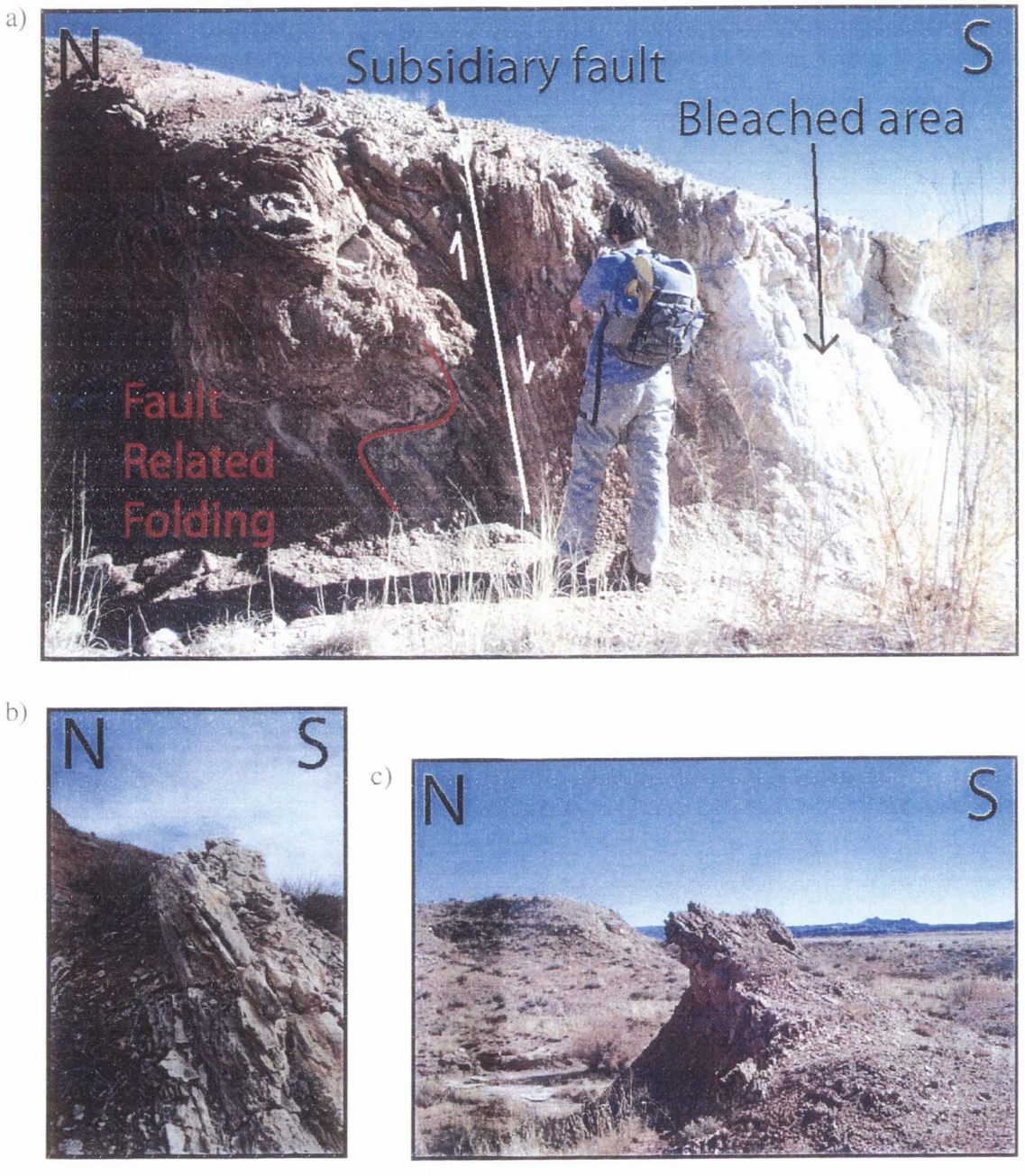


Figure 26 Structures seen in the Salt Wash fault zone area. a) Looking to the east at a subsidiary fault with small-scale folded beds in the damage zone and bleached host rock. b) Looking to the east at rotated calcite mineralizations associated with the fault. c) Looking to the east at rotated beds associated with the north Salt Wash fault damage zone.

In the center of the graben, the north fault juxtaposes the Jurassic upper Entrada Sandstone in the footwall of the faults against the Cretaceous Cedar Mountain Formation (Fig. 27). Stratigraphic separation along this fault is 300 m. The Cedar Mountain Formation in the hanging wall of this fault is folded and forms a shallow syncline with a northwest trend. The north limb dips 8° S and the south limb dips 10° N (Fig. 27). In this center region, the stratigraphic separation of the Cedar Mountain Formation along the southern fault occurred on two fault stands (Fig. 25 and 27). These faults offset the Cedar Mountain Formation against the Morrison Formation. With the use of the bedding contact between the Morrison Salt Wash and Summerville Members, the total stratigraphic separation along these two faults is estimated to be 250 m.

Varying degrees of rotated bedding, directly associated with faulting, were noted at all studied outcrop locations. This altered bedding is illustrated on the fault strands of the cross section (Fig. 27).

Evidence for fault leakage

The Salt Wash faults, similar to the Little Grand Wash fault, affect present-day gas and water flow. Five carbonate springs, an active $CO_2$-charged geyser, and actively forming travertine deposits are localized along this system (Fig. 25). Field mapping and oblique air photos show that leakage areas are constrained to the center of the graben near the north strand (Fig. 28). All but the Ten Mile Geyser are in the footwall of this strand (Fig. 28). At this location, the Entrada Sandstone in the footwall has been bleached.

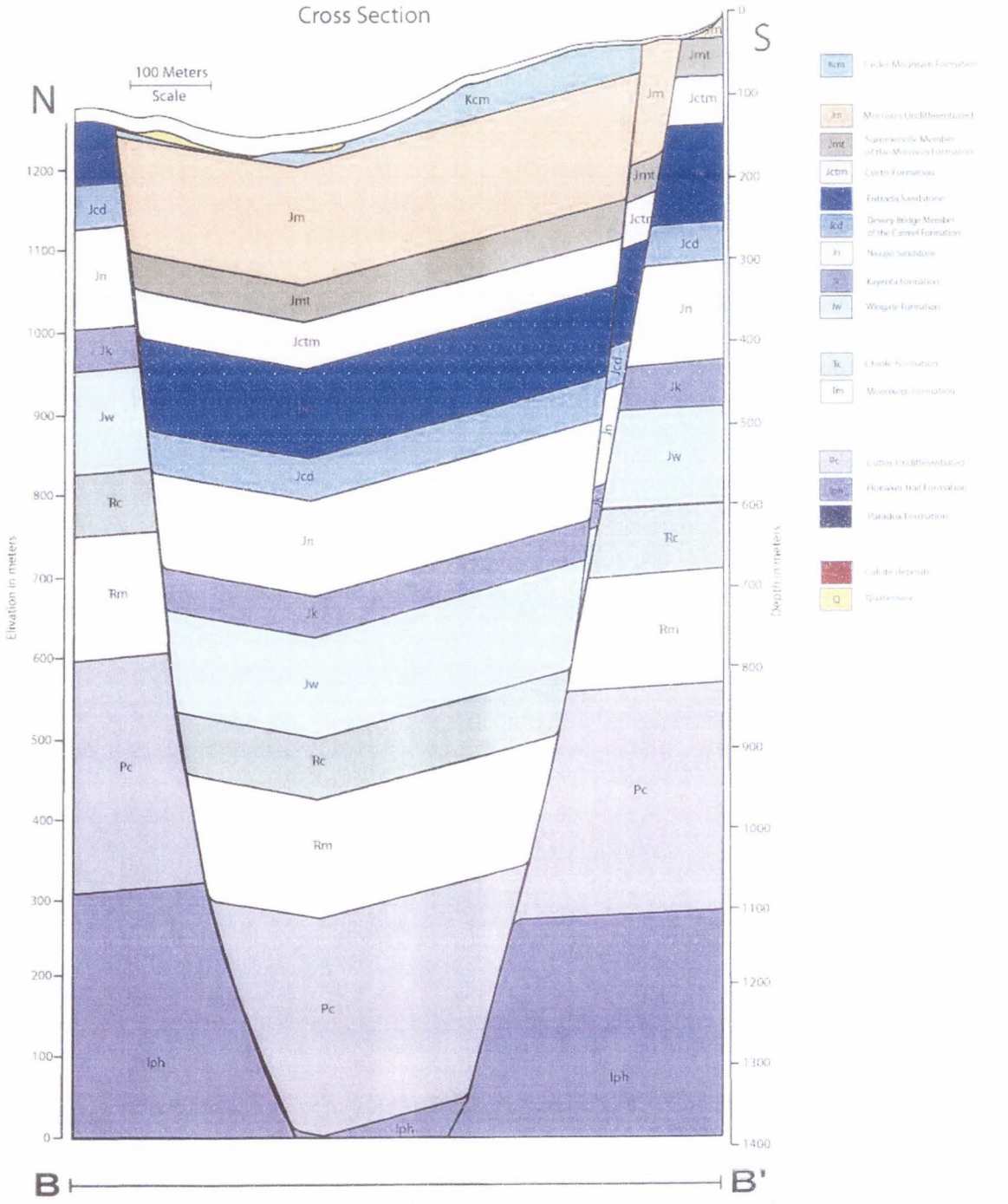


Figure 27 Cross section of the Salt Wash fault.

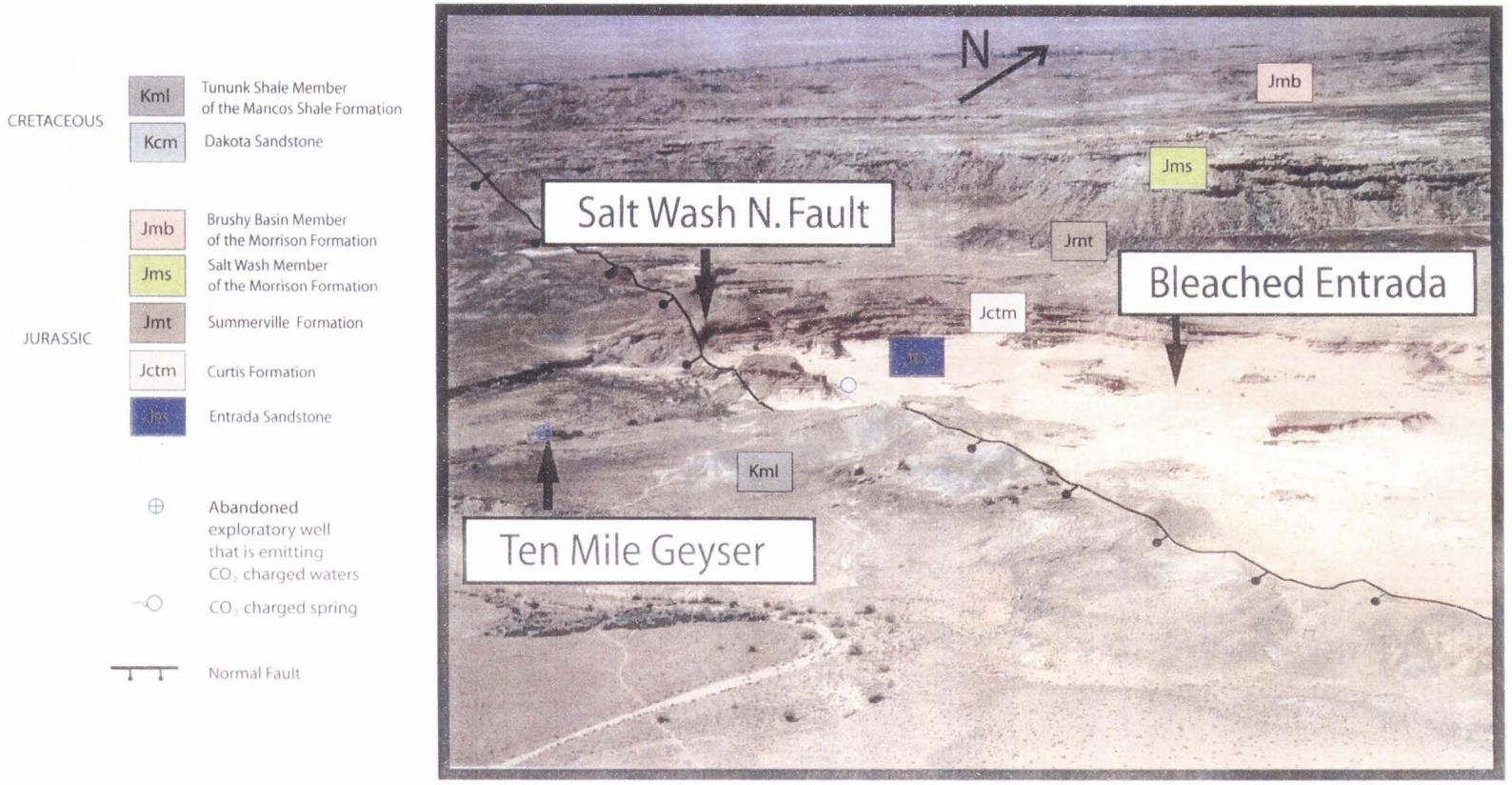


Figure 28 Oblique air photo showing that leakage areas are constrained to the center of the graben near the north strand.

The active Ten Mile $CO_2$-charged geyser erupts from a 0.5-m-high well casing near cross section B to B' (Fig. 25), seen on Figure 29 c. There are no well records of this borehole and its depth is unknown. The water chemistry of the Ten Mile Geyser is similar to the Crystal Geyser (Glen Ruby et al. no 1-X well) on the Little Grand Wash fault (Heath, 2004), and there is poorly-developed, orange-stained calcite deposited from these waters. The Ten Mile Geyser has erupted infrequently in the past, with 1-m to 1.5-m- high eruptions. A similar mineral-charged spring is located in an open wash 120 m north of the footwall of the north fault strand (Fig. 25). The (Pseudo-Ten Mile) spring has been excavated and refilled during this study. Someone (unidentified by the author) dug this once small, bubbling pool (Fig. 28 and 29 b) into a pit about 2 m wide, 15 m long and 1.5 m deep. Since then, the pool has been backfilled to a smaller pool similar to the original.

About 2.5 km east of the geyser, a small, bubbling $CO_2$-charged spring lies in the Entrada Sandstone in the footwall of the northern fault (Fig. 25). The spring (Torrey Spring) appears to be at the location of the Delaney Petroleum Corp. no 1 drillhole drilled in 1949, which had a total depth of 980 ft (299 m). At this location, orange-stained calcite is actively being deposited at the surface in a 15-m-diameter area (Fig. 29 d). This mound has increased in size, during this four-year study. This increase was not realized in time to take detailed measurements over time. The water now trickles over the mound and cascades into a dry wash. This water precipitates calcite sub-vertically, forming flowstone along its path.

One km to the northwest of the Ten Mile Geyser, in the footwall of the fault, there is a series of small springs (Fig. 25). These springs flow continuously and are actively

forming orange-stained travertine deposits (Fig. 29 a). The Three Sister Springs are in close proximity to each other and are located in a topographically low wash, and may be linked in the subsurface. Water can be found within 10 cm of the surface throughout the region and a white saltpan crust borders this same area (Fig. 29 a).

## Ten Mile Graben

### Fault characteristics

The Ten Mile fault system is the eastern continuation of the Salt Wash fault system. The Ten Mile fault system is a set of normal faults that form a graben over 9 km long. Unlike the Little Grand Wash fault and the Salt Wash Graben, this system does not cut the Cane Creek Anticline (Fig 12). The two faults that bound the graben are sub-parallel and maintain an average orientation of 283° (Fig. 30). At the surface they displace Jurassic and Cretaceous sandstones, siltstones, and clays (Fig 12).

### Structures related to the Ten Mile Graben

The slip on this graben is accommodated along two primary faults. The dip of the north fault is 82° S and the dip of the south fault is 85° N (Fig. 30). These faults splay at the west end of the graben and begin to step over to the Salt Wash fault (Fig. 31). In this complex zone, the slip of the fault is distributed over at least seven faults. There are two fault-bounded tilt blocks associated with these faults (Fig. 32). In general, the fault zones are 0.5-m to 5-m wide, and consist of fractured host rock. Clay-rich fault gouge can be seen in many places along the fault. A variety of structures is present in the fault zones, including small-displacement synthetic faults and fractures.

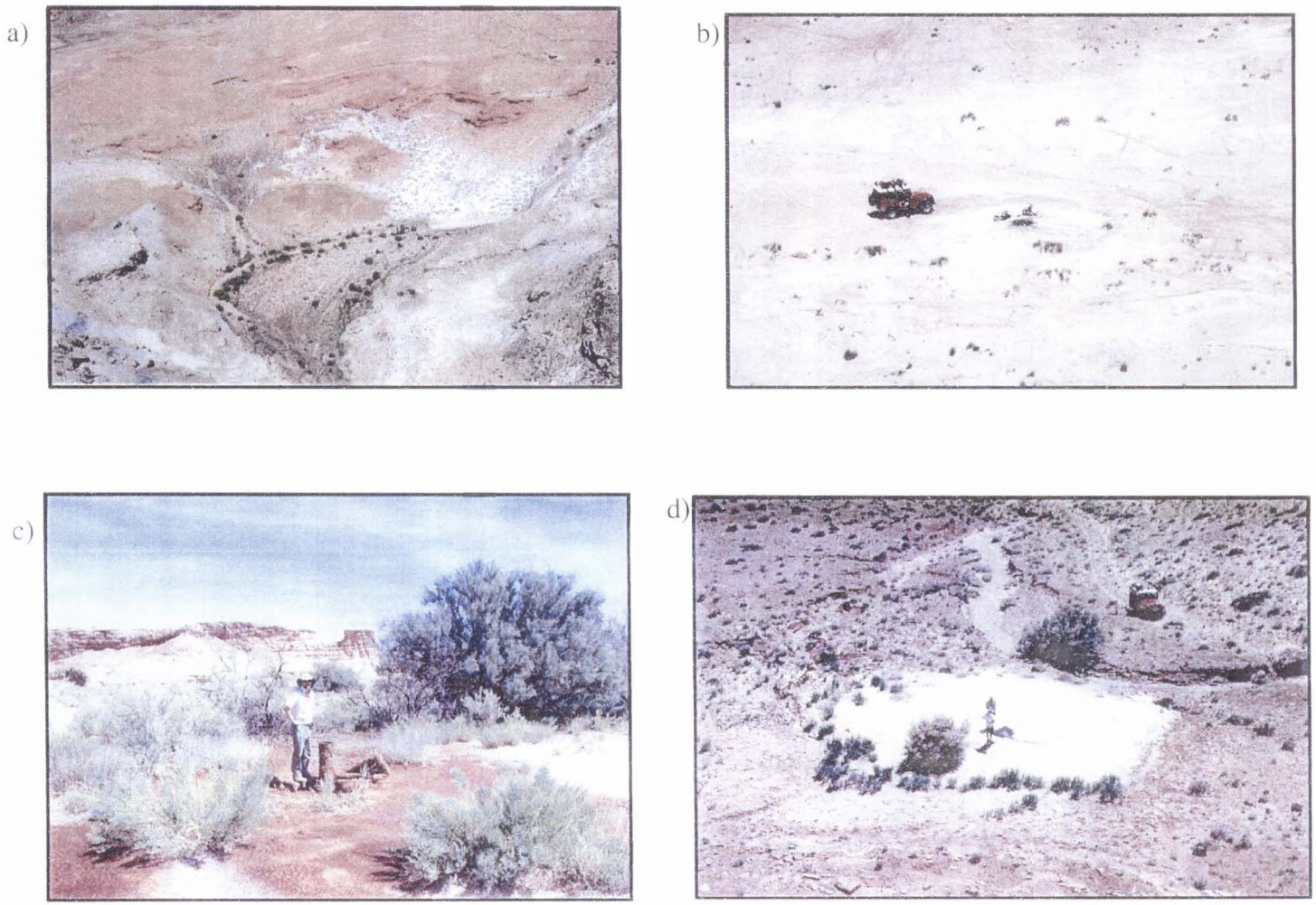


Figure 29 Springs and geysers in the Salt Wash Graben. a) The Three Sister Springs 1 km west of the Ten Mile Graben. b) Ten Mile Spring 120 m north of Ten Mile Geyser. c) Ten Mile Geyser (no drilling records). d) Torrey's Spring (well #21).

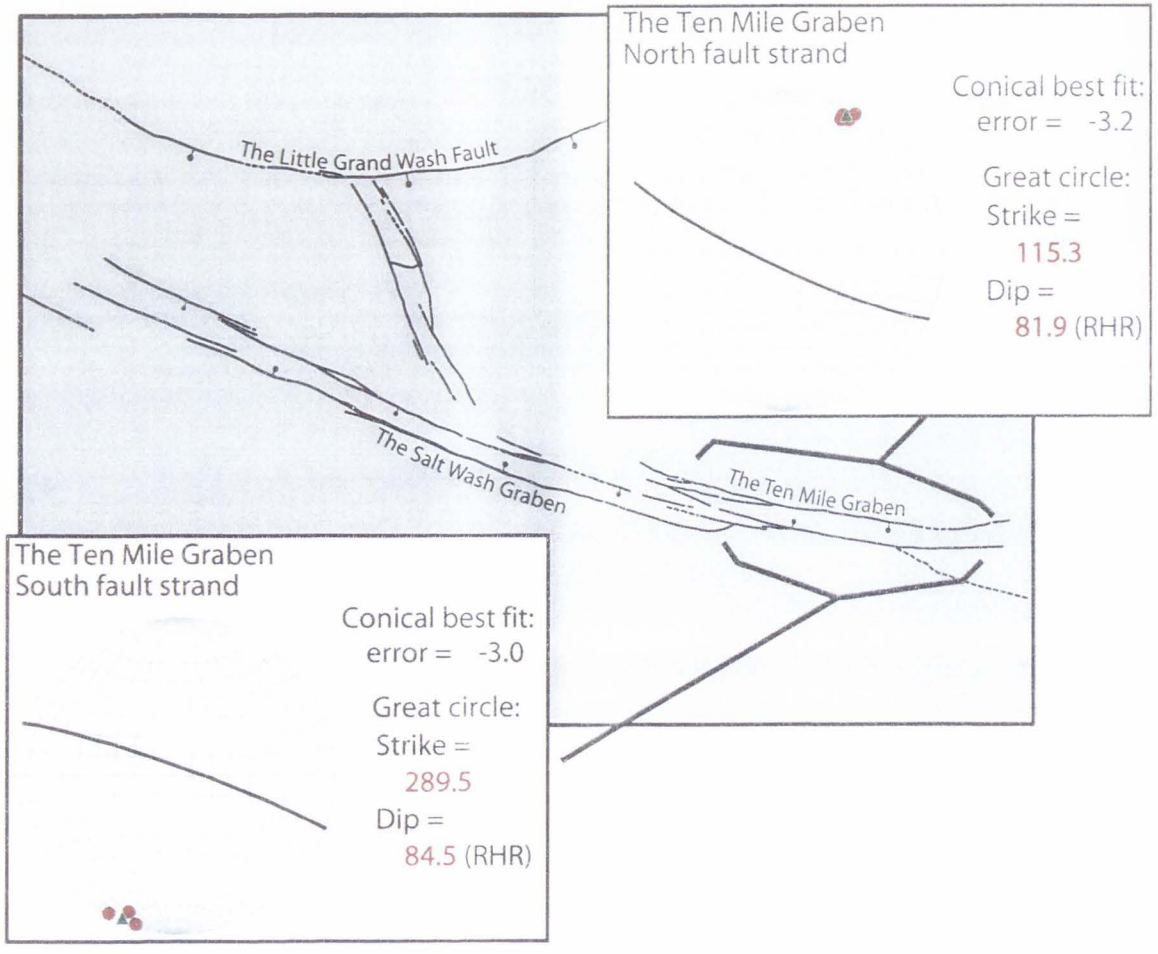


Figure 30 Stereograms compiled from fault data showing fault strike and dip along the Ten Mile Graben.

Evidence for fault leakage

Unlike the Little Grand Wash fault and the Salt Wash Graben, there are no calcite deposits, and none of the structures seen suggest any type of past leakage in the area studied.

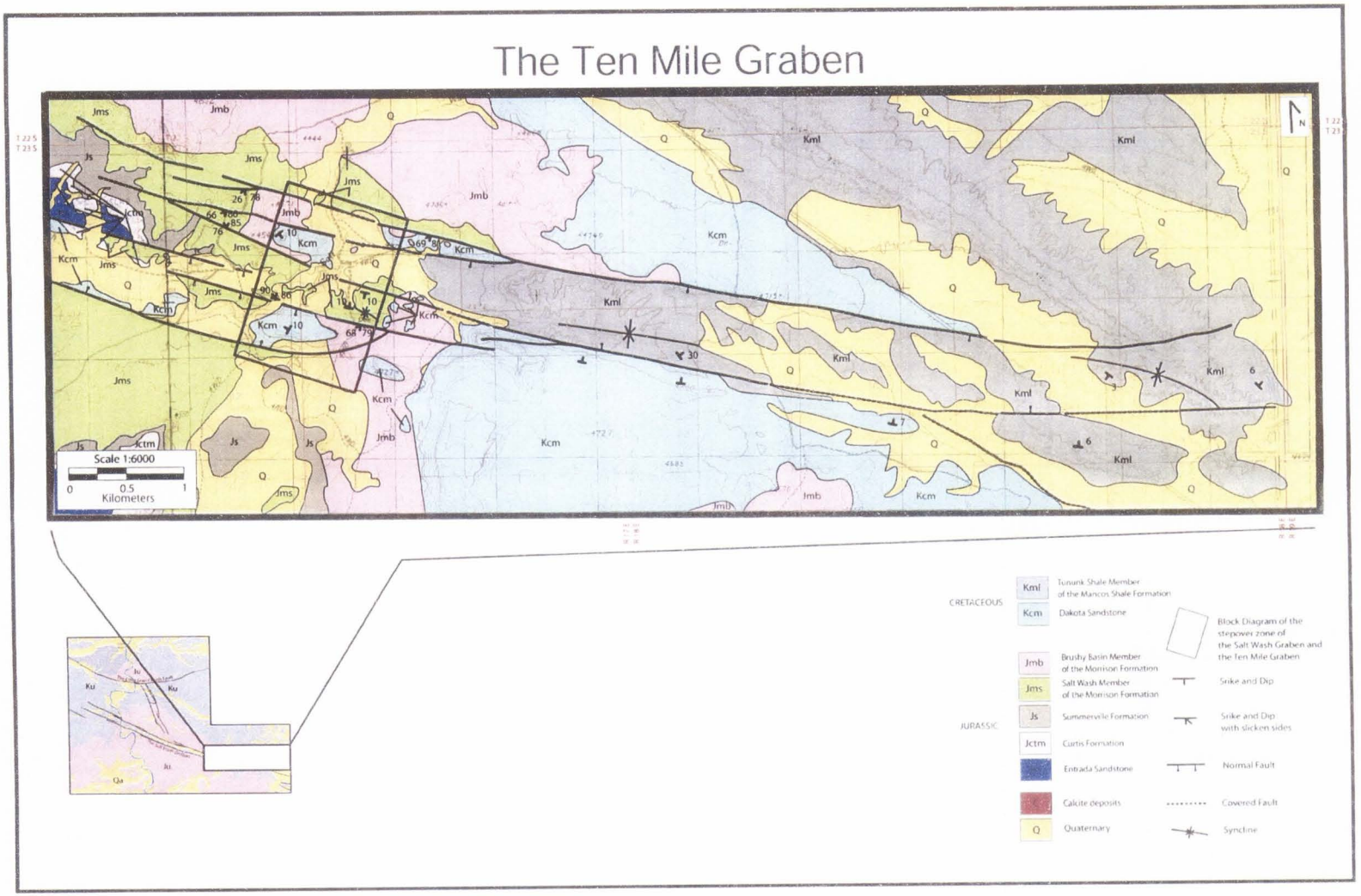


Figure 31 A detailed geologic map showing the Ten Mile Graben.

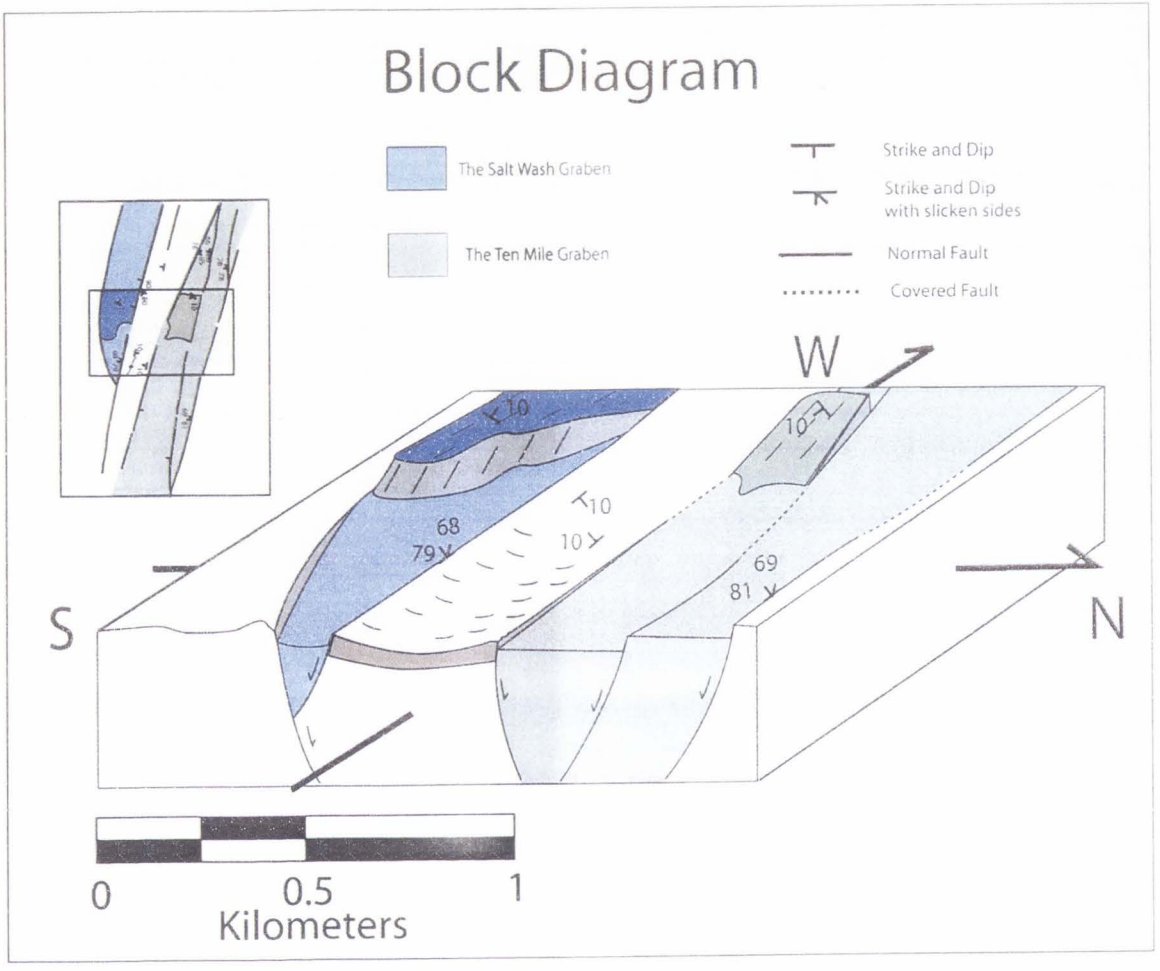


Figure 32 The Salt Wash and Ten Mile Grabens step-over zone block diagram. Location box in the upper left corner can also be seen on Figure 31.

## Calcite Deposits

A variety of calcite deposits (Fig. 6) is found along the fault trace of the Little Grand Wash fault and the northern fault trace of the Salt Wash Graben (Fig. 14; Fig. 25). All deposits on the fault systems are situated where the structurally high part of the Cane Creek-Big Flat salt anticline is cut. The majority of the tufa deposits are found in the footwall of the faults, with little spilling over to the hanging wall (Fig. 20; Fig. 25). The

tufa is divided into active deposits and ancient, inactive deposits as described by (Dockrill et al., in review). The active deposits form around geysers and springs, and many are the result of uncapped wells penetrating the reservoir. The ancient, inactive deposits tend to be situated at higher elevations, capping buttes that are aligned along both fault traces (Dockrill et al., in review). Due to the poor preservation potential of terrestrial tufa deposits, it has been suggested that all of the deposits are Pleistocene or younger in age (Baer and Rigby, 1978).

## Geochronology

The faults cut the Mancos Shale, indicating that fault activity occurred at least up to the middle Cretaceous. Calcite deposits along the fault trace must have been deposited after this. In areas where calcite deposits are present, the host rock is magnificently veined—in some cases obliterating primary sedimentary structures (Fig. 15 d). Some of these deposits cut though the fault zone and are also are cut by the fault (Fig. 15 e). Samples of vein deposits can be used for uranium-series dating and have been taken from the Little Grand Wash fault zone.

The faults cut a north-plunging anticline, which could be related to salt movement in the Paradox Formation at depth (Fig. 22), and according to the well log data the faults cut down at least to the Permian Cutler Formation (Fig. 22). The development of a basin-wide system of salt anticlines initiated when the salt was loaded by the Pennsylvanian/Permian clastics that shed off the Uncompagre uplift to the northeast. Reactivation of the salt-related anticlines and faults occurred during Laramide (Eocene) compression (Fig. 5).

Direct dating of the clay in the fault gouge was done by ExxonMobil with $^{40}Ar/^{39}Ar$ methods outlined in van der Pluijm et al. (2001), Pevear et al. (1998) and Dung et al. (2000). The uninterpreted $^{40}Ar/^{39}Ar$ results were provided by personnel at Exxon Mobil Upstream Technology Company (P. Vrolijk, written comm. 2002). Three samples were analyzed from shallow wells drilled by ExxonMobil within their seismic survey area, and the results (Table 3; P. Vrolijk, written comm. 2002) constrain the Tertiary history of the fault. The results presented here are for the model ages of the smallest and largest grain fractions—interpreted to be the end-member authigenic and detrital components, respectively.

The smallest (< 2 μm) fractions yield ages of 25.47 to 46.89 Ma, with mean ages of 36 to 41.42 Ma and median values of 36.36 to 41.62 Ma. The detrital components range in ages from 114 to 197 Ma. Detrital ages are consistent with clays that developed in the middle Jurassic to early Cretaceous. The fault cuts rocks from ~100 to 157 Ma at the surface; older grains were likely transported into the sediments.

The authigenic components point to fine-grained clay development in the fault zone between the middle Eocene to the end of the Miocene. During this time, the region is interpreted to have been experiencing rapid uplift (Fig. 33). The middle Jurassic, upper Jurassic, and Cretaceous rocks at the surface have been uplifted approximately 1.8 km since the end of the Eocene. This uplift may have influenced fault movement in the Colorado Plateau, along the Little Grand Wash fault, and in the Salt Wash and the Ten Mile Grabens.

Fault activity from 25 to 42 Ma would correspond to Jurassic and Cretaceous rocks being as deep as 8,000 ft. at a temperature of 250° F (Fig. 33). This temperature is

in the oil generation window. The uplift from the Oligocene to the present exhumed the Little Grand Wash fault.

Rocks from the top of the Paleocene, interpreted by Heath (2004) to be the source of $CO_2$, have just recently reached a shallow enough level to allow $CO_2$ to change to the gas phase.

| Well | Depth | Size Fraction | K/Ar data | | XRD data | | Illite Age Analysis data | | | |
|---|---|---|---|---|---|---|---|---|---|---|
| | | | Age (Ma) | Error (+/-) | % Detrital Illite ($2M_1$) | Error (+/-) | Mean Diagenetic Age | $\alpha_{90}$ | Mean Detrital Age | $\alpha_{90}$ |
| DS3 | 30.8 | Coarse | 86.5 | 2.2 | 39 | 3 | 40 | 26 - 47 | 160 | 142 - 197 |
| | | Medium | 74.3 | 1.9 | 28 | 3 | | | | |
| | | Fine | 61.1 | 1.6 | 18 | 3 | | | | |
| DS9 | 30.5 | Coarse | 68.2 | 1.8 | 28 | 2 | 41 | 35 - 46 | 133 | 114 - 156 |
| | | Medium | 62.4 | 1.6 | 20 | 3 | | | | |
| | | Fine | 51.4 | 1.3 | 12 | 3 | | | | |
| DS9 | 32 | Coarse | 74.1 | 1.9 | 35 | 2 | 36 | 25 - 42 | 151 | 131 - 185 |
| | | Medium | 64.1 | 1.7 | 25 | 3 | | | | |
| | | Fine | 54.9 | 1.4 | 16 | 3 | | | | |

Table 3 The uninterpreted $^{40}Ar/^{39}Ar$ results provided by personnel at ExxonMobil Upstream Technology Company.

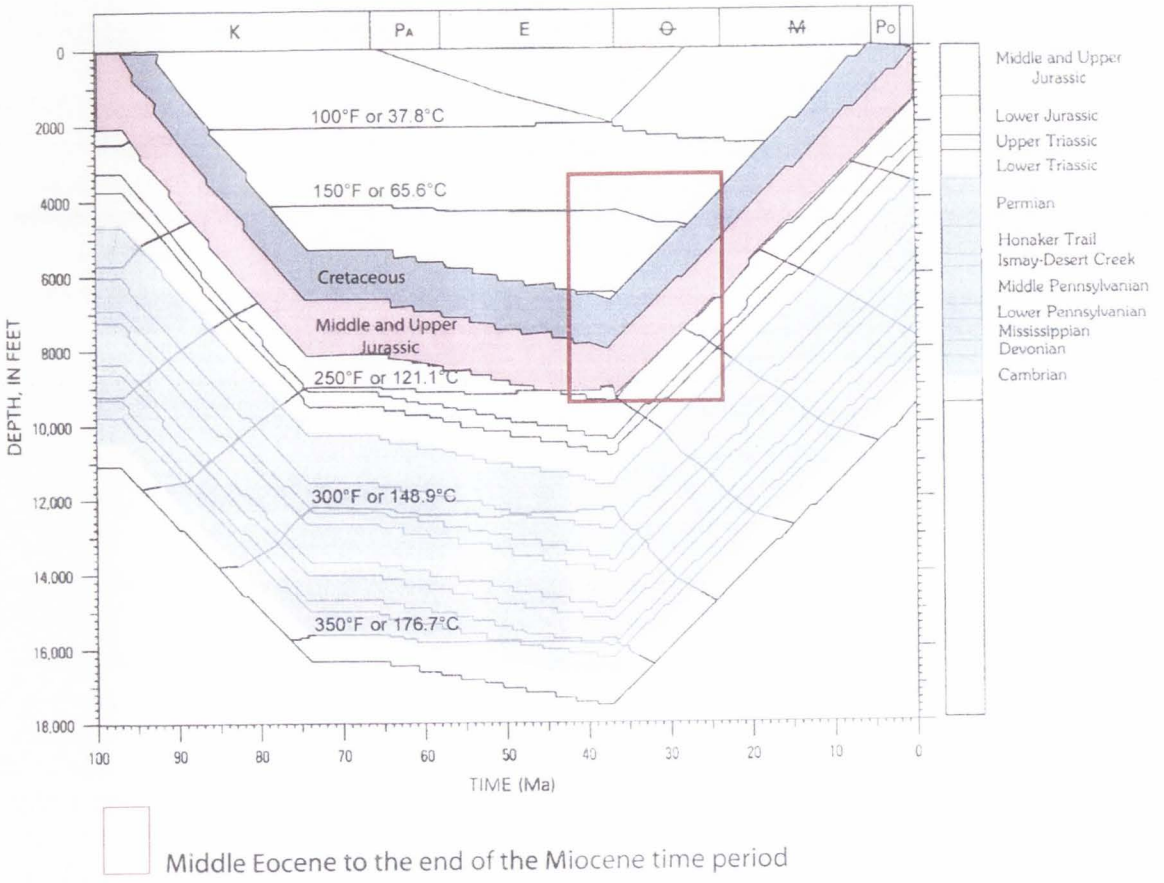


Figure 33 Thermal burial history curve for the area near Green River, Utah (adapted from Nuccio and Condon, 1996). Geochronological $^{40}Ar/^{39}Ar$ direct dating of the clay in the fault gouge suggests movement at 36.36 to 41.62 Ma. Rocks at the surface have been uplifted approximately 1.8 km during the middle Jurassic, upper Jurassic, and Cretaceous since the end of the Eocene. This uplift may have influenced fault movement in the Colorado Plateau and on the Little Grand Wash fault, and Salt Wash and the Ten Mile Graben. Permian and deeper rocks have been at an adequate depth, temperature, and time for oil generation (shaded in gray).

# DISCUSSION

This field-based structural analysis of clay-rich fault zones can be used to help constrain the geometry and properties of leaky subsurface aquifers, and $CO_2$ and oil reservoirs. Data was collected over a variety of scales along the Little Grand Wash and Salt Wash faults, and in the Ten Mile Graben, that may contribute to understanding why faults can act as barriers or conduits to fluid flow as outlined by Caine et al. (1996).

Mapping at the scale of 1:24,000 (Fig. 12) shows the Little Grand Wash fault is an arcuate south-dipping normal fault system comprised of two to eight strands. Most of the slip occurred on two strands, and the internal fault structure at all scales is complex. The Salt Wash and Ten Mile Grabens are bounded by two primary faults that bifurcate into a complex step-over zone linking the two fault systems. Both the Little Grand Wash fault and the Salt Wash Graben cut the Caine Creek Anticline and fail to constrain fluids, but the Ten Mile Graben does not cut the Caine Creek Anticline, nor does it show any evidence of leakage. Based on the results of the 1:6,000 mapping (Fig. 14 and 25), the data suggest that all evidence of leakage is located along the northernmost traces of the Little Grand Wash fault and the Salt Wash Graben at or near the fold axis of the Caine Creek Anticline.

## Structures in Leakage Areas

The data provided in this study include detailed outcrop mapping of fault damage zones at and near areas of leakage. Unconsolidated clay-rich gouge in the fault core, highly fractured fault zones, the presence of surficial mineralization and fracture-fill mineralization, and thickness changes, both down dip and along strike of the rocks cut by

the fault, are all seen in the field area. These data can aid in making interpretations of these leaky subsurface reservoir-scale faults.

## Sources of the Fluids

The Ten Mile Graben and the complex step-over zone to the Salt Wash Graben are not included as locations of leakage, although in the complex step-over zone the slip is distributed over at least seven faults (Fig. 31 and 32). In many places along these faults and the faults that bound the Ten Mile Graben, clay-rich fault gouge can be seen, and a variety of structures are present in the fault zones. These structures include fractures and small-displacement synthetic faults. Similar fault structures are seen along the Little Grand Wash fault and the Salt Wash Graben, except there is evidence of leakage. In addition to the absence of fault zone leakage along the Ten Mile Graben, no evidence of leakage was observed in this study south of the northernmost faults of the Little Grand Wash fault and the Salt Wash Graben. This is also the case for all of the abandoned, uncapped boreholes except the Ten Mile Geyser. No well log data for the geyser are available for this study, but it likely encounters the north fault of the graben at depth and ultimately soles out in the footwall of the fault.

Well logs near the Little Grand Wash fault used in Figure 22 show the source of these fluids is as shallow as the middle Jurassic Navajo Sandstone (300 m) and as deep as the upper Permian (800 m) (Fig. 34). These rocks provide a stacked aquifer system with higher-porosity aeolian and fluvial sandstone aquifers, underlying lower-porosity mudstone, siltstone and shale caps (Fig. 7).

This evidence suggests that regional fluids migrate up-plunge along the Caine Creek Anticline in the Jurassic Wingate and Navajo Sandstones, and that this regional flow system is affected by the northernmost traces of Little Grand Wash fault and the Salt Wash Graben (Fig. 34). Considering the mud-, silt-, and shale-rich nature of the cap rocks (the Carmel and Kayenta formations), one might expect that the faults cutting these aquifers would be poor conduits for flow. The highly fractured fault damage zones may create higher hydraulic conductivity in the vertical (up-dip) direction of the faults (Fig. 35). Similar clay-rich faults have been reported as being barriers to lateral flow and conduits for vertical flow (Perkins, 1961; Smith, 1966; Weber et al., 1978).

The hydraulic conductivity decreases near the surface when calcite begins to precipitate out of solution, filling the fractures. The specific locations of these deposits and other areas of leakage also may be influenced by the varying thicknesses of the formations throughout the field area. The damage zones of these faults appear to impede lateral cross-fault flow, but act as baffles, allowing fluids to travel vertically to the surface (Fig. 35). Multiple slip surfaces, an increase in fracture density in the faults' damage zones, and thickness variations in the formations cut by the fault may all affect the sealing integrity of the faults.

Deeper fluids (oil and gas) and the shallower groundwater migrate up-plunge from the northwest and are sealed from further migration by the northern faults of the Little Grand Wash fault and the Salt Wash Graben. This may be a result of the clay gouge seen in the field area, and may be similar to what is reported for other fault studies (Aydin and Yehuda, 2002). The reduction of pore space through granulation in

sandstones may also explain the lateral seal in areas where sandstones are juxtaposed in the fault zones (Aydin and Yehuda, 2002).

The Permian or deeper source of $CO_2$ (Heath, 2004) is cut by the fault, which migrates up-dip along the fault traces, allowing the $CO_2$ to mix with the shallower groundwater system. Gas analysis can be found in Heath (2004). These $CO_2$- charged waters then migrate up-dip to the surface. The Jurassic Wingate Sandstone and Navajo Sandstone are good candidate aquifers (Heath, 2004; and this study).

This interpretation is consistent with the gas analysis of the $CO_2$ and the geochemical analysis of the waters of all springs and geysers in the area done by Heath (2004). The oil seep found along the Little Grand Wash fault, seen on Figures 14, and 23 d, was sampled by Lillis et al. (2003), and the geochemical fingerprint of this oil suggests that it was sourced in the lower Permian.

## Geometry of the Aquifers

### Regional geometry and timing

The rocks in the area of the Little Grand fault, Salt Wash Graben, and Ten Mile Graben have been subjected to numerous tectonic loads. Repeated salt movement, Tertiary intrusive igneous activity, burial, and uplift occurred in the Cretaceous to early Tertiary. The area is currently under NNE extension (Davatzes et al., 2003; Reinecker et al., 2004).

Early Tertiary conditions may have folded the rocks within the Colorado Plateau, including the rocks in the field area, forming the Caine Creek Anticline. This implies the Caine Creek Anticline presently is under NNE extension (Reinecker et al., 2004). Rapid

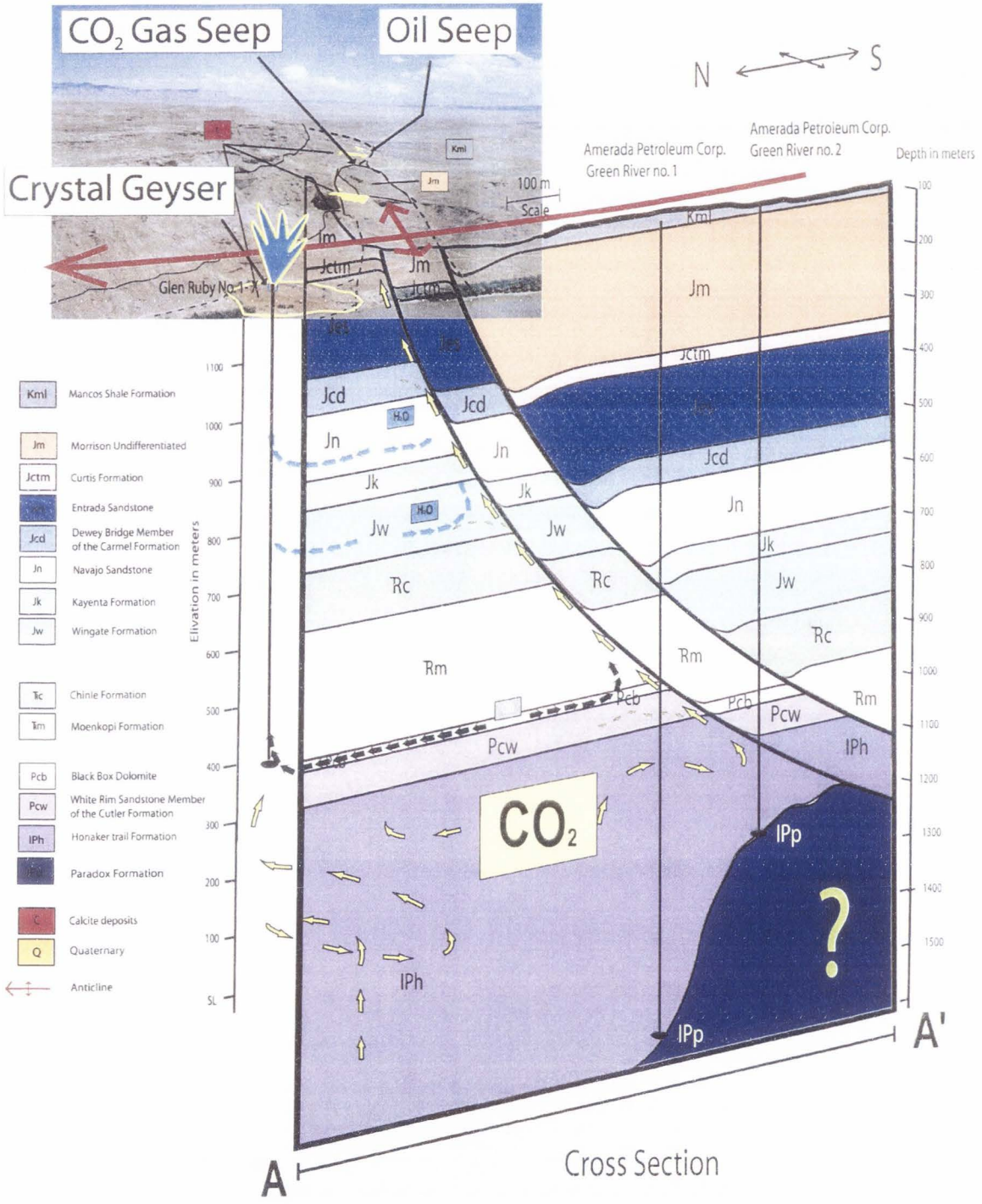


Figure 34 Cartoon showing that regional fluids migrate up-plunge along the Caine Creek Anticline, and that this regional flow system is affected by the northernmost traces of Little Grand Wash Fault and the Salt Wash Graben. Air photo animations are explained in Figure 19.

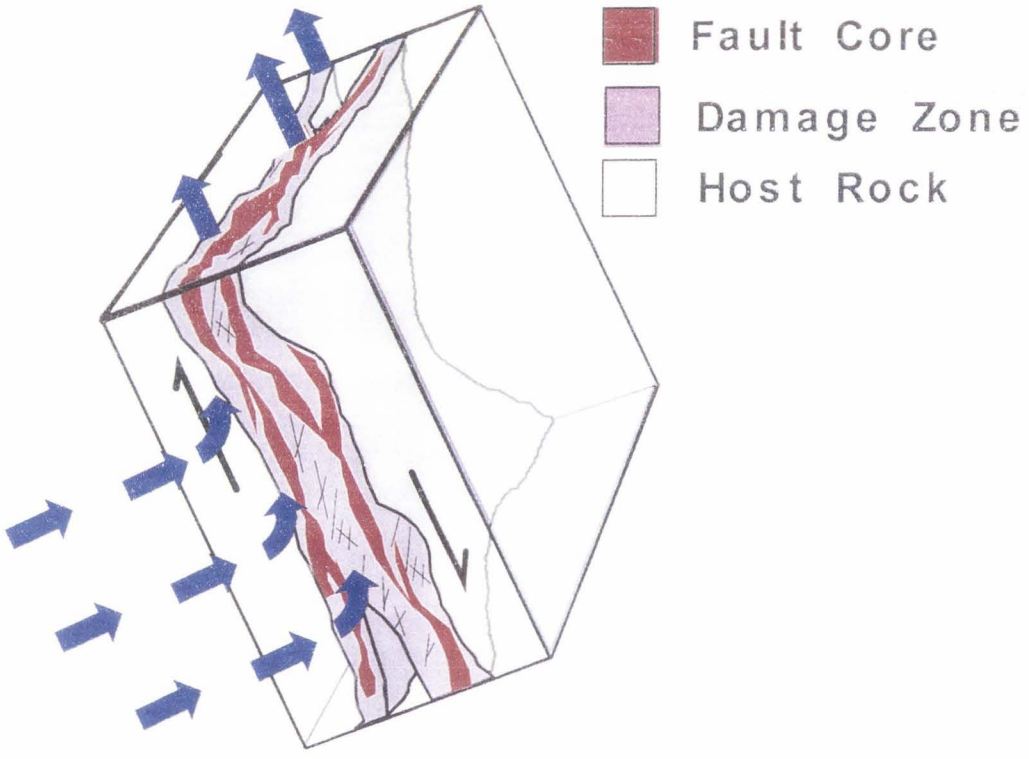


Figure 35 Cartoon illustrating vertical fluid migration. The three primary components of faults (core, damage zone, and protolith) that help determine whether they act as conduits, barriers, or combined conduit-barrier systems are illustrated (modified from Caine et al., 1996).

uplift of the Colorado Plateau (approximately 1.8 km since the end of the Eocene; Fig. 33) may be at least one of the catalysts for such extension. This agrees with the median ages, (36.36 to 41.62 Ma) of the clay in the fault gouge. The fault movement along the Little Grand Wash fault, the Salt Wash Graben, and the Ten Mile Graben can also be better constrained with the aid of $^{230}Th/^{234}U$ values, which can be used to estimate ages

if the carbonates are less than 250,000 to 300,000 years old. As of this writing, samples are still being analyzed by E. Dixon (Los Alamos National Lab).

## Aquifers

There are at least two candidate aquifers seen in the wells near the Little Grand Wash fault that contribute to the overall flow system in and around these faults. They are the Wingate Sandstone and Navajo Sandstone (Fig. 36). These two aquifers have been folded into a shallow, north-plunging anticline with shallow-dipping limbs of varied thickness both down-dip and along strike, and have been cut by south-dipping normal faults. Damage zones created by the faults allow water in these aquifers to migrate vertically up-dip along the Little Grand Wash fault and the Salt Wash Graben. These aquifers are charged with $CO_2$ that has used this same damage zone conduit system to migrate up-section from deeper formations.

## Oil reservoirs

Oil shows have been limited to a few wells (Table 1) and there are minimal surficial data available for the interpolation of the reservoirs containing oil. It is likely that at least one of the oil sources is in the lower Permian (Lillis et al., 2003). These formations have clay-carbonate lithologies and have been at an adequate depth and temperature for a sufficient length of time (2,800 m and $100^{o}$+C for a time of 75 to 35 Ma) for oil generation (Fig. 33). It is probable that the damage zone pathways created by

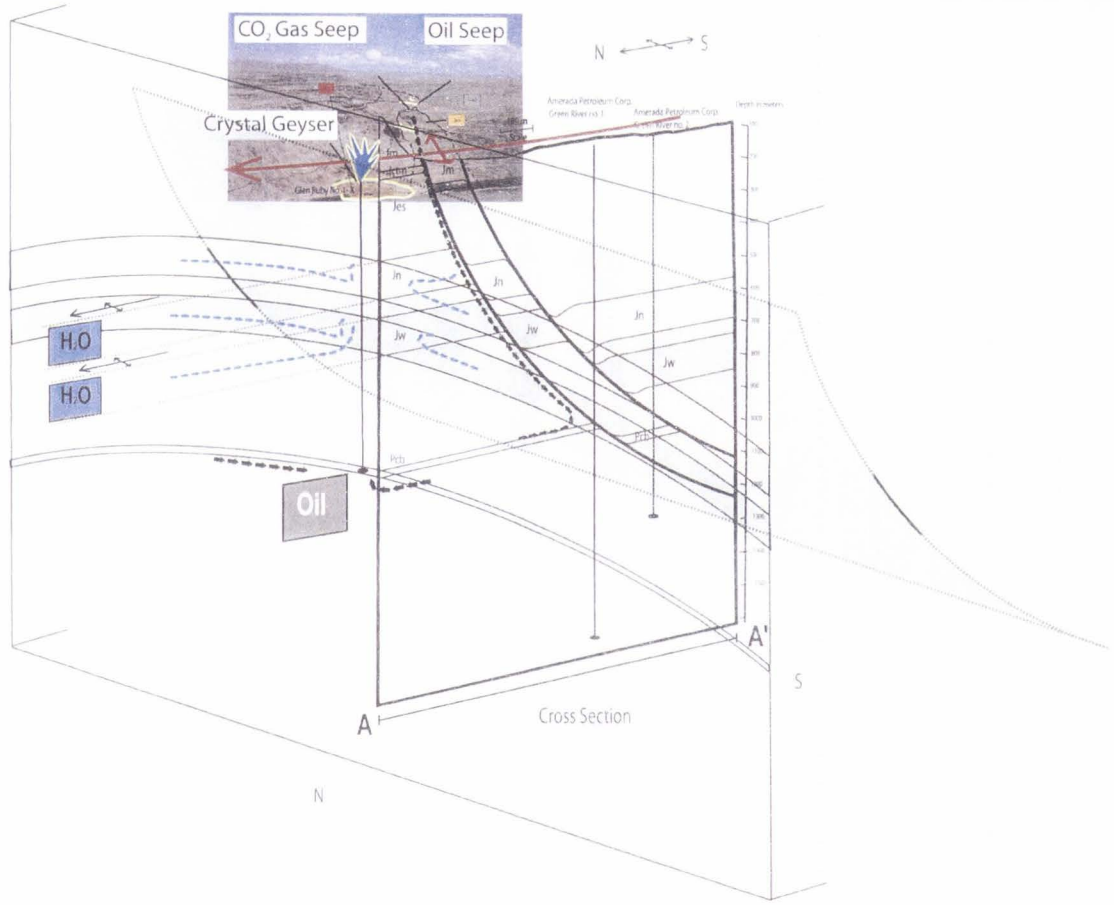


Figure 36 Cartoon showing a cross-sectional slice, perpendicular to the axis of the Caine Creek Anticline, of the Navajo Sandstone, the Wingate Sandstone, and the Black Box Dolomite being truncated by the north strand of the Little Grand Wash Fault. This figure shows the predicted flowpaths of the oil and water in the system. Dips of the anticline limbs have been vertically exaggerated.

the faults have allowed the oil generated in the lower Permian to migrate up, breaching the clay-rich possible cap rocks. This would allow the oil generated at depth to mix with water in the shallower aquifers (Wingate and Navajo Sandstones) up section and ultimately reach the surface (Fig. 36).

$CO_2$ reservoirs

Carbon dioxide has probably been generated by clay-carbonate reactions (Heath 2004). Formations containing siliceous-carbonate rocks are needed for these reactions. The Moenkopi, Honaker Trail, and the Elephant Canyon Formations have all been deep enough to experience temperatures ranging from 100° to 200°C (Fig. 33). These are the temperatures needed to generate $CO_2$ (Heath, 2004). The $CO_2$ from these formations has migrated up section, mixing with the waters of shallower aquifers (Fig. 37).

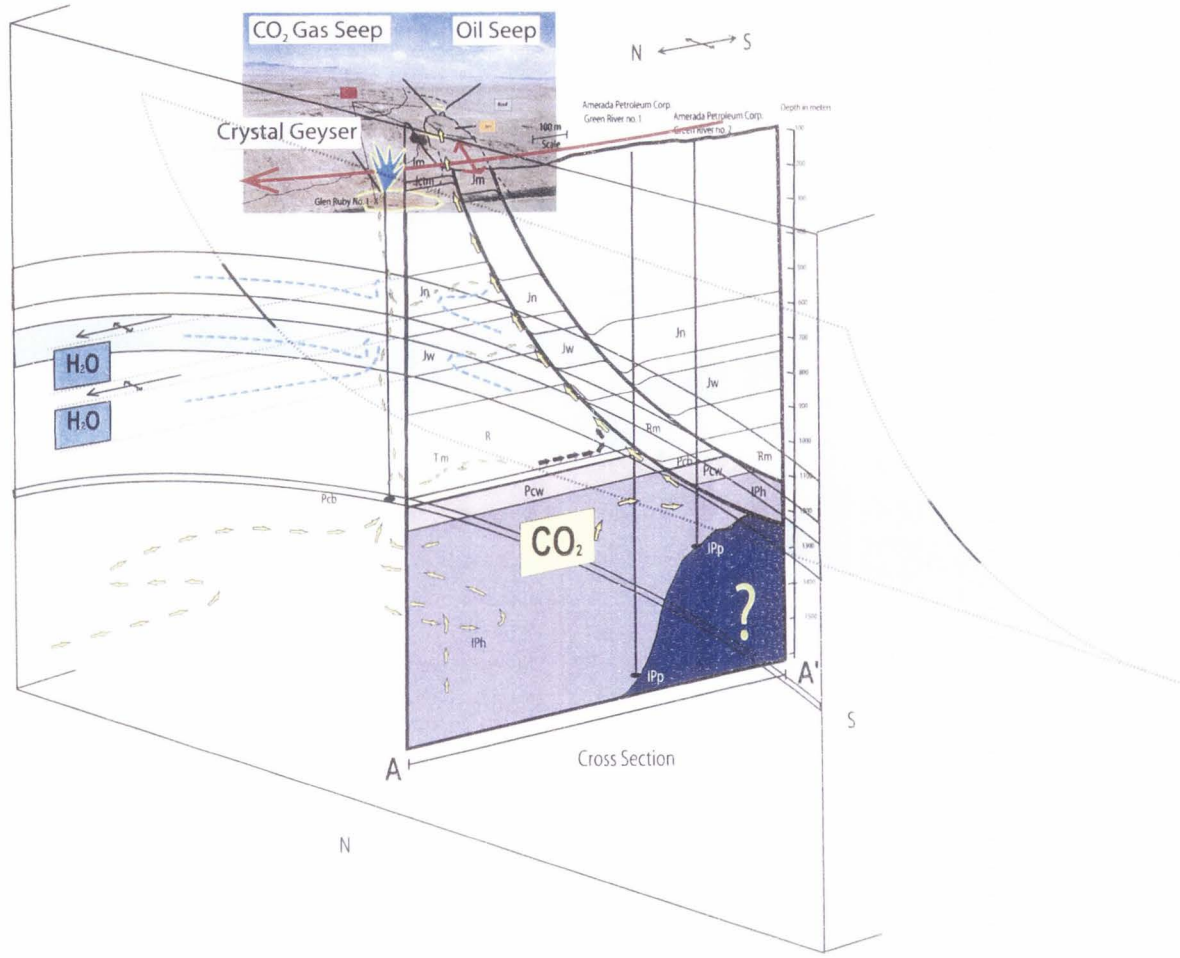


Figure 37 This cartoon, in addition to showing the cross-sectional slice, perpendicular to the axis of the Cane CreekAnticline, of the Navajo Sandstone, Wingate Sandstone and the Black Box Dolomite, shows the deeper Permian formations from the Little Grand Wash cross section (Fig.22). This figure shows the predicted flow paths of the oil and water in the system and the $CO_2$ reservoirs feeding the system. Dips of the limbs of the anticline have been vertically exaggerated.

# CONCLUSIONS

This study clearly shows that clay-rich faults that cut subsurface fluid reservoirs may act as conduits, barriers, or combined conduit-barrier systems that enhance or impede fluid flow in different flow directions. This study concludes that the damage zones of the Little Grand Wash fault and the northern fault of the Salt Wash Graben do impede lateral cross-fault flow, but act as baffles, allowing fluids to travel vertically to the surface. It is probable that the damage zone pathways created by the faults have allowed the oil generated in the lower Permian reservoir and the Permian or deeper $CO_2$ reservoir to migrate vertically, breaching the clay-rich possible cap rocks. This migration has occurred and is occurring in spite of, in some areas, 100+ m of mud, silt, and shale cap rocks, and at the surface, the presence of mineralization in the damage zones.

This research has examined a natural laboratory that can be used to understand $CO_2$ sequestration. Deep $CO_2$ reservoirs have contaminated shallower groundwater aquifers near the Little Grand Wash fault and the Salt Wash Graben. It is clear that faults of this nature can and do create fluid pathways, effectively breaching anticlinal reservoirs. This occurs regardless of the presence of obstacles in these pathways at the surface. In this study, there is sufficient evidence suggesting that cap-rocks faulted candidate $CO_2$ sequestration reservoir, despite their sealing capabilities, may act as combined conduit-barrier systems. Faults can effectively allow fluid flow even in clay-rich formations that are often considered to be cap rocks of these candidate sequestration $CO_2$ reservoirs. This may negate these reservoirs' sealing integrity. The results of this

study clearly show that much consideration and planning is essential when implementing geologic storage of carbon dioxide in faulted, clay-rich reservoir.

# REFERENCES

Allis, R., Chidsey, T., Gwynn, J., Morgan, C., White, S., Adams, M., and Moore, J., 2000, Natural $CO_2$ reservoirs on the Colorado Plateau and Southern Rocky Mountains– Candidates for $CO_2$ Sequestration: First National Conference on Carbon Sequestration, May 11-14, 2000, U.S. Department of Energy, National Energy Technology Laboratory, compact disk DOE/NETL-2001/1144.

Anonymous, 1912, The Green River, Utah, oil field: The Salt Lake Mining Review, v. 13, no. 22.

Antonellini, M., and Aydin, A., 1994, Effect of Faulting on Fluid Flow in Porous Sandstones: Petrophysical Properties: American Association of Petroleum Geologists Bulletin, v. 78, p. 355-377.

Aydin, A., and Yehuda, E., 2002, Anatomy of a normal fault with shale smear: Implications for fault seal; American Association of Petroleum Geologists Bulletin, v. 86, p. 1367-1381.

Baer, J.L., and Rigby, J.K., 1978, Geology of the Crystal Geyser and environmental implications of its effluent, Grand County, Utah: Utah Geology, v. 5, p. 125-130.

Bouvier, J.D., Sijpesteijn, K., Kluesner, D. F., Onyejekwe, C.C., and Van der Pal, R.C., 1989, Three-dimensional seismic interpretations and fault sealing investigations, Nun River field, Nigeria: American Association of Petroleum Geologists Bulletin, v. 73, p. 1397-1414.

Caine, J. S., and Forster, C. B., 1999, Fault zone architecture and fluid flow; insights from field data numerical modeling: Geophysical Monograph, v. 113, p. 101-127.

Caine, J.S., Evans, J.P., and Forster, C.B., 1996, Fault zone architecture and permeability structure: Geology, v. 18, p. 1025-1028.

Campbell, J.A., and Baer, J.L., 1978, Little Grand Wash fault–Crystal Geyser area, *in* Fasset, J.E., and Thomaidis, N.D., eds., Oil and gas fields of the Four Corners Area: Four Corners Geological Society, p. 666-669.

Davatzes, N.C., Aydin, A., and Eichhubl, P., 2003, Overprinting faulting mechanisms during the development of multiple fault sets in Sandstone, Chimney Rock, Utah. Tectonophysics, v. 363, p. 1-18.

Dockrill, B., Kirschner, D., and Shipton , Z.K. ernal structure and evolution of travertine deposits overlying a normal fault system, SE Utah, USA. (*Chemical Geology*, in press).

Doelling, H., 2001, Geologic map of the Moab and eastern part of the San Rafael Desert 30' X 60' quadrangles, Grand and Emory Counties, Utah and Mesa County, Colorado., Utah Geological Survey. Salt Lake City, UT, United States, 3 sheets.

Doelling, H., 1975, Geology and mineral resources of Garfield County, Utah: Utah Geological and Mineral Survey Bulletin 107, 175 p.

Doelling, H., 1994, Tufa deposits in western Grand County: Utah Geological Survey, v. 26, 8-10, p. 13.

Dong, H., Hall, C.M., Peacor, D.R., and Halliday, A.N., 1995, Mechanisms of argon retention in clays revealed by laser $^{40}Ar$ - $^{39}Ar$ dating: Science v. 267, p. 355-359.

Downey, M. W., 1984, Evaluating seals for hydrocarbon accumulations: American Association of Petroleum Geologists Bulletin, v. 68, p. 1752-1764.

Dula, W. F., 1991, Geometric models of listric normal faults and rollover folds: American Association of Petroleum Geologists Bulletin, v. 75, p. 1609-1625.

Gale, J., 2002. Geological storage of $CO_2$: What's known, where are the gaps and what more needs to be done. 6th International Conference on Greenhouse Gas Technologies. Kyoto. Retrieved from http://www.ieagreen.org.uk/ghgt6%20papers/GHGT61.pdf

Gibson, R. G., 1994, Fault-zone seals in siliciclastic strata of the Columbus Basin, offshore Trinidad: American Association of Petroleum Geologists Bulletin, v. 78, p. 1372-1385.

Hager, D., 1956, The Little Grand fault and the Green River nose, Emery and Grand Counties, Utah: Intermountain Association of Petroleum Geologists.

Harding, T. P., and Tuminas, A. C., 1988, Interpretation of footwall (lowside) fault traps sealed by reverse faults and convergent wrench faults: American Association of Petroleum Geologists Bulletin, v. 72, p. 738-757.

Hardman, R. F. P., and Booth, J. E., 1991, The significance of normal faults in the exploration and production of North Sea hydrocarbons. *in*: Roberts, A. M., Yielding, G., and Freeman, B., eds., The geometry of normal faults.

Heath, J.E., 2004, Hydrogeochemical characterization of leaking carbon dioxide-charged fault zones in east-central Utah. [M.S. Thesis], Logan , Utah State University. 175 p.

Helgesen, J. and Vold, J., 2003, Sealing properties of faults and their influence on water-alternating-gas injection efficiency in the Snorre Field, northern North Sea: American Association of Petroleum Geologists Bulletin, v. 87, p. 1437-1458.

IPCC, 2001: Climate Change 2001: Synthesis Report. A Contribution of Working Groups I, II, and III to the Third Assessment Report of theIntegovernmental Panel on Climate Change [Watson, R.T. and the Core Writing Team (eds.)]. Cambridge University Press, Cambridge,United Kingdom, and New York, NY, USA, 398 p.

Johnson, J.A., 1988. The sedimentology, paleohydrology, and paleogeography of the Brushy Basin Member, Morrison Formation in the Henry Basin, Wayne and Garfield Counties, Utah, PhD Thesis, University of California, Berkeley, Berkeley, CA, USA 117 p.

Lillis, P.G., Warden, A., and King, J.D., 2003. Petroleum systems of the Uinta and Piceance Basins—Geochemical characteristics of oil types. In: Petroleum Systems and Geologic Assessment of Oil and Gas in the Uinta-Piceance Province, Utah and Colorado, chap. 3, Digital Data Series DDS-69-B, U.S. Geological Survey, Denver. 25 p.

McKnight, E.T., 1940, Geology of area between Green and Colorado Rivers, Grand and San Juan Counties, Utah: U.S. Geological Survey Bulletin 908, 147 p.

Nelson, R., A., 1985 Geologic analysis of naturally fractured reservoirs: Houston, Texas, Gulf Pulishing Company, 320 p.

Nuccio, V.F., and Condon, S.M., 1996, Burial and thermal history of the Paradox Basin, Utah and Colorado, and petroleum potential of the middle Pennsylvanian Paradox Formation: U.S. Geological Survey Bulletin 2000 p. O1-O41.

O Sullivan, R.B., 1992, The Jurassic Wanakah and Morrison Formation in the Telluride-Ouray-western Black Canyon area of southern Colorado: U.S. Geological Survey Bulletin 1927, 24 p.

Pearce, J.M., Holloway, S., Wacker, H., Nelis, M.K., Rochelle, C., and Bateman, K., 1996. Natural occurrences as analogues for the geological disposal of carbon dioxide. Energy Conversion and Management 37, p. 1123-1128.

Pevear, D. R., Vrolijk, P. J., and Longstaffe, F. J., 1997, Timing of Moab Fault displacement and fluid movement integrated with burial history using radiogenic and stable isotopes, *in* Geofluids II, Hendry, J. P., Carey, P., Parnell, J., Ruffell, A, and Worden, R., eds., Belfast, U.K., Queens University of Belfast, p. 42-45.

Perkins, H., 1961, Fault closure-type fields, southeast Louisiana: Gulf Coast Association Geological Society Transaction, v. 11, p. 203-212.

Peterson, F., 1988, Stratigraphy and nomenclature of Middle and Upper Jurassic rocks, western Colorado Plateau, Utah and Arizona: U.S. Geological Survey Bulletin 1633-B, p. 17-56.

Peterson, F., and Turner-Peterson, C. E., 1989, Sedimentation and basin analysis in siliciclastic rocks sequences; Volume 1, Geology of the Colorado Plateau. *in* Hanshaw, P. M., ed., Field trip guidebook T 130, Field trips for the 28th international geological congress. .American Geophysical Union, Washington, DC, United States. 65 p.

Petersen, L.M., and Roylance, M.M., 1982, Stratigraphy and depositional environments of the Upper Jurassic Morrison Formation near Capitol Reef National Park, Utah: Brigham Young University Geological Studies, v. 29, p. 1-12.

Powell, J. W., 1875, Exploration of the Colorado River of the west and its tributaries, 1869-72: Publisher unknown, Washington D.C., U.S.

Ramsay, J. G., and Huber, M. I., 1987, The techniques of modern structural geology: , Folds and Fractures, v. 2, London, U.K., Academic press Inc.

Randolph, L., and Johnson, B., 1989, Influence of faults of moderate displacement on groundwater flow in the Hickory sandstone aquifer in central Texas: Geological Society of America with Programs, v. 21. p. 242.

Reinecker, J., O. Heidbach, M. Tingay, P. Connolly, and B. Müller, 2004, The 2004 release of the World Stress Map (available online at www.world-stress-map.org)

Scholz, C., H., 1990 The mechanics of earthquakes and faulting: Cambridge, Cambridge University Press, 439 p.

Seeburger, D. A., Aydin, A., Warner, J. L., and White, R. E., 1991, Structure of fault zones in sandstone and its effect on permeability, American Association of Petroleum Geologists Bulletin, v. 75, 699 p.

Shipton, Z.K., Evans, J.P., Robeson, K.R., Forster, C.B., Snelgrove, S., 2002, Structural heterogeneity and permeability in faulted eolian sandstone; implications for subsurface modeling of faults, American Association of Petroleum Geologists Bulletin, v. 86, p. 863-883.

Shipton, Z.K., Evans, J.P., Kirchner, D., Kolesar, P.T., Williams, A., and Heath, J., 2004,Analysis of $CO_2$ leakage through "low-permeability" faults from natural reservoirs in the Colorado Plateau, southern Utah. In: Baines, S. J. & Worden, R. H. (eds.) 2004. *Geological Storage of Carbon Dioxide: Reducing Greenhouse Gas Emissions.* Geological Society, London, Special Publications 233.

Smith, D.A., 1966, Theoretical considerations of sealing and nonsealing faults: American Association of Petroleum Geologists Bulletin, v. 50, p. 363-374.

Smith, D.A., 1980, Sealing and non-sealing faults in Louisiana Gulf Coast Salt basin: American Association of Petroleum Geologists Bulletin, v. 64, p. 145-172.

Trimble, Larry M. and Doelling, Hellmut H., 1978, Geology and Uranium-Vanadium Deposits of the San Rafael River Mining Area, Emery County, Utah: Utah Geological and Mineral Survey, Bulletin 113.

Utah AGRC, 2002, State of Utah – Division of Information Technology Services see website http://agrc.utah.gov, last referenced 12/31/04.

van der Pluijm, B. A., Hall, C. M., Vrolijk, P. J., Pevear, D. R., Covey, M. C., 2001, The dating of shallow faults in the Earth's crust, Nature 412; 6843, p. 172-175.

Vrolijk, P., Myers, R., Sweet, M. L., Shipton, Z. K., Evans, J. P., Heath, J., Williams, A. P., 2005, Anatomy of Reservoir-Scale Normal Faults in Central Utah: Stratigraphic Controls and Implications for Fault Zone Evolution and Fluid Flow, in: Pederson, J. P., and Dehler, C. M., eds., Field trip guidebook for the Annual meeting, Geological Society of America, Salt Lake City.

Watts, N. L., 1987, Theoretical aspects of cap-rock and fault seals for single- and two-phase hydrocarbon columns: Marine and Petroleum Geology, v. 4, p. 274-307.

Weber, 1997; A historical overview of the efforts to predict and quantify hydrocarbon trapping features in the explorations phase and in field developments planning, *in* P. Moller-Pedersen and A. G. Koestler, eds., Hydrocarbon seal: importance for exploration and production: Norwegian Petroleum Society Special Publication 7, p. 1-13.

Weber, K. J., and Daukoru, E., 1975, Petroleum geology of Niger delta: 9th World Petroleum Congress Proceedings, v 2, p. 209-221.

Weber, K., J., Mandl, G., Polaar, W. F., Lehner, F., and Precious R. G., 1978, The role of faults in hydrocarbon migration and trapping in Nigerian growth fault structures, *in* American Institute of Mining Metallurgical and Petroleum Engineers and Society of Petroleum Engineers Tenth Annual Offshore Technology Conference Proceeding, v. 4, p. 2643-2653.